JOURNAL OF APPLIED PHYSICS

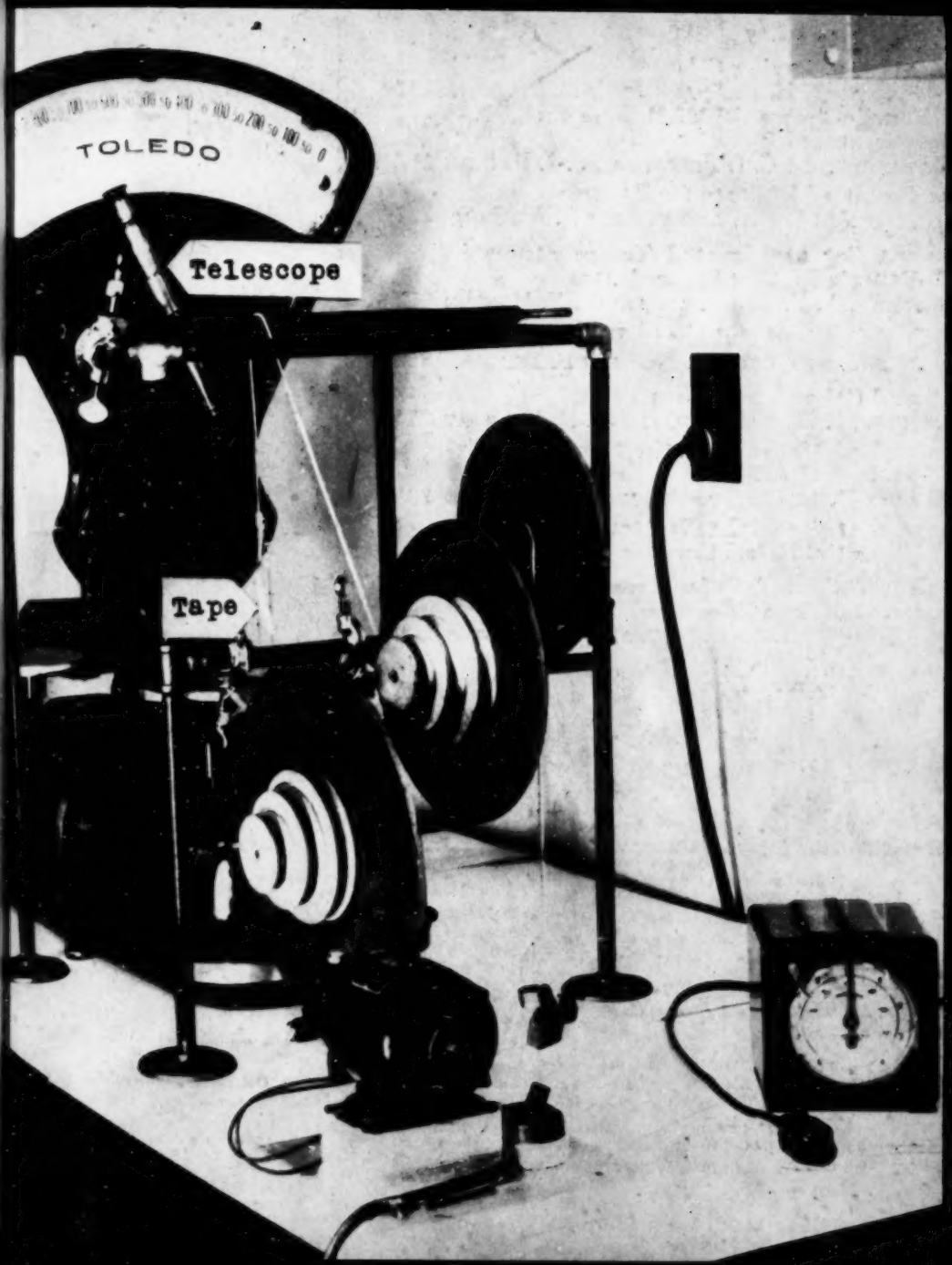

JOURNAL OF APPLIED PHYSICS

Vol. 17, No. 5 MAY, 1946

In This Issue

Special Issue on High Polymers

		Page
Editorial	E. H.	313
Elastic Properties of Cork. I. Stress Relaxation of Compressed Cork	S. L. Dart and Eugene Guth	314
Formation of Ionized Water Films on Dielectrics under Conditions of High Humidity	Robert F. Field	318
Thermal Polymerization of Drying Oils	H. E. Adams and P. O. Powers	325
Electrostatic and Tensile Properties of Rubber and GR-S at Elevated Temperatures	R. S. Havenhill, H. C. O'Brien, and J. J. Rankin	338
Significance of the Equation of State for Rubber	Eugene Guth, Paul E. Wack, and Robert L. Anthony	347
Theory of Permanent Set at Elevated Temperatures in Natural and Synthetic Rubber Vulcanizates	R. D. Andrews, A. V. Tobolsky, and E. E. Hanson	352
Crystallization of Unvulcanized Rubber at Different Temperatures	Lawrence A. Wood and Norman Bekkedahl	362
Tackiness of GR-S and Other Elastomers	W. F. Busse, J. M. Lambert, and R. B. Verdery	376
Applications of Infra-Red Methods in the Structural Examination of Synthetic Rubber	J. E. Field, D. E. Woodford, and S. D. Gehman	386
Photoelectric Instrument for Light Scattering Measurements and a Differential Refractometer	P. P. Debye	392
Thermal Expansion and Second-Order Transition Effects in High Polymers. III. Time Effects	R. S. Spencer and R. F. Boyer	398
Abstracts		405

In Every Issue

Calendar of Meetings	361
Here and There	408
New Books	408
New Booklets	410
Index to Advertisers	xxx

BOARD OF EDITORS

Elmer Hutchisson, *Editor*

Associate Editors

R. Bowling Barnes
Otto Beeck
W. F. Busse
S. H. Caldwell
Clark Goodman
Selig Hecht
W. James Lyons
Paul E. Sabine
Frederick Seitz
J. R. Townsend

Publication of the American Institute of Physics

ADMINISTRATIVE STAFF

Henry A. Barton, *Director*

Margaret S. Griffin *Publications Manager*

Theodore Vorburger, *Business Manager*

John T. Tate, *Adviser on Publications*

GOVERNING BOARD

Paul E. Klopsteg, *Chairman*

Wallace Waterfall, *Secretary*

George B. Pegram, *Treasurer*

R. B. Dow
L. A. DuBridge
W. F. Fair, Jr.
Floyd A. Firestone
Harvey Fletcher
R. C. Gibbs
K. S. Gibson
W. H. Markwood, Jr.
A. H. Pfund
John T. Tate
L. W. Taylor
A. G. Worthing

The Journal of Applied Physics, published monthly at Prince and Lemon Sts., Lancaster, Pa., is devoted to physics in its role as the science basic to other natural sciences and to the arts and industries. Previous to 1937 this publication was known as Physics. The Journal of Applied Physics publishes editorials, news of physicists, and reviews, as well as technical papers of applied physics.

Manuscripts should be submitted to Elmer Hutchisson, Editor, Case School of Applied Science, Cleveland 6, Ohio.

Subscriptions and orders for back numbers should be addressed to Prince and Lemon Streets, Lancaster, Pa. or to the American Institute of Physics, 57 East 55 Street, New York 22, N. Y.

Subscription Price

	U. S. AND CANADA	ELSEWHERE
To members of scientific societies	$5.00	$5.70
To all others	7.00	7.70

Back Number Prices

Complete set: Vol. 1, July, 1931–Vol. 16, 1945—$101.50
Yearly back number rate: $7.70
Single copies: $0.70 each.

Changes of address and proofs should be addressed to the Publications Manager.

Advertising rates supplied on request. Orders, advertising copy, and cuts should be sent to the American Institute of Physics.

Entered as second class matter January 22, 1937, at the Post Office at Lancaster, Pennsylvania, under the Act of March 3, 1879
Accepted for mailing at the special rate of postage provided for in the Act of February 28, 1925, authorized May 2, 1932.

Copyright 1946, by the American Institute of Physics.

Journal
of
Applied Physics

Volume 17, Number 5 May, 1946

The Control of Atomic Energy

DURING the past few months much progress has been made in the formulation of a type of control of atomic energy which, if adopted, would not only make it difficult for atomic bombs to be used as weapons of war, but would also encourage and stimulate the beneficial application of atomic energy in science, medicine, and industry. The progress that has been made is remarkable not only in its extent but also in the large number of individuals who have taken part in it. It is reported that over 70,000 letters have been written to the special Senate Committee on Atomic Energy headed by Senator Brien McMahon. Great credit for this activity should go to the Atomic Scientists of Chicago and their bimonthly Bulletin,[1] to the striking report to the public on the meaning of the atomic bomb entitled *One World or None*,[2] and the very extensive public appearances of the leading scientists in this field.

One concrete result of this aroused public interest is the unanimous approval by the McMahon committee of a bill which sets up for the domestic control of atomic energy a full-time Commission consisting of five civilians, with three supplementary committees which may act as checks. These are (1) a military liaison committee; (2) a general advisory committee consisting of nine civilians; and (3) a joint Congressional committee consisting of nine members. The Commission will assume title to all sources of fissionable material, all such materials, and all facilities for developing them, but will allow the use of fissionable material by industry, individuals, and medical and educational institutions. The effect of this bill on the dissemination of scientific information is not absolutely clear, and close scrutiny of the bill from this point of view will be necessary when it is reported out of the Committee.

The most important of the recent publications on the international control of atomic energy is the report of the Secretary of State's Committee on Atomic Energy.[3] In an extremely fascinating and lucid style this report describes how a group of distinguished consultants studying the control problem for the Committee changed their outlook from one of deep pessimism to optimism as their study progressed. There gradually evolved what seems like a workable scheme which now carries the full endorsement of the Committee. An essential feature of the scheme is that an international Atomic Development Authority would be established which would take the lead in developing peacetime applications of atomic energy as well as performing an inspection service to reduce the possibility of surreptitious activities which may lead to atomic warfare. The plan divides activities in the field of atomic energy into "safe" and "dangerous." The "dangerous" consist chiefly in the provision of raw materials, quantity production of fissionable materials, and use of these materials in atomic weapons. The "safe" consist of almost all other applications in science, medicine, and technology in which U235 and plutonium can be used in a denatured state without loss of effectiveness. The proposal is that the dangerous activities be carried on only by the international Authority, and the safe by interested individuals or groups in any nation. Thus the inspection service would not be prohibitive, and peaceful applications would be stimulated rather than retarded. The reading of this important report by all physicists is highly recommended.—E. H.

[1] *Bulletin of the Atomic Scientists*, Office 1126 East 59 Street, Chicago, Illinois. Subscription $2 a year.

[2] *One World or None* (Whittlesey House, McGraw-Hill Book Company, Inc., New York, 1946). $1.

[3] *A Report on the International Control of Atomic Energy*, Department of State Publication 2498. For sale by Superintendent of Documents, U. S. Government Printing Office, Washington 25, D. C. Price 20 cents.

Special Issue on High Polymers

All of the papers in this issue were presented at the second regular meeting of the Division of High Polymer Physics of the American Physical Society at Columbia University, January 24-26, 1946.

Elastic Properties of Cork

I. Stress Relaxation of Compressed Cork

S. L. Dart and Eugene Guth
Polymer Physics Laboratory, University of Notre Dame, Notre Dame, Indiana

The stress relaxation of corky materials is of theoretical significance for the understanding of such two-phase (corky material+air) systems, and is of great practical interest, since these materials are commonly used as gaskets, seals, etc. Stress relaxation was studied at various degrees of compression and at temperatures ranging from 30°C to 200°C. The experimental data were obtained from an automatic stress-relaxation machine which employed the principle of a chainomatic balance. It was found that the stress-time curves for various compressions could be obtained from each other by multiplication. This experimental fact is generalized by the statement that the stress is a product of two functions. The first factor is essentially identical with the S-shaped load-compression curve of cork and is independent of time. The second factor is shown to be a linear function of $\log t$ and is independent of compression. The linear stress-log time curve is found to persist over a wide range of times and to continue until the stress has decayed to zero at the higher temperatures. The decay time as obtained either by actual experiment or by extrapolation is shown as a function of temperature. This gives a fairly complete picture of the stress-time-temperature behavior of cork under compression.

INTRODUCTION

IT is surprising how little the average person knows about cork even though he uses it every day in his car as gaskets, vibration insulation, and in many other ways, such as closures, stoppers, heat insulation, etc.

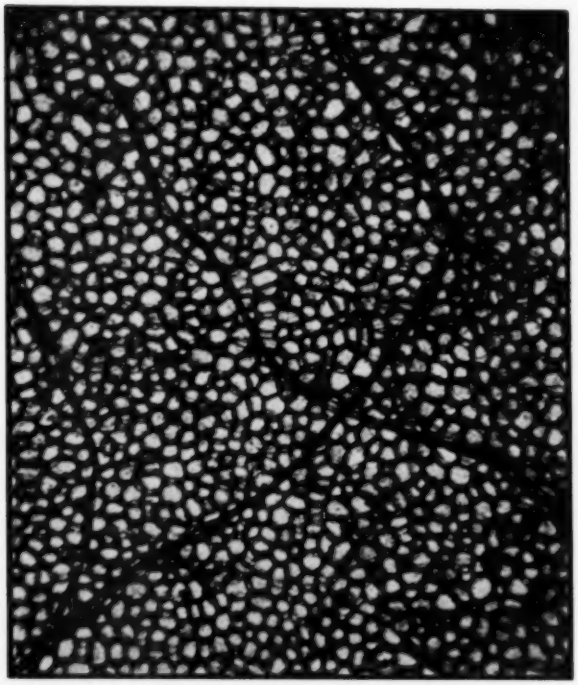

FIG. 1. Natural cork with cotton fibers. 80×.

Since the literature on cork, especially the scientific literature, is quite meager, it will not be out of place to give a brief outline of what cork really is before presenting any detailed work.*

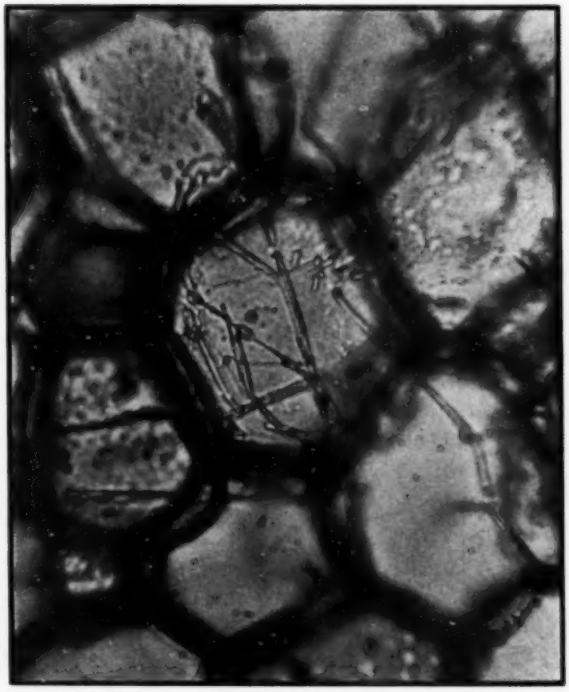

FIG. 2. Natural cork. 800×.

* Taken from the very interesting book *Cork and the American Cork Industry* by Arthur L. Faubel, published by the Cork Institute of America in 1941.

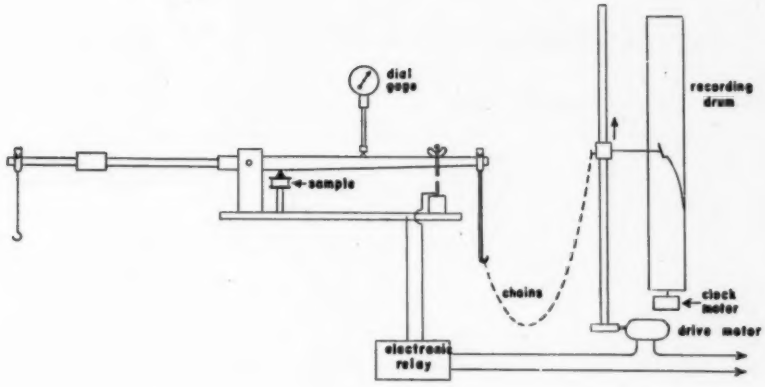

FIG. 3.

Cork is the outer bark of an evergreen oak tree. The tree grows this outer bark as a protection against the hot dry winds which are common around the Mediterranean sea. The cork oak is native to the Mediterranean area only, although attempts have been made to introduce it into the United States with some success in California. The corky outer bark of this oak tree is not a living part of the tree and hence may be stripped off when it gets sufficiently thick, without injuring the tree. A tree cannot be stripped until it is about 30 years old and thereafter every 10 years or so. This yields a piece of cork an inch or two thick. The average life of the tree is about 150 years but many live 200 years or more.

If we take a piece of this cork and look at it under a microscope, we will notice that it is made up entirely of tiny cells, as shown in Fig. 1. Thus, cork might be thought of as a solidified foam. The black lines on the slide are cotton fibers included to give a size comparison. The cells are fairly uniform in size and average about one thousandth of an inch in diameter. It is interesting to note that the shape of these cells is tetrakaidecahedral. This is the shape as shown by Lord Kelvin that one would expect from minimum surface conditions.

The cellular structure of cork accounts for most of its useful properties. This structure explains immediately the low density and also the high coefficient of friction due to the many "cups" or opened cells at the surface. The fact that the cells are closed explains the low thermal conductivity, the resistance to moisture and liquid penetration, and to a certain extent the resilience and ability to absorb vibration. Cork is also decidedly inert chemically. Figure 2 shows the cork cells at a higher magnification. This indicates the structure of the cell walls and shows the presence of crystalline material within the cells. With this brief outline of what cork is, we can proceed to a more detailed study of some of its properties.

DESCRIPTION OF EXPERIMENTAL METHOD

The apparatus used is shown schematically in Fig. 3. It consists essentially of a lever arm with a 1 to 10 ratio between the force due to the weights and that on the sample. The compression was indicated by a dial gauge on a 5 to 1 ratio with the sample. Stress-strain curves were taken by adding weights at a constant rate and reading the corresponding compression on the dial gauge. For relaxation the machine was made automatic by using the principle of the chainomatic balance. A number of chains were used as a variable weight. The moving end of the chains was driven by a motor actuated by contact points on the lever arm as indicated in Fig. 3. This set-up kept the forces balanced at all times and hence gave a very accurate picture of the relaxation. The motion of the chain drive was recorded by a pen on a clock driven drum. Thus, the machine recorded a continuous force *vs.* time curve.

STRESS-STRAIN

Because of the cellular structure of cork one can explain qualitatively the shape of the stress-strain curve in compression. Figure 4 shows the stress-strain curve for cork. At low compressions there is a region in which Hooke's law holds. At stresses slightly higher there seems to be a general breakdown of the structure and hence a region where compression changes rapidly, with small stress changes. Beyond this is the final region where the cells have all been collapsed and the material itself is compressed. This, of course,

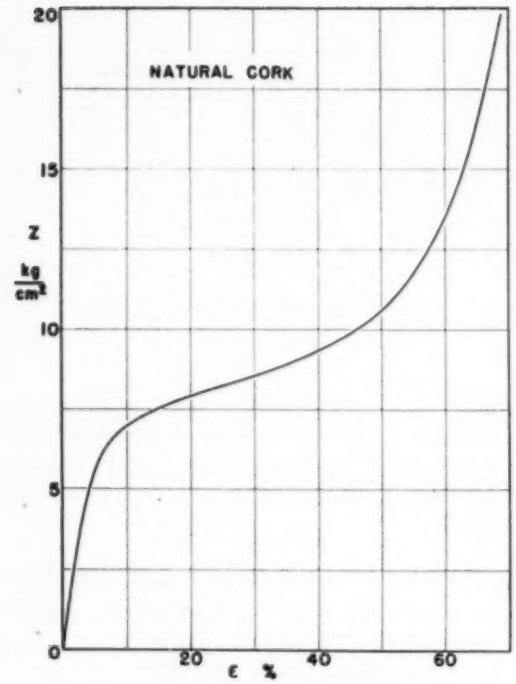

FIG. 4.

results in a final steep upward trend in the curve. Cork is not the only substance whose stress-strain curve is of this shape. Most woods, when compressed perpendicular to the grain (and hence in a direction to collapse the cells), give a similar curve. Dry Balsa wood in particular gives a curve with a very abrupt breakdown of the cells and hence that portion of the curve is almost horizontal. Metals also show an S-shaped compression curve, but here the final upward trend is due to a change in cross section of the metal. However, the unique thing about cork is that after a deformation it recovers its original dimensions to a remarkable degree. This is what gives cork its resilience and makes it useful for gaskets, stoppers, etc. We shall mention the stress-strain curve again a little later.

RELAXATION

The stress *vs.* time curves for natural cork in an ordinary plot have much the same appearance as that of many materials, i.e., a decay of stress whose rate of decay decreases with increasing time. Many types of plots were tried and it was found that if we plot the stress against the logarithm of the time we get almost exactly a straight line. Such a plot for 2 percent compression is shown in Fig. 5. This behavior was checked for times of as long as a couple of weeks without deviations from linearity. At high compressions it is found that there are deviations for short times (less than 10 minutes) which may be due to the air diffusing out of the compressed cork cells. In these cases we have taken the linear behavior of the sample after the first 10 minutes as the true cork behavior.

Figure 6 shows a number of relaxation curves at various degrees of compression plotted on a semi-log graph. One can immediately see a number of interesting things. The intercept values at t equal to one minute show a variation with compression entirely similar to that shown on the stress-strain curve; in fact, within the experimental error (due to the use of many different samples) these are identical with the stress-strain curve. Although one would expect this behavior, it is not an obvious conclusion since the stress-strain curve previously shown was obtained by an entirely different process and used but one sample. Another interesting thing about this graph is the fact that the extrapolation

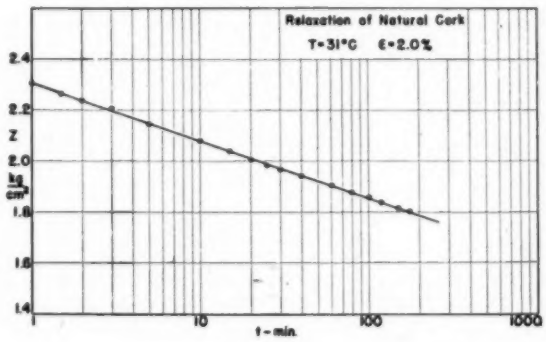

FIG. 5.

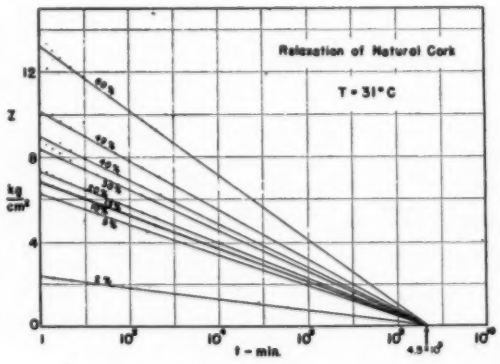

FIG. 6.

of the straight lines to zero stress yields the same decay time τ for all curves. Thus, assuming the extrapolation to be correct, we can say that no matter what the compression, the stress will decay to zero in about 980 years.

Let us see what conclusions we can draw from this fact. The equation of a single relaxation curve must be of the form.

$$Z = A_{(\epsilon T)} - B_{(\epsilon T)} \log_{10} t, \qquad (1)$$

where Z is the stress, t is the time in minutes, and $A_{(\epsilon T)}$ and $B_{(\epsilon, T)}$ are functions of the compression and temperature. We have already seen that the dependence of $A_{(\epsilon, T)}$ the intercept, on the compression, ϵ, is given by the stress-strain curve. Now, since all curves pass through the same point and since this point is at $Z=0$, we can say that the slope of the lines must be proportional to the intercept for all compressions. To state this a little differently, we can say that the ratio of $B_{(\epsilon T)}$ to $A_{(\epsilon, T)}$ must be independent of compression. Thus, we may say that

$$B_{(\epsilon T)}/A_{(\epsilon, T)} = \lambda_{(T)}, \qquad (2)$$

where $\lambda_{(T)}$ is a function of the temperature only. Rewriting Eq. (1) we have

$$Z = A_{(\epsilon, T)}(1 - \lambda_{(T)} \log t) = F(\epsilon, T)G(t, T). \qquad (3)$$

Thus, ignoring the temperature dependencies for the moment, we have split the stress function into two factors, the first depending on the compression only and the second depending on the time only. The form of the first factor, i.e., the stress-strain curve was shown graphically and explained qualitatively. The second factor was explained quantitatively and is given in analytical

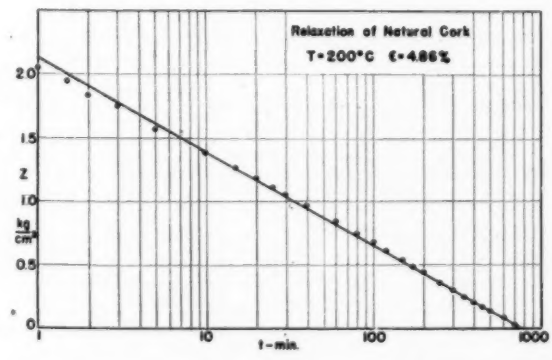

FIG. 7.

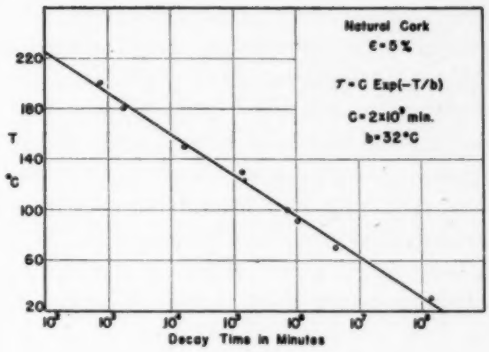

FIG. 8.

form. It should be pointed out that the decay time τ is related to λ by the equation

$$\tau = 10^{1/\lambda}.$$

TEMPERATURE DEPENDENCY

There remains to be found the temperature dependencies. One would expect that a process like relaxation would be accelerated by an increase in temperature. This proves to be the case and what is more interesting is the fact that the form is unchanged. That is, the relaxation curves are found to be linear on semi-log plot for all temperatures studied. Figure 7 shows the relaxation curve taken at 200°C. The curve is seen to be practically linear all the way to zero stress. Since raising the temperature means increasing the rate of relaxation, it seems that it was a good assumption that the semi-log plot is linear all the way to zero stress.

Figure 8 shows a plot of the temperature *vs.* the log of the decay time. There is a spread of the experimental points but this seems to be a straight line. The equation of this line would be of the form

$$\tau = \exp_{10}\left(\frac{\alpha - T}{\beta}\right) = Ce^{-T/\beta}. \qquad (4)$$

A theoretical consideration would predict a linear relation between $\log \tau$ and $1/T$. However, this does not check the experimental evidence as well as the above form.

Thus, we have as the generalized equation of state of cork

$$Z_{(\epsilon, T, t)} = A_{(\epsilon, T)}\left(1 - \frac{\beta}{\alpha - T} \log t\right). \qquad (5)$$

The analysis is not quite complete as we have not given the stress temperature relationships. There

has been a great deal of experimental difficulty in determining this. Besides the usual difficulties of variations between samples and the large number of variables encountered (i.e., density and humidity as well as stress, temperature, time, and compression) we have to correct for thermal expansion *and rate* of thermal expansion in the apparatus. However, the experimental difficulties have been pretty well cleared up and it is hoped that this last phase of the study will be completed soon.

ACKNOWLEDGMENT

The authors wish to express their appreciation to Dr. H. A. Robinson, Chief Physicist, Armstrong Cork Company for valuable discussions and for furnishing the samples used in this investigation. They also appreciate the benefit of discussions and the support of this work by Mr. E. Claxton, Director of Research and Dr. R. B. Rohrer, Assistant Director of Research, Armstrong Cork Company.

The Formation of Ionized Water Films on Dielectrics under Conditions of High Humidity

ROBERT F. FIELD

General Radio Company, Cambridge, Massachusetts

When a dielectric is placed in an atmosphere of 100 percent relative humidity, an ionized film of water forms, whose conductivity at the end of one minute is within a factor of ten of its equilibrium value, which is usually attained within an hour. This equilibrium conductivity ranges from essentially zero for certain hydrocarbon waxes, silicone resins and silicone-treated glass to 100 micromhos for ordinary glass and quartz. The ionized water film also produces interfacial polarization at its interface with the dielectric, which produces a marked increase in both capacitance and dissipation factor at audiofrequencies. This polarization builds up in the same manner as the conductivity. Its relaxation frequency appears to be in the audio-range.

THE effect of high humidity on dielectrics is so important that methods of conditioning samples have already been established. The properties studied have been mechanical, such as tensile strength and impact strength. Hence the conditioning has been for volume absorption, not for surface film. These conditioning procedures have been carried over to the testing of

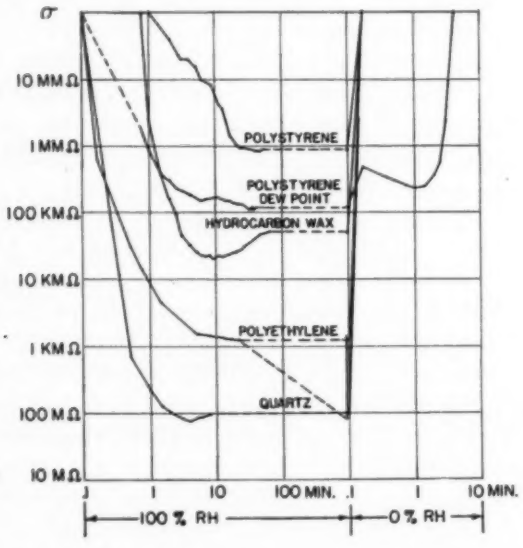

FIG. 1. Change of surface resistivity with time for materials having negligable volume absorption; exposure to 100 percent RH on left, recovery at 0 percent RH on right.

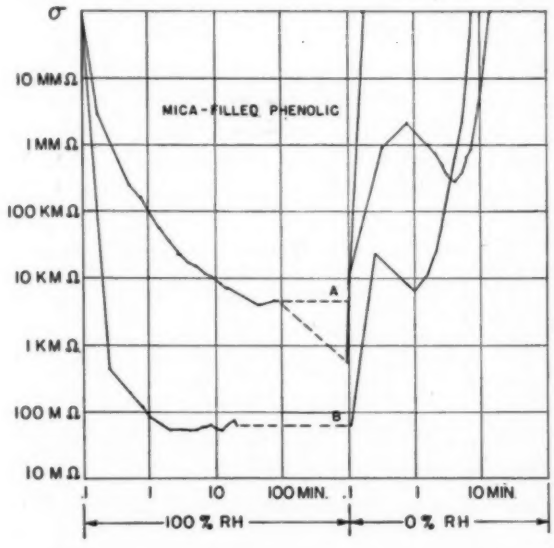

FIG. 2. Exposure and recovery curves for materials whose surface films are so thick that natural diffusion cannot cause them to vanish quickly.

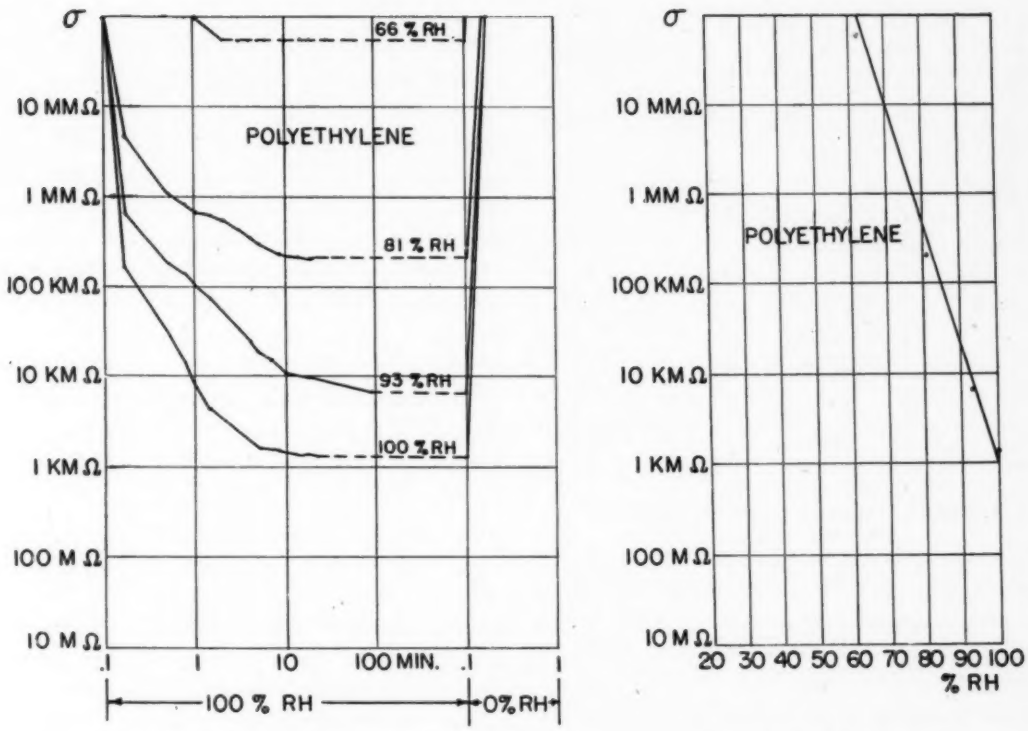

FIG. 3. (left) Effect of relative humidity on magnitude of exposure curve. (right) Relation of equilibrium surface resistivity to relative humidity.

electrical properties, where actually the effect of a surface film is of the greater immediate importance. The effect of volume absorption appears only after hours or days, while the surface film forms in minutes.

D.C. PHENOMENA

The formation of surface films has been studied by measuring the resistance between two pairs of electrodes bolted to opposite ends of thin slabs of dielectric.[1] This resistance is greater than 1 MΩ and is measured on a megohm bridge.[2] The slab is mounted on polystyrene terminals set in the metal top of a glass desiccator jar. Leakage over the surface of these terminals is eliminated by connecting the metal top to the guard terminal of the bridge. The base of the jar is filled with water for 100 percent RH, with saturated solutions of various salts for lower humidities[3] and with silica gel for 0 percent RH.

[1] ASTM Test Method, D257-38, Figs. 1 and 2.

[2] General Radio Type 544-BS8 Megohm Bridge, having upper resistance limit of 10 MMΩ.

[3]

%RH	93	81	66	52	43	32
Salt	$NaSO_4$	$(NH_4)_2SO_4$	$NaNO_2$	$Na_2Cr_2O_7$	K_2CO_3	$CaCL_2$

The rate of formation of surface film is shown in Fig. 1 for several dielectrics which have no appreciable volume absorption. Within a minute after being placed in 100 percent RH the surface resistivity is reduced from greater than 20 MMΩ to a value about a decade above the final equilibrium value, which is usually attained within 1 hour. Evidence to be given later suggests that the film forms very rapidly and that it is the ionization of the film that is observed by measuring resistance. Surface resistivity may decrease steadily to its equilibrium value, as for polyethylene, or overshoot, as for quartz and wax. In the latter case, excess ions are swept to the electrodes by the steady voltage. This action is well shown by polyethylene which has been allowed to stand overnight with the voltage off. Resistivity dropped by a decade, but recovered in a few minutes.

The film is actually very thin and vanishes within 10 seconds at 0 percent RH except for the thicker films which result from dew point condensation, shown here for polystyrene. In this case natural diffusion in the desiccator jar cannot

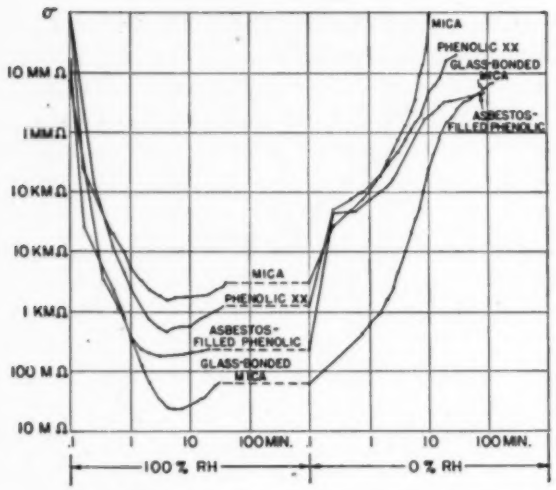

FIG. 4. Effect of volume absorption on shape of recovery curve.

maintain 0 percent RH at the surface. A curve with a maximum and minimum results, which appears to be typical. Forced ventilation removes the film within 10 seconds.

Similar typical recovery curves for two mica-filled phenolics are shown in Fig. 2. They illustrate the importance of small differences in composition or surface finish on the thickness and tenacity of the film. Type A requires 16 hours to give the typical recovery curve which Type B produces in 30 minutes. This is not caused by volume absorption, for forced ventilation removes the films from both materials in less than 10 seconds.

The effect of lower values of relative humidity is shown in Fig. 3 for polyethylene. The equilibrium value is a logarithmic function of relative humidity. This relation has been found for all the materials studied and agrees with the conclusions to be drawn from the classic work of Curtis.[4]

The effect of volume absorption first appears in the shape of the recovery curve, as shown in Fig. 4. Water stored just below the surface maintains the surface film without adding appreciable conductivity of its own. Surface forces acting on the water molecules must play a very important part, for the volume absorption of asbestos-filled or laminated phenolics differs greatly from that of natural mica and glass-bonded mica.

[4] H. L. Curtis, Bull. Bur. Stand. 2, 359 (1915).

The effect of volume absorption on the exposure curve is shown in Fig. 5 for polyamide, which has a high volume absorption as compared to its surface film. Conductivity from the absorbed water becomes comparable with that from the surface film before an equilibrium value is attained. Vulcanized fibre has so much surface film that its equally great volume absorption does not prevent equilibrium at 100 percent RH. At 81 percent RH however its surface film is reduced while the volume absorption is unchanged, so that there is no equilibrium value.

Some 40 different materials have been studied in this manner. Their parameters are shown in Table I, arranged in order of decreasing surface resistivity. For a material to be water repellant there must be some hydrophobic radical strategically placed on the surface. Methyl, ethyl, butyl, and propyl radicals seem to meet this requirement. The position of cellulose acetate butyrate as second in the list is the more remarkable because it maintains its high resistivity even after absorbing 4 percent of water. Silicone rubber and other silicone materials contain a methyl radical. Non-absorbent materials containing silicon, like quartz, glass, and steatite, can be made completely water repellant by coating with special silicone resins which provide a layer several hundred molecules thick. The exact position in the table of many of the other materials is determined by the condition of their surface. The samples measured were cleaned with grain alcohol and then baked at 60°C.

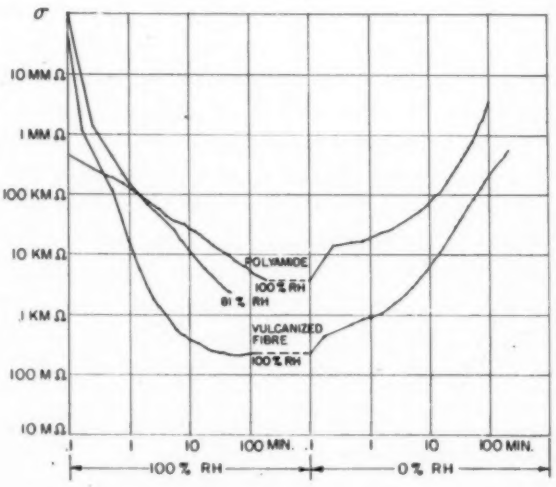

FIG. 5. Effect of volume absorption on exposure curve.

This provides as clean a surface as will exist in normal use, but does not completely remove oil films and other substances. Only one sample of a kind was tested so that there is no measure of the magnitude of normal variations. Values on the same specimen are repeatable within 50 percent.

The second column in the table gives the slope of the straight line plot of surface resistivity against relative humidity with values ranging from 4 to 18 percent RH per decade change in resistivity. The third and fourth columns give the recovery times in minutes after exposure to 100 percent RH for 1 and 16 hours. Any time up to 0.25 minute (15 seconds) indicates no volume absorption. Any longer time which is starred (*) is for a recovery curve typical of non-porous materials, for which forced ventilation will give a recovery time of less than 0.25 minute. Other large times indicate volume absorption under the conditions noted.

TABLE I.

Material	σ	% RH per decade change of σ	Recovery time in minutes after 100% RH for 1 hr.	16 hr.
	MMΩ			
Hydrocarbon wax, modified	>20		.0	.0
Cellulose acetate butyrate	>20		.0	.0
Silicone rubber	10		.13	
Polytetrafluoroethylene	3.6		.17	.17
	kMΩ			
Polystyrene (sheet)	840		.13	.13
Polydichlorostyrene 2–5	29	7	.17	
Hydrocarbon wax	20	13	.17	
Ethyl cellulose	13	9	.33	.5
Cellulose acetate	7.0	6	1.0	6
Polyvinyl chloride acetate	5.7	12	6*	
Polystyrene (plasticized)	5.0	4	.17	62*
Phenolic, mica-filled	5.0	9	.17	13*
Aniline formaldehyde	4.2	4	.17	20*
Polyamide	3.8	14	200	
Porcelain, glazed	3.7	15	2.5*	
Glass (high K)	3.4	10	17*	20*
Mica	3.0	12	11	
Polystyrene (molded)	2.4	10	.17	.17
Polystyrene (plasticized)	2.4	8	.11	.17
Steatite (L-3)	1.6		.17	.75
Quartz	1.4			
Polyethylene	1.3	9	.17	.17
Phenolic, XX	1.3	16	80	
Phenolic, asbestos filled	1.2	9	1.5*	100*
	MΩ			
Phenolic, XXXP	660	15	300	
Steatite (L-4)	640		.5	1
Phenolic, LE	500	18	400	
Phenolic, mica-filled	320	8	40*	
Steatite (L-4)	280		.33	
Polydichlorostyrene 3–4	240	6	.33	5.3*
Phenolic, cellulose filled	240	10	400	
Aniline formaldehyde, glass matte	240	9	14	1000
Phenolic, C	220	16	300	
Vulcanized fibre	220		6000	
Aniline formaldehyde, glass cloth	200	12	3	
Quartz	190			
Phenol formaldehyde (plasticized)	100	12	25	
Glass (sintered)	90			
Glass bonded mica	64	18	400	
Melamine, glass cloth	38	14	300	
Phenolic, mica filled	30	11	7*	

Starred (*) times indicate that forced ventilation will give a recovery time of less than 0.25 minute.

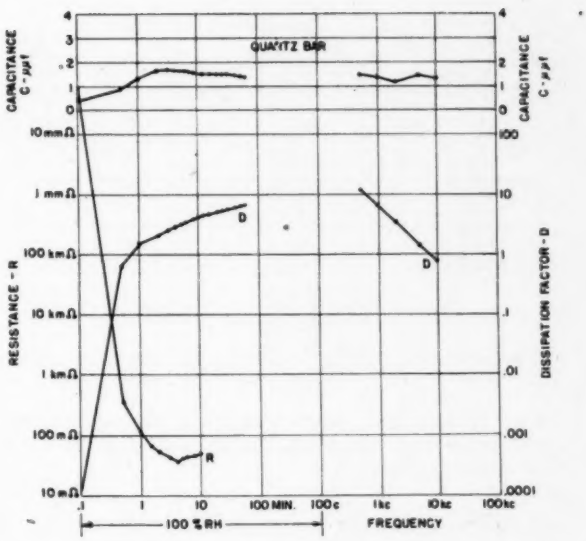

FIG. 6. Change of capacitance and dissipation factor with time and, after equilibrium, with frequency.

A.C. PHENOMENA

The effect of surface films on the dielectric constant and dissipation factor of dielectrics has been studied by measurements on a Schering bridge,[5] both at a single frequency as the film is forming and vanishing and over a considerable frequency range under equilibrium conditions. It is obvious that, as the film forms, both capacitance and dissipation factor should increase, because the water film itself must have a dielectric constant of 80 and must provide a shunt resistance because it is conducting.

The behavior of a quartz bar at 100 percent RH is shown in Fig. 6. Both capacitance and dissipation factor at 1 kc increase to steady values as the surface film builds up and its

[5] General Radio Type 716-C capacitance bridge.

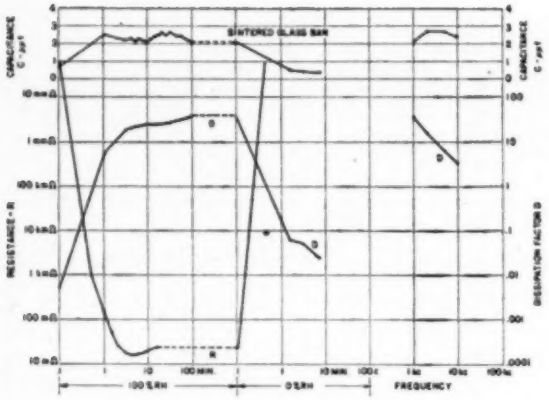

FIG. 7. Exposure, equilibrium, and recovery curves. Capacitance and dissipation factor recover more slowly than surface resistivity.

resistance decreases to its equilibrium value. For frequencies in the audio-range capacitance is constant within the limits of error for such small values. Dissipation factor varies inversely with frequency and has the value to be determined by the equilibrium resistance. There is no evidence of any interfacial polarization.

Similar curves for a sintered glass bar are shown in Fig. 7. The 1 kc recovery curves, taken after equilibrium conditions are attained, show that, after the film breaks within 0.25 minute and raises surface resistance above 10 MMΩ, there are ionized water droplets on the surface, for capacitance and dissipation factor do not return to their original values for nearly 10 minutes.

The behavior of an L-4 grade steatite is shown in Fig. 8. Both capacitance and dissipation factor at 1 kc continue to rise up to the time of surface resistance equilibrium. Their equilibrium values

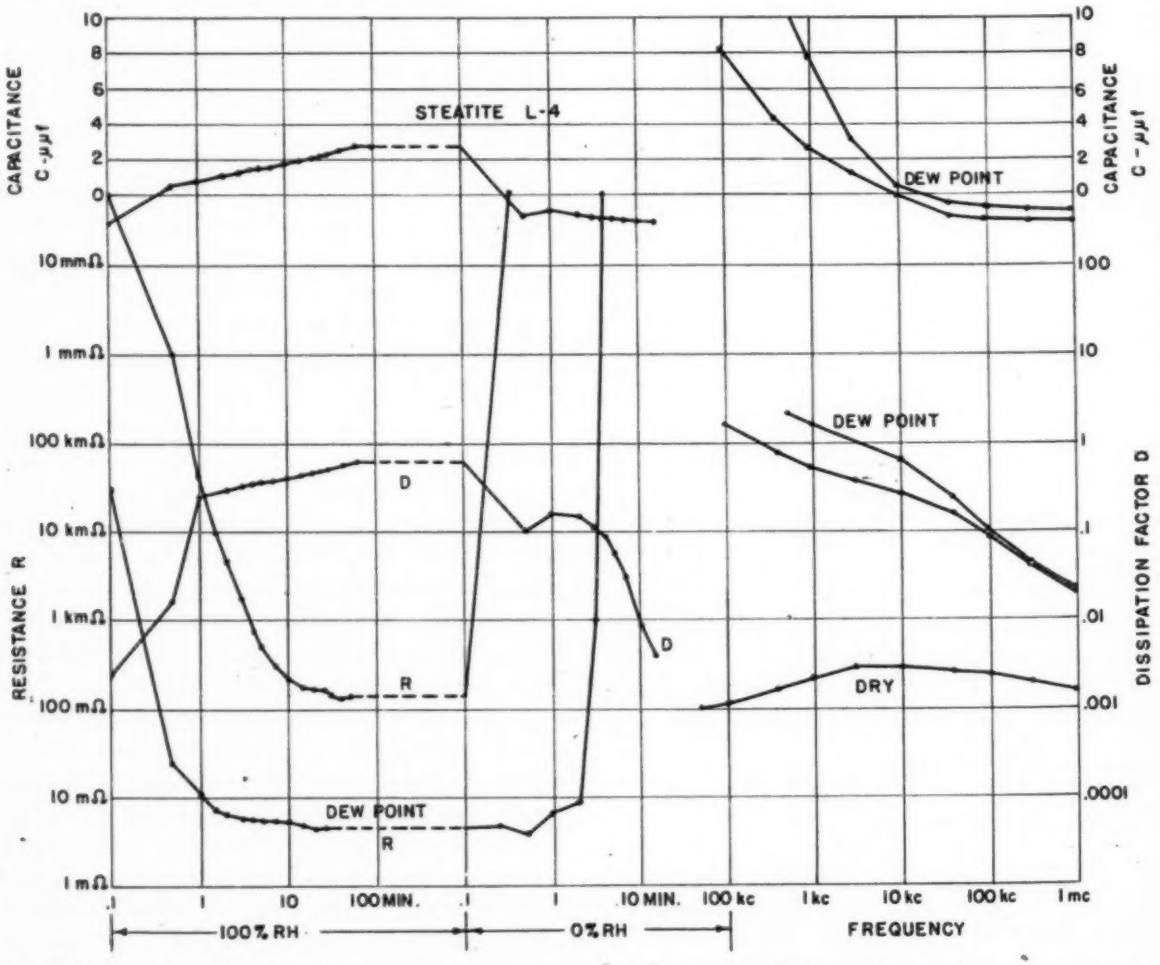

FIG. 8. Exposure, equilibrium, and recovery curves for material showing polarization at the interface of water film and dielectric. Also effect of dew-point condensation.

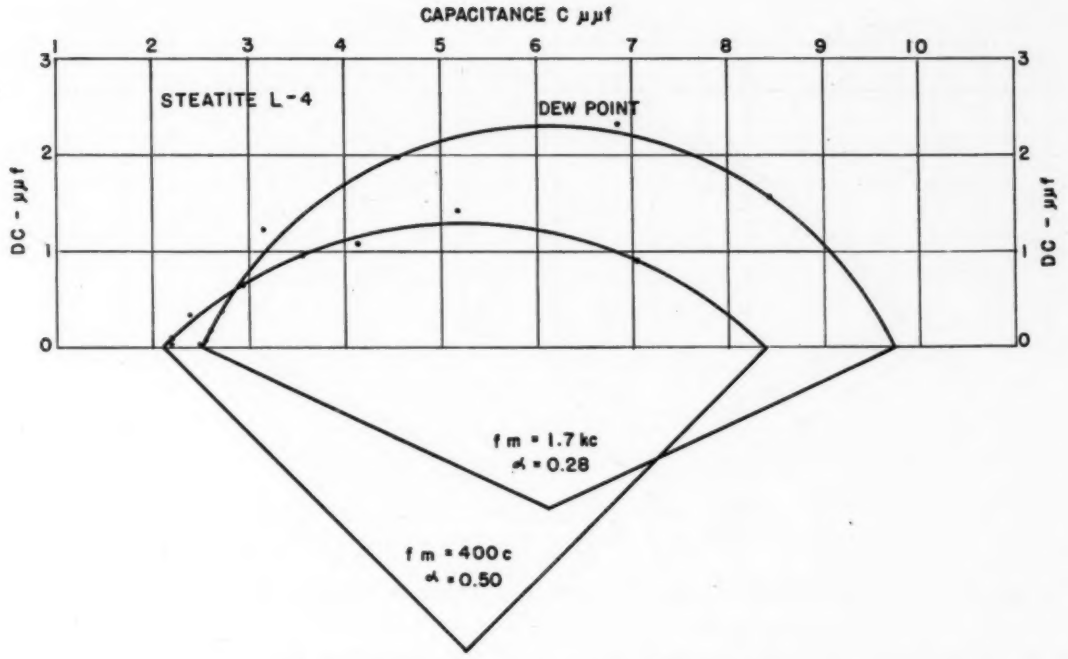

FIG. 9. Circular arcs for equilibrium data of Fig. 8.

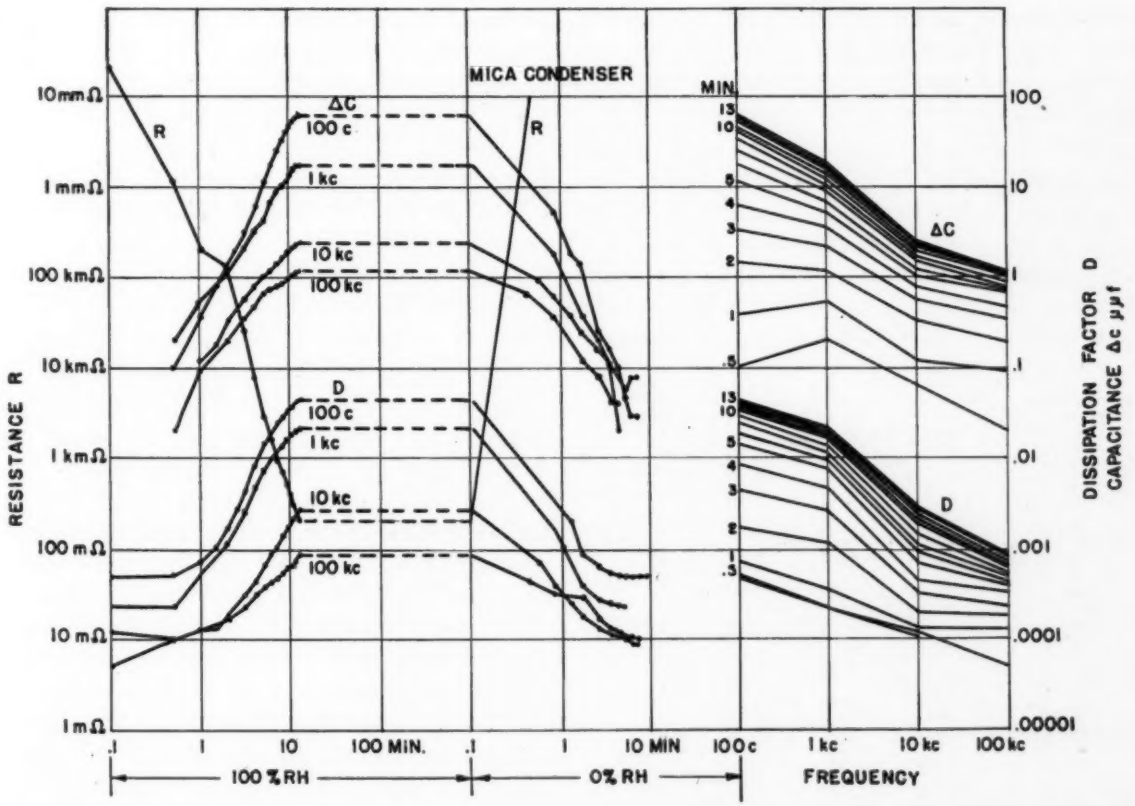

FIG. 10. (left) Exposure and recovery curves at four different frequencies plotted against time. (right) Exposure curves at one-minute intervals up to 13 minutes plotted against frequency.

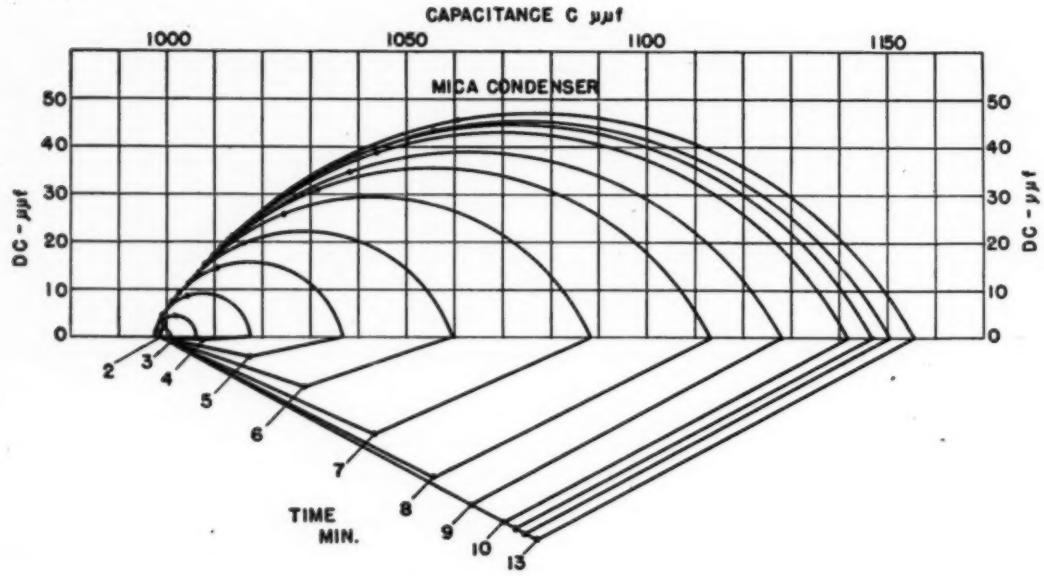

FIG. 11. Circular arcs for exposure curves at one-minute intervals.

at other frequencies definitely indicate interfacial polarization. Capacitance is no longer independent of frequency, but increases rapidly with decreasing frequency. Dissipation factor no longer decreases inversely with frequency, but changes more slowly. After subtracting the values of dissipation factor resulting from the equilibrium surface resistance, the circular arc plot[6] of the product DC of dissipation factor and capacitance against capacitance appears as shown in Fig. 9. This is an audiofrequency polarization with a relaxation frequency f_m of 400 c, a storage coefficient α of 0.50, and a change in capacitance ΔC of 6.18 $\mu\mu$f. Observations were also taken on the thicker film produced by dew-point condensation. Its circular arc plot as shown in Fig. 9 gives a higher relaxation frequency, 1.7 kc, a smaller storage coefficient, 0.28, and a slightly larger change in capacitance, 7.22 $\mu\mu$f. This indicates that the ion concentration is less in the thicker film, which is reasonable.

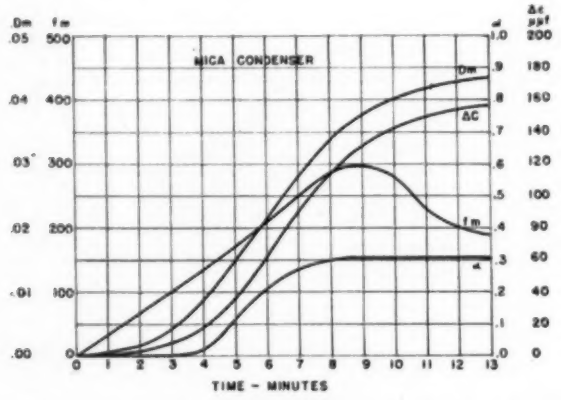

FIG. 12. Change of polarization parameters with time.

A more complete study of this type of interfacial polarization was made on an unprotected 1000 $\mu\mu$f mica condenser.[7] This condenser was exposed to 100 percent RH five times to obtain the resistance curve and the capacitance and dissipation factor curves at four different frequencies, as shown in Fig. 10. Only capacitances changes are given. The remarkable consistency of these successive exposures is shown by the fact that in the frequency plots at one-minute intervals no curves cross except those for the shortest times. After subtracting the effect of surface resistance the circular arc plots of Fig. 11 were obtained. There is an increase with time in all three polarization parameters, change in capacitance, relaxation frequency, and storage coefficient, the latter increasing from 0.0 to 0.31. This is the evidence which indicates that the film forms rapidly and then ion concentration slowly increases, for storage coefficient α can be zero (semicircle) only for dilute solutions. The

[6] K. S. Cole and R. H. Cole, J. Chem. Phys. **9**, 341 (1941).

[7] General Radio Type 505-F, uncased.

changes with time in the numerical values of the three parameters are shown in Fig. 12.

These a.c. measurements are far from complete, for they must be taken for most of the materials studied for d.c. leakage before broad conclusions can be drawn. It will be important to establish the order in which these materials are arranged in terms of either fractional change in capacitance or maximum dissipation factor and to determine the corresponding values of storage coefficient and relaxation frequency in order to set a frequency limit beyond which humidity has no appreciable effect.

ACKNOWLEDGMENT

The author is indebted to Mr. D. H. Chute for mounting the various materials and for carrying out most of the measurements for both resistance and capacitance and dissipation factor.

Thermal Polymerization of Drying Oils

H. E. Adams and P. O. Powers*

Armstrong Cork Company, Lancaster, Pennsylvania

A statistical analysis of the thermal polymerization of drying oils has been made, and equations have been derived which predict the amount of a specific polymer present as a function of the extent of reaction and the original composition of the oil. Several samples of oils have been heat bodied to test the validity of this analysis. Certain discrepancies are apparent. The presence of an intrapolymer is postulated to explain these discrepancies. Indirect evidence for the presence of such a compound is presented. Additional studies of the heat polymerization of drying oils have been made by conducting the polymerization in dilute solution. After the reaction has been carried out, the solvent is removed and the properties of the oils compared with oils similarly treated without solvent. It has been found that iodine values of the oils are substantially the same regardless of the concentration of oil, and depend only on the time and temperature of heating, but that the viscosity decreases with lower concentration of the oils. This behavior substantiates the formation of an intrapolymer. By using the values at various concentrations it may be possible to estimate the extent of intrapolymer formation in heat bodied oils.

IT is well known that drying oils such as linseed, tung, and soybean oils increase in body or viscosity when heated at elevated temperatures. This increase in viscosity is due to a chemical reaction between the unsaturated fatty acids present in the oils as glycerides. Various types and varying amounts of fatty acids account for the differences in reactivity and properties of the different oils. The vegetable oils are composed chiefly of glycerides of eighteen carbon atom fatty acids, while the fish oils contain, in addition to eighteen carbon atom fatty acids, fatty acids with twenty to twenty-six carbon atoms. These fatty acids contain from none to six double bonds and in some cases an hydroxyl group is attached to the chain. In most cases the double bonds are isolated, but conjugated double bonds do occur such as in eleostearic acid in tung oil. It has been observed that non-conjugated double bonds undergo a slow but progressive shift to the conjugated position at elevated temperatures.[1] Thus, a conjugated double bond system is postulated as a prerequisite for polymerization. Extensive work has been done on the polymerization of conjugated systems such as butadiene, isoprene, etc.[2] Vinylcyclohexene is obtained in the dimerization of butadiene by the addition of one mole-

* Present Address: Battelle Memorial Institute, Columbus, Ohio.

[1] T. F. Bradley and W. B. Johnston, Ind. Eng. Chem. **32**, 802 (1940); **33**, 86–89 (1941). T. F. Bradley and D. Richardson, *ibid.* **32**, 963 (1940). J. S. Brod, W. G. France, and W. L. Evans, *ibid.* **31**, 114 (1939).

[2] F. Hofmann and L. Tank, Zeits. f. angew. Chemie **25**, 1465 (1912). S. Lebedev and S. Sergienko, Comptes rendus Acad. Sci. U.S.S.R. **3**, 79 (1935). K. Alder and H. F. Rickert, Ber. d. d. Chem. Ges. **71B**, 373 (1938). G. S. Whitby and W. Gallay, Can. J. Research **6**, 280 (1932).

cule of butadiene in the 1–4 position to another molecule in the 1–2 position. This Diels-Alder reaction is taken as the mechanism of the polymerization that takes place during heat bodying of drying oils. It is possible that three or more fatty acids could combine. The formation of trimer fatty acids has been suggested,[3] but the extent of their formation in heat bodying has not been established. Since it is not the free fatty acid but the glyceride of the fatty acids which occurs in the drying oils, highly branched structures or molecules are formed during the heat bodying process.

COMPOSITION OF LINSEED OIL

It is fairly well established that linseed oil consists of glycerides of eighteen carbon atom acids and that the chief acids present are stearic, oleic, linoleic, and linolenic. Since the iodine value of linseed oil varies somewhat, the relative amounts of the various fatty acids must vary accordingly. Equations[4] have been proposed to correlate the iodine number with the composition of the oil. Two recent articles have studied the percentages of the various fatty acids in linseed oil by the determination of thiocyanate and iodine values of the oils and by determining the ultraviolet absorption of the alkali isomerized acids. The work of Mitchell, Kraybill, and Zscheile[5] has shown that estimates of the linolenic and linoleic acid content, by determining absorption at 2340 and 2680A after isomerization with alkali at 180°C in glycol, give good agreement with the Kaufman method, which depends on determination of the thiocyanogen value. Their estimate for a linseed oil having a Wijs iodine value of 180 is:

Linolenic acid	47 percent,
Linoleic	18 percent,
Oleic acid	29 percent,
Saturated acids	6 percent.

These results indicate a much higher content of oleic acid and a much lower content of linoleic acid than the prior estimates. This difference is rather large and would suggest a much lower degree of reactivity. Using the thiocyanogen value, Painter and Nesbitt[6] have examined samples of linseed oil varying in iodine value from 127 to 203. Saturated acids were determined by the Bertram method. They did not attempt to correlate the composition of the oils with their iodine values.

It is obvious that the saturated fatty acids cannot polymerize, and since oleic acid does not readily undergo polymerization, the acid distribution may be simplified by considering two types of acids, those that undergo polymerization and those that do not. Thus, oleic acid and the saturates would be considered as non-polymerizing acids (v), and linoleic acid and linolenic acid would constitute the polymerizing acids (u). The assumption that the linoleic acid group has the same reactivity as the linolenic acid group is highly questionable, but for the present it will be assumed to be true. This point will be discussed further, later in the article. According to the analysis of Mitchell, referred to above, linseed oil fatty acids would be comprised of 65 percent polymerizable acids and 35 percent non-polymerizable acids. If the fatty acids can be considered to be randomly distributed[7] in the glycerides, the relative amounts of the different types of glycerides are given by the following equation.

$$1=(u+v)^3=u^3+3u^2v+3uv^2+v^3. \qquad (1)$$

Thus, (u^3) is the fraction of glyceride molecules containing three polymerizing acids, ($3u^2v$) the fraction of glyceride molecules containing two polymerizing acids and one non-polymerizing acid, ($3uv^2$) the fraction of glyceride molecules containing one polymerizing acid and two non-polymerizing acids, and (v^3) is the fraction of glyceride molecules containing three non-polymerizing acids. Thus, the drying oils according to this analysis are composed of four types of molecules, trireactive (u^3), direactive ($3u^2v$), monoreactive ($3uv^2$), and zero-reactive (v^3). If the distribution is assumed to be random, the glyceride composition of some of the more im-

[3] J. C. Cowan, L. B. Falkenburg, and H. M. Teeter, Ind. Eng. Chem. Anal. Ed. **16**, 90 (1944). W. C. Ault, J. C. Cowan, J. P. Kass, and J. E. Jackson, Ind. Eng. Chem. **34**, 1120 (1942).

[4] P. O. Powers, Oil and Soap **22**, 52 (1945). E. P. Painter, *ibid.* **21**, 345 (1944). H. R. Sallons and G. D. Sinclair, Can. J. Research **22F**, 132 (1944).

[5] J. H. Mitchell, H. R. Kraybill, and F. P. Zscheile, Ind. Eng. Chem. Anal. Ed. **15**, 1 (1943).

[6] E. P. Painter and L. L. Nesbitt, Ind. Eng. Chem. Anal. Ed. **15**, 123 (1943).

[7] H. E. Longenecker, Chem. Rev. **29**, 201 (1941).

TABLE I. Glyceride composition of various drying oils.

Oil	u	v	u^3	$3u^2v$	$3uv^2$	v^3
Linseed oil	0.65	0.35	0.275	0.444	0.238	0.043
Cottonseed oil	0.43	0.57	0.082	0.323	0.416	0.180
Tung oil	0.79	0.21	0.496	0.384	0.100	0.009
Perilla oil	0.84	0.16	0.602	0.333	0.061	0.004
Oiticica oil	0.84	0.16	0.595	0.338	0.064	0.004
Soybean oil	0.61	0.39	0.227	0.436	0.278	0.059

portant drying oils are listed in Table I. The original fatty acid compositions are according to Mattil.[8]

Let the subscripts 100, 010, and 001 refer to trireactive, direactive, and monoreactive glycerides, respectively. Then the original mole fractions (N^0) and group fractions (M^0) of the different types of glyceride are given by the following equations. By group fraction is meant the fraction of reactive groups that is attached to the particular glyceride.

$$\left.\begin{aligned} N^0_{100} &= \frac{n^0_{100}}{n^0} = u^3 \\ N^0_{010} &= \frac{n^0_{010}}{n^0} = 3u^2v \\ N^0_{001} &= \frac{n^0_{001}}{n^0} = 3uv^2 \end{aligned}\right\}, \qquad (2)$$

$$\left.\begin{aligned} M^0_{100} &= \frac{3n^0_{100}}{m^0} = u^2 \\ M^0_{010} &= \frac{2n^0_{010}}{m^0} = 2uv \\ M^0_{001} &= \frac{n^0_{001}}{m^0} = v^2 \end{aligned}\right\}. \qquad (3)$$

The functionality (f) is defined as the average number of reactive groups per molecule. That is,

$$f = \frac{m^0}{n^0} = 3N^0_{100} + 2N^0_{010} + N^0_{001} = 3u. \qquad (4)$$

MECHANISM OF POLYMERIZATION

During heat bodying it is considered that these three types of glycerides combine to form polymers. It is fairly well established, although not definitely proven, that the bond between two fatty acids is a six-membered ring formed by the following mechanism.[9]

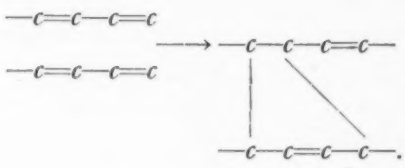

All the changes in physical properties are in accord with this mechanism, but they do not necessarily eliminate other mechanisms. Irrespective of the mechanism it is sufficient for present purposes to know that some sort of bond is formed between the reactive fatty acid groups.

The equations giving the relative amounts of the different types of polymers formed can be derived if the following assumptions are made, that during the polymerization two reactive groups disappear in the formation of one bond between two molecules, that the formation of a ring structure or intrapolymer is excluded, and finally, that all of the groups are equally reactive. The equivalence of linolenic and linoleic acid in the polymerization reaction has been previously discussed. The second assumption of the absence of ring formation is very doubtful due to the formation of highly branched structures. It is impossible to estimate the amount of ring formation. Consequently, it will be neglected for the present.

For the formation of a bond, it is necessary that two molecules collide in such a position for the reaction to take place. Thus, if we assume that the polymerization reaction is second order, the following differential equation for the instantaneous change of a definite polymer molecule is obtained.

$$\frac{dn_{abc}}{dt} = m^0 k \sum_{i=0}^{a}\sum_{j=0}^{b}\sum_{k=0}^{c} m_{ijk} m_{a-i,b-j,c-k} - m^0 k m_{abc} \sum_{i=0}^{\infty}\sum_{j=0}^{\infty}\sum_{k=0}^{\infty} m_{ijk}, \qquad (5)$$

[8] W. H. Mattil, Oil and Soap **21**, 197 (1944).

[9] C. P. A. Kappelmeier, Farben Ztg. **38**, 1018, 1077 (1933).

where n_{abc} is the number of molecules made from (a) trireactive glycerides, (b) direactive glycerides, and (c) monoreactive glycerides, and m_{abc} is the number of reactive groups attached to (abc) polymers. k is the specific rate constant. The first term of the right-hand side of Eq. (5) accounts for the synthesis of the (abc) polymer from all of the possible combinations of lower polymers, while the second term accounts for the disappearance of the (abc) polymer as it combines with other molecules to form higher polymers. Equation (5) may be expressed in terms of group fractions (M) and extent of reaction (p), thus eliminating the time factor, by means of the following equations

$$m = m^0(1-p), \tag{6}$$

$$dp/dt = m^0 k(1-p)^2, \tag{7}$$

$$M_{abc} = \frac{(a-c+2)n_{abc}}{m}. \tag{8}$$

Therefore,

$$\frac{d(M_{abc})}{dp} + \frac{(a-c+1)}{1-p} M_{abc} = \frac{(a-c+2)}{1-p} \sum_{i=0}^{a} \sum_{j=0}^{b} \sum_{k=0}^{c} M_{ijk} M_{a-i,b-j,c-k}. \tag{9}$$

The following equation is a solution of this linear differential equation

$$M_{abc} = K_{abc} p^{a+b+c-1}(1-p)^{a-c+1}, \tag{10}$$

where

$$K_{abc} = \frac{a-c+2}{2(a+b+c-1)} \sum_{i=0}^{a} \sum_{j=0}^{b} \sum_{k=0}^{c} K_{ijk} K_{a-i,b-j,c-k}, \tag{11}$$

and

$$k_{000} = 0,$$

$$k_{100} = M^0{}_{100},$$

$$k_{010} = M^0{}_{010},$$

$$k_{001} = M^0{}_{001}.$$

It is evident that (a) and (b) can have any value from 0 to ∞, while (c) can only assume values from 0 to $(a+2)$.

It has been found, by trial and error, that it is possible to solve the above recursion formula involving the constants. The following result is obtained.

$$K_{abc} = \frac{(2a+b)!}{(a-c+1)!} \frac{(M^0{}_{100})^a}{a!} \frac{(M^0{}_{010})^b}{b!} \frac{(M^0{}_{001})^c}{c!}. \tag{12}$$

Then the complete expression for the group fraction of an (abc) combination is given by

$$M_{abc} = \frac{(2a+b)!}{(a-c+1)!} \frac{(M^0{}_{100})^a}{a!} \frac{(M^0{}_{010})^b}{b!} \frac{(M^0{}_{001})^c}{c!} p^{a+b+c-1}(1-p)^{a-c+1}. \tag{13}$$

In addition the molecular weight on a number basis (A_n) and on a weight basis (A_w) are given by the following equations after the proper summations are made.

$$A_n = \frac{A_1}{1-\frac{f}{2}p}, \tag{14}$$

$$A_w = A_1\left(1+\frac{f_p}{1-(1+M^0{}_{100}-M^0{}_{001})p}\right). \tag{15}$$

The same method of attack may be extended to cover the polymerization of any mixture of other polyfunctional molecules. The differential equation and its solution follow.

$$\frac{d(M_{x_1\cdots x_k})}{dp}+\frac{(Y_{x_1\cdots x_k}-1)}{1-p}M_{x_1\cdots x_k}=\frac{Y_{x_1\cdots x_k}}{1-p}\sum_{i_1=0}^{x_1}\cdots\sum_{i_k=0}^{x_k}M_{i_1\cdots i_k}M_{(x_1-i_1)\cdots(x_k-i_k)}, \tag{16}$$

$$M_{x_1\cdots x_k}=\frac{(Z_{x_1\cdots x_k}-1+Y_{x_1\cdots x_k}-1)!}{(Y_{x_1\cdots x_k}-1)}\prod_{x_1}^{x_k}\frac{(M^0{}_{0\cdots1\cdots0})^{x_i}}{x_i!}p^{Z_{x_1\cdots x_k-1}}(1-p)^{Y_{x_1\cdots x_k-1}} \tag{17}$$

where

$$Z_{x_1\cdots x_k}=\sum_{i=1}^{k}x_i,$$

$$Y_{x_1\cdots x_k}=2+\sum_{i=1}^{k}(i-2)x_i.$$

$(Z_{x_1\cdots x_k})$ is the number of original molecules making up the $(x_1\cdots x_k)$ molecule and $(Y_{x_1\cdots x_k})$ is the number of reactive groups attached to the $(x_1\cdots x_k)$ polymer.

Likewise, the molecular weights are given by Eqs. (18) and (19)

$$A_n = \frac{A_1}{1-\frac{f}{2}p}, \tag{18}$$

$$A_w = A_1\left(1+\frac{f_p}{1-p(1+\sum_{i=1}^{k}(i-2)M^0{}_{0\cdots1\cdots0})}\right). \tag{19}$$

The fundamental Eqs. (13) and (19) are in agreement and substantiate the earlier work of Flory[10] and Stockmayer.[11]

EXPERIMENTAL PROCEDURE

In an effort to check the validity of this analysis several oils have been heat bodied. Three samples of linseed oil, one sample of linseed oil plus 1 percent litharge, one sample of soybean oil, and one sample of tung oil have been bodied under a vacuum or inert atmosphere. Samples were taken at various times of reaction, and physical constants such as viscosity, molecular weight, density, etc., determined. The results are shown in Figs. 1 to 6 as a function of time. Table II contains the data obtained for the tung oil and soybean oil, while the results for linseed oil are given in an earlier report.[12] Reference to this report should be made for methods of determining the physical constants.

The bodying of the soybean oil was stopped after it was discovered that the viscosity had

[10] P. J. Flory, J. Am. Chem. Soc. **63**, 3083, 3091, and 3096 (1941).

[11] W. H. Stockmayer, J. Chem. Phys. **11**, 45 (1943); **12**, 125 (1944).

[12] H. E. Adams and P. O. Powers, Ind. Eng. Chem. **36**, 1124 (1944).

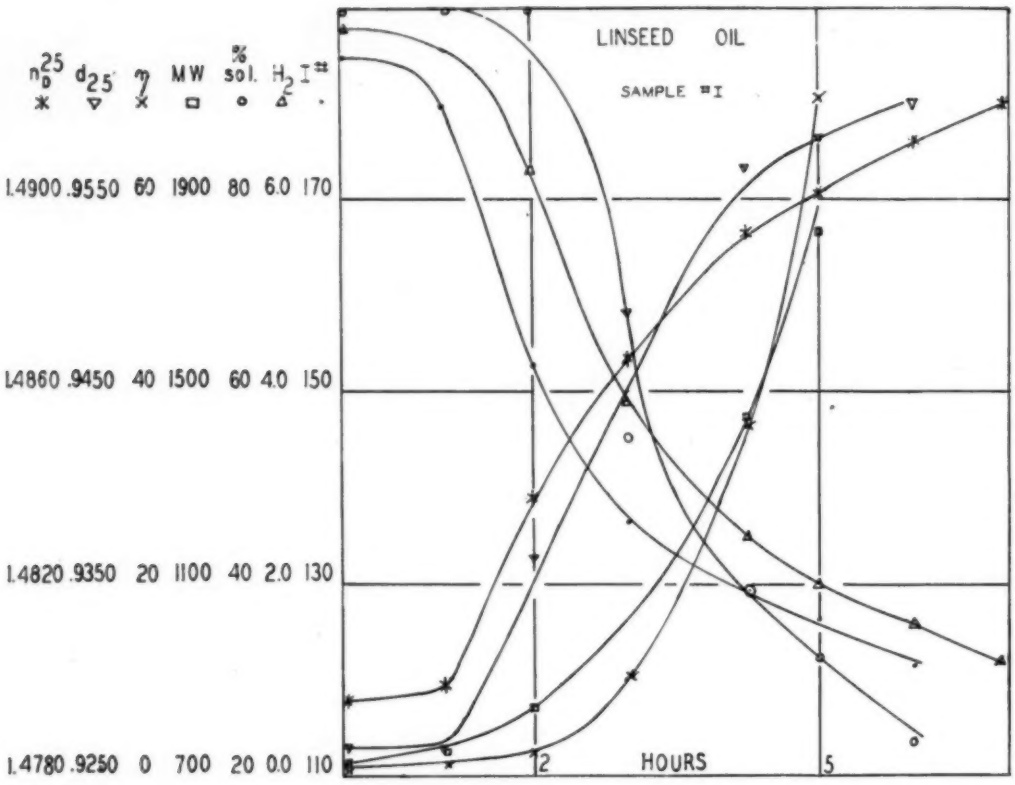
LINSEED OIL
SAMPLE #I
n_D^{25} d_{25} η MW % sol. H_2 I#
1.4900 .9550 60 1900 80 6.0 170
1.4860 .9450 40 1500 60 4.0 150
1.4820 .9350 20 1100 40 2.0 130
1.4780 .9250 0 700 20 0.0 110
2
HOURS
5

FIG. 1.

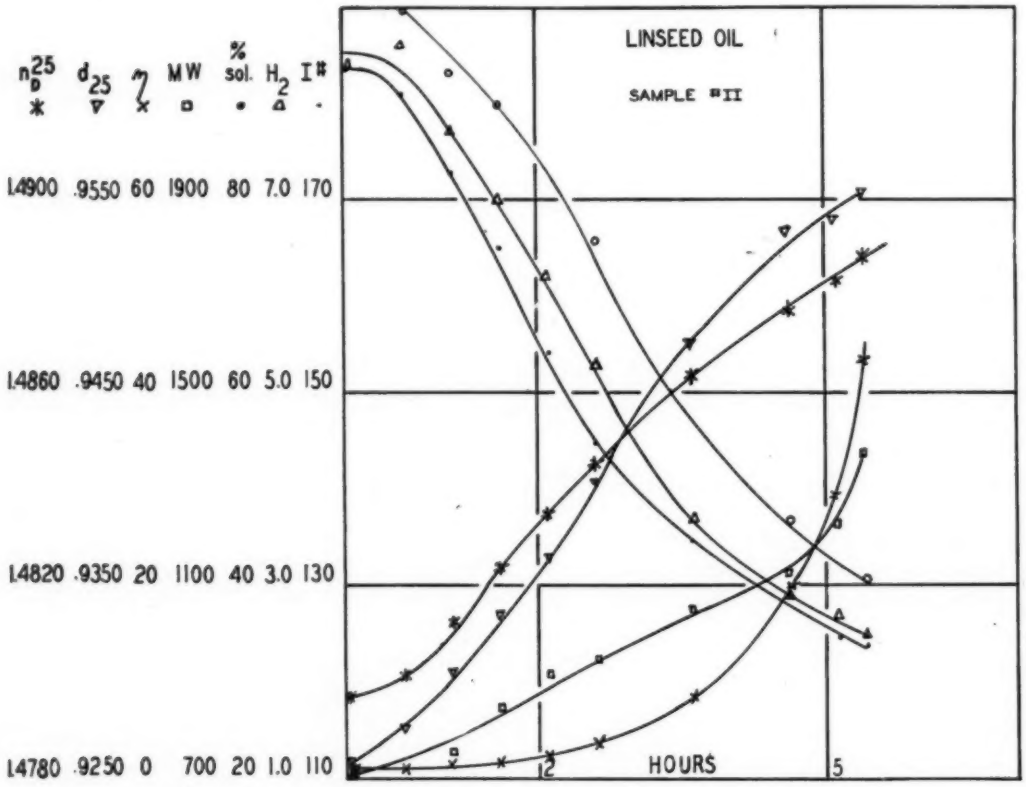
LINSEED OIL
SAMPLE #II
n_D^{25} d_{25} η MW % sol. H_2 I#
1.4900 .9550 60 1900 80 7.0 170
1.4860 .9450 40 1500 60 5.0 150
1.4820 .9350 20 1100 40 3.0 130
1.4780 .9250 0 700 20 1.0 110
2
HOURS
5

FIG. 2.

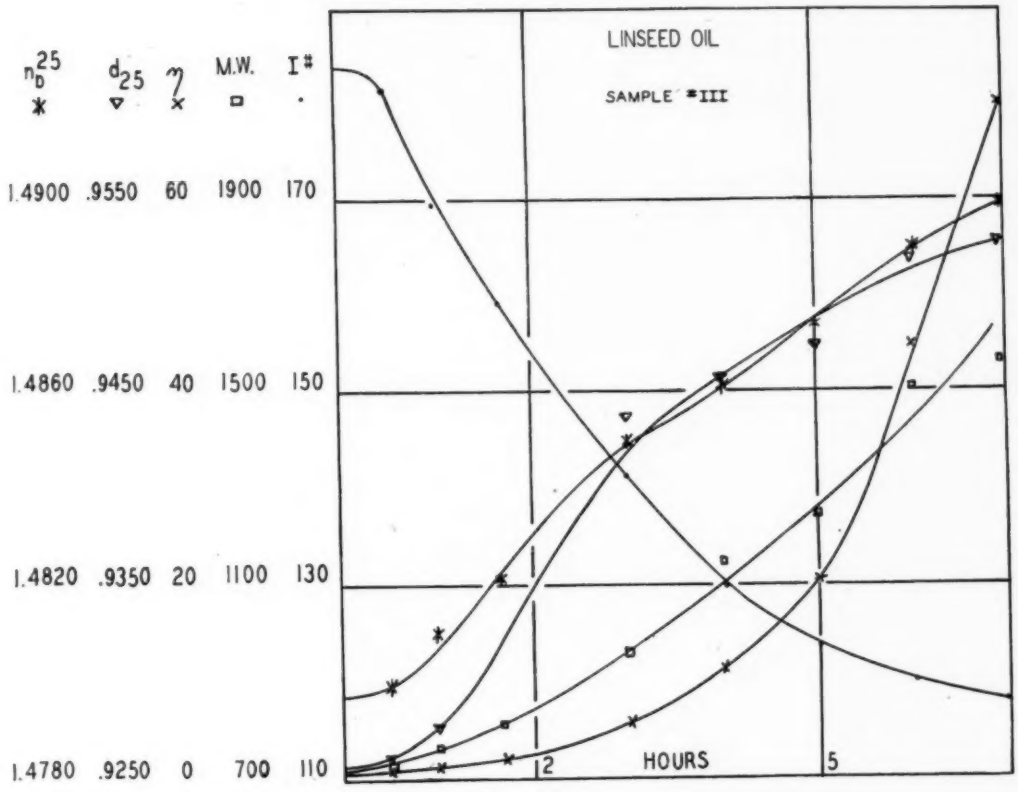
n_D^{25} d_{25} η M.W. I#
1.4900 .9550 60 1900 170
1.4860 .9450 40 1500 150
1.4820 .9350 20 1100 130
1.4780 .9250 0 700 110
LINSEED OIL
SAMPLE #III
2
HOURS
5

FIG. 3.

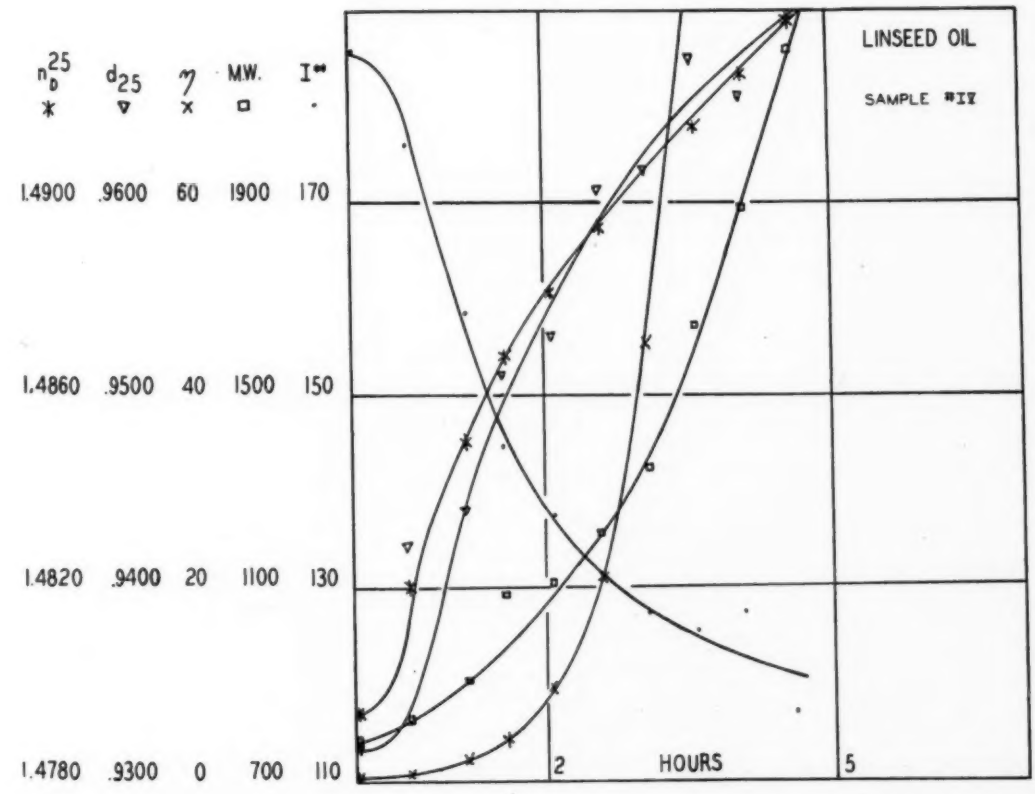
n_D^{25} d_{25} η M.W. I#
1.4900 .9600 60 1900 170
1.4860 .9500 40 1500 150
1.4820 .9400 20 1100 130
1.4780 .9300 0 700 110
LINSEED OIL
SAMPLE #II
2
HOURS
5

FIG. 4.

ACID ■	D_{25} Δ	η ×	M.W. □	I # ·
60	940	60	1300	130
40	930	40	1100	110
20	920	20	900	90
0	.910	0	700	70

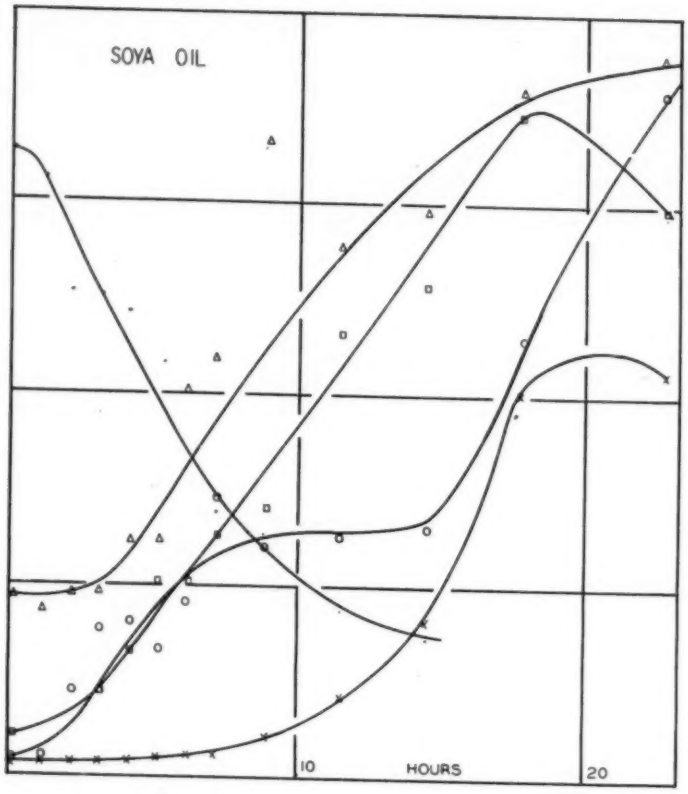

FIG. 5.

N_D^{25} ×	H_2 Δ	I #
1.534	9	170
1.530	7	150
1.526	5	130
1.522	3	110

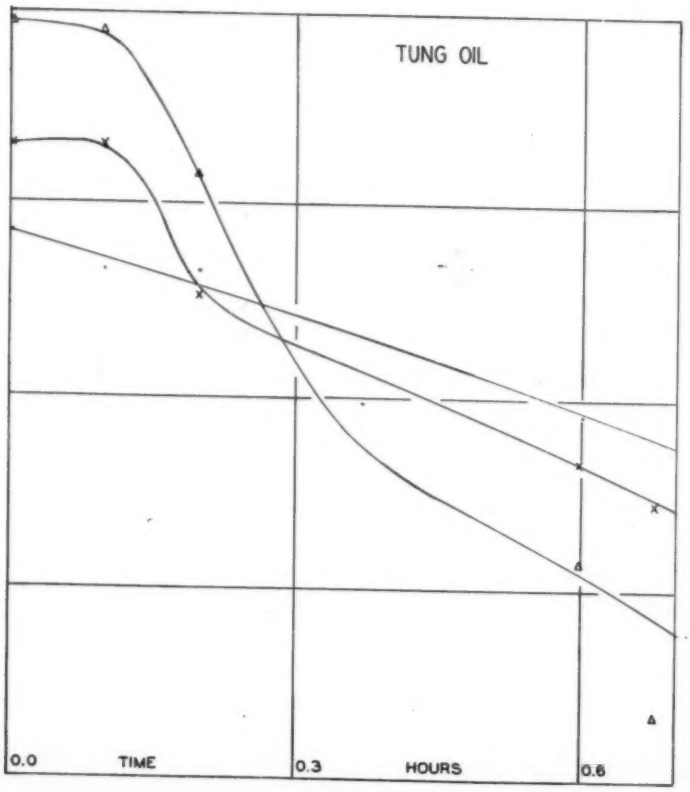

FIG. 6.

started to decrease and the acid number to increase greatly, showing that the glycerides were being hydrolyzed.

During the heat bodying the temperature of the reaction was controlled manually by means of a ring burner. Because of the extremely high temperature of 305°C it was difficult to maintain an entirely constant temperature. However, the maximum variation was seldom over two degrees.

DISCUSSION OF RESULTS

Rate of Reaction

Since the iodine number may be accurately determined and measures the unsaturation present in bodied oils, the values have been used to measure the extent of the combination of fatty acid groups (p). Since the loss of one double bond per fatty acid chain is equivalent to a decrease of 86.6 in iodine number, the actual decrease divided by 86.6 indicates the extent of reaction. Consequently, $(1-p)$ is a measure of the remaining double bonds or the reactivity left. Since it is postulated that in the disappearance of a double bond two fatty acid chains are bonded together through a six-membered ring, the rate of disappearance of unsaturation should vary as the

TABLE II.

Soybean oil bodied at 305°C under nitrogen

Sample No.	Time hr.	Density	Viscosity sec.	Iodine No.	Mole weight	Acid No.
V-1	0	0.9197	1.3	135.2	746	2.0
-2	1.167	0.9188	1.3	132.4	571	2.3
-3	2.167	0.9198	1.4	120.6	572	9.4
-4	3.167	0.9198	1.7	120.3	792	15.7
-5	4.167	0.9226	1.9	117.1	834	16.5
-6	5.167	0.9226	2.1	113.0	902	13.3
-7	6.167	0.9304	2.4	99.5	903	18.3
-8	7.167	0.9320	2.6	97.9	956	29.2
-9	8.167	0.9433	4.6	95.5	984	24.5
-10	11.417	0.9379	8.7	87.6	1165	25.4
-11	14.417	0.9399	16.5	85.0	1219	26.4
-12	17.750	0.9461	40.6	—	1395	46.0
-13	22.750	0.9479	42.9	—	1299	72.0

Tung oil bodied at 225°C under vacuum

Sample No.	Time hr.	Refractive index	Iodine No.	H_2 absorption lb.
VI-1	0.0	1.5352	167	10.9
-2	0.1	1.5351	163	10.8
-3	0.2	1.5321	163	9.3
-4	0.6	1.5287	148	5.3
-5	0.68	1.5278	147	3.7
-6	0.70 (gel)	—	—	2.5

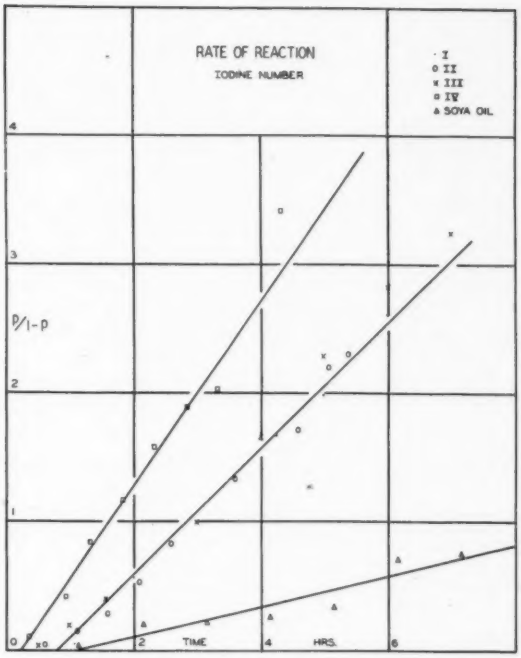

FIG. 7.

second power of the remaining reactivity. That is

$$dp/dt = k(1-p)^2, \qquad (20)$$

where k is the second-order rate constant. Integration of this equation gives

$$p/(1-p) = kt. \qquad (21)$$

In Fig. 7 $(p/1-p)$ has been plotted against the time (t) for the linseed oil and soybean oil samples. Because of the high amount of conjugation present in tung oil, Wijs iodine numbers do not give a true indication of the change in unsaturation. Consequently, these results have not been included in this graph. The results clearly indicate that the disappearance of unsaturation as indicated by the iodine number is a second-order reaction. The three linseed oil samples have the same rate constant of $k=0.49$, while the presence of 1 percent litharge increases this rate constant to $k=0.73$. Soybean oil has a much smaller constant of $k=0.40$.

Mattiello[13] has bodied linseed oil at three different temperatures and determined the resulting changes in the various physical properties. With these data the extents of reaction have been

[13] J. J. Mattiello, *Protective and Decorative Coatings* (John Wiley and Sons, Inc., New York, 1943), Vol. III, p. 50.

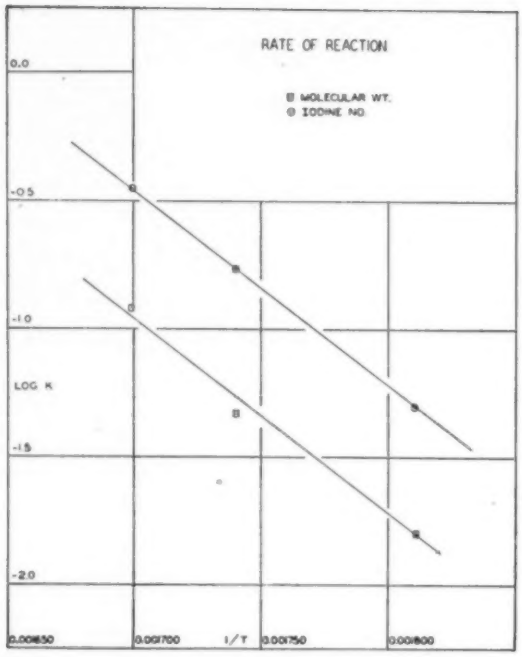

FIG. 8.

calculated from the change in iodine number and change in molecular weight. Straight lines were obtained when $(p/1-p)$ obtained from the change in iodine number and (p) as calculated from the molecular weight were plotted against time. Two parallel lines were obtained when the logarithm of the respective rate constants was plotted against the reciprocal of the absolute temperature. As shown in Fig. 8 this gave a value of 36.5 kcal. for the activation energy, as obtained from both the iodine value change and the molecular weight change. The value of 36.5 kcal. for the energy of activation is in good agreement with the estimate of the energy change (34.4 kcal.) involved in the formation of the six-membered ring as determined from the bond energies.[14]

Viscosity

An unsuccessful attempt has been made to obtain a relationship between the viscosity and molecular weight by means of the above equations. Flory's[15] equation, which indicates that the logarithm of the viscosity is a linear function of the square root of the molecular weight on a weight basis, does not hold for the bodied oils. A possible explanation is that the linseed oil polymer is highly branched, while Flory's equation may only be true for linear polymers.

H. Eyring[16] has developed a theory of viscous flow based on reaction kinetics. Viscous flow in liquids takes place by the movement of molecules into "holes" in the liquid which in turn is governed by an energy barrier ΔE or energy of activation. This energy of activation has been found to be roughly equal to $\frac{1}{4}$ the molar heat of vaporization, consequently, it has been possible to estimate the number of molecules comprising a segment of flow. Flory[15] in his work with polyesters has shown that the energy of activation is independent of molecular weight. Therefore, the segment of flow is constant. There are about 28–34 chain atoms per unit of flow.

The viscosities of heat bodied linseed oil at several stages of reaction have been measured over the temperature range of 30°C to 75°C by means of Gardner-Holt viscosity tubes. The temperature of the bath was maintained constant

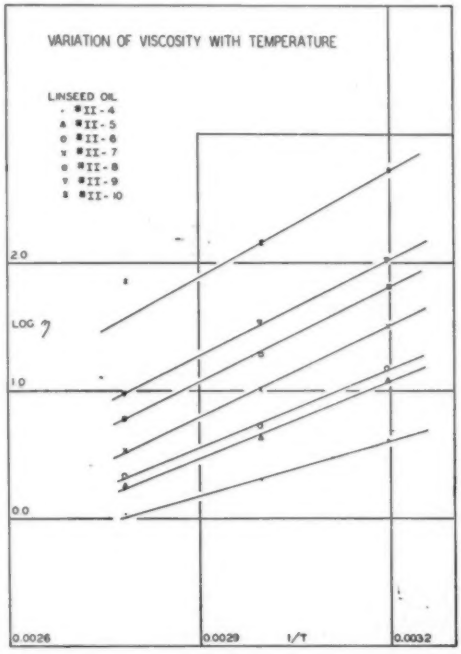

FIG. 9.

[14] L. Pauling, *Nature of the Chemical Bond* (Cornell University Press, Ithaca, 1940).
[15] P. J. Flory, J. Am. Chem. Soc. **62**, 1057 (1940).
[16] R. H. Ewell and H. J. Eyring, J. Chem. Phys. **5**, 726 (1937). H. Eyring, *ibid.* **9**, 268 (1941). W. Kauzmann and H. Eyring, J. Am. Chem. Soc. **62**, 3113 (1940).

to ±0.5°C. The results are listed in Table III and plotted in Fig. 9. A straight line is obtained when the logarithm of the viscosity is plotted against the reciprocal of the absolute temperature.

It is apparent from Fig. 9 that the slope of the various lines is not constant but increases with increasing molecular weight or viscosity. The energy barrier calculated from the individual slopes is plotted as a function of the extent of reaction as calculated from the change in iodine number and molecular weight, in Fig. 10, and the data are assembled in Table IV. A linear relationship exists between the extent of reaction and the energy of activation in contrast to the result of Flory, who found the energy of activation independent of the extent of reaction in his work on polyesters. The answer to this discrepancy lies in the fact that Flory prepared only linear polyesters, and consequently, the shape of the molecule would change only in length as the polymerization proceeded. In the case of linseed oil, a highly branched molecule would be produced by polymerization. Since the distance between branches in the linseed oil polymer is of the same order of magnitude as the segment of flow, it is logical that this branched structure would increase the unit of flow.

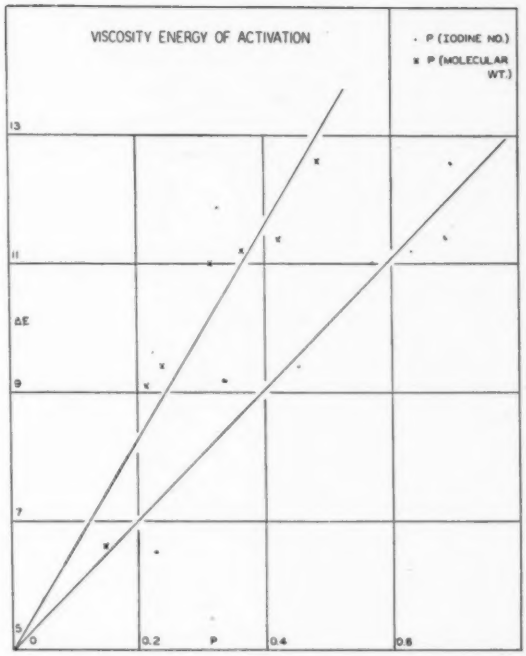

FIG. 10.

INTERMEDIATE COMPOUND FORMATION

The results as shown in Figs. 1–6 are in good agreement with the reported changes in properties[13] of drying oils on heat bodying. Linseed oil and soybean oil give analogous results in contrast to tung oil. Tung oil contains a high proportion of conjugated fatty acids which in a large measure accounts for its greater reactivity. For both soybean oil and linseed oil, the iodine number, hydrogen absorption, and percent soluble in acetone decrease rapidly at the beginning of the reaction and tend to approach a constant value at the later stages, while the density and refractive index increase rapidly at the start and then level off. On the other hand, the viscosity and molecular weight experienced relatively little change at the beginning and increased very rapidly at the later stage.

If (p) the extent of reaction is calculated from both the iodine number and molecular weight, different values are obtained from the two properties. To explain this discrepancy the presence of an intrapolymer has been postulated. This idea has been suggested by several other investigators.[17] An intrapolymer consists of either a

TABLE III. Temperature coefficient of viscosity of heat bodied linseed oil sample No. II.

Number	Logarithm of viscosity 30°C	50°C	75°C
II-4	0.623	0.301	0.041
-5	1.076	0.634	0.256
-6	1.170	0.732	0.322
-7	1.510	1.013	0.544
-8	1.808	1.292	0.792
-9	2.030	1.525	0.977
-10	2.706	2.154	1.846

TABLE IV. Viscous energy of activation.

Number	$\bar{p}$ Iodine No.	$\bar{p}$ Molecular wt.	ΔE kcal.
II-4	0.223	0.150	6.6
-5	0.346	0.216	9.1
-6	0.454	0.240	9.4
-7	0.570	0.316	11.0
-8	0.631	0.366	11.2
-9	0.688	0.423	11.4
-10	0.697	0.485	12.6

[17] T. F. Bradley, Ind. Eng. Chem. **30**, 689 (1938). A. Schwarcman, Oil and Soap **21**, 204 (1944).

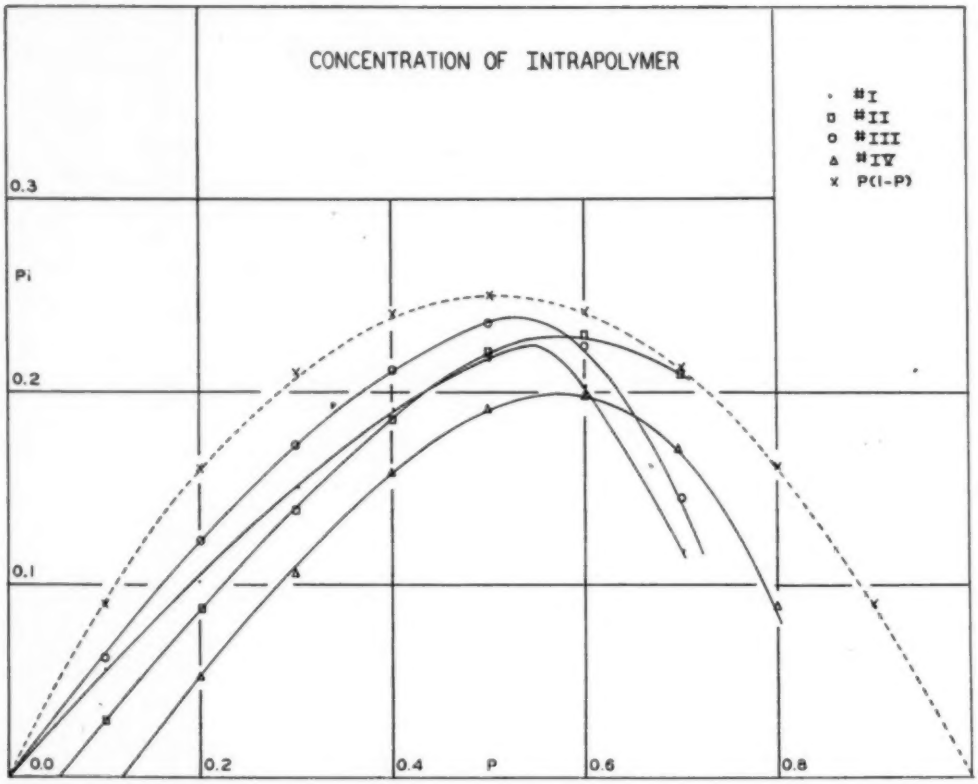

FIG. 11.

monomer glyceride which has two of its fatty acid groups joined together or a polymer that contains a ring. Figure 11 shows the magnitude of this difference between the iodine number and molecular weight changes as ordinate and the extent of the reaction as calculated from the iodine number as abscissa. The fact that the concentration of the intrapolymer reaches a maximum at about $p=\frac{1}{2}$, and then decreases, indicates that most of the ring formation is on the monomers. Thus, the intrapolymer is being formed simultaneously with the interpolymer (bonds between fatty acid groups on different glyceride molecules) and at the same time the intrapolymer is continually being changed to an interpolymer by ester interchange which occurs readily at the temperature of heat bodying.

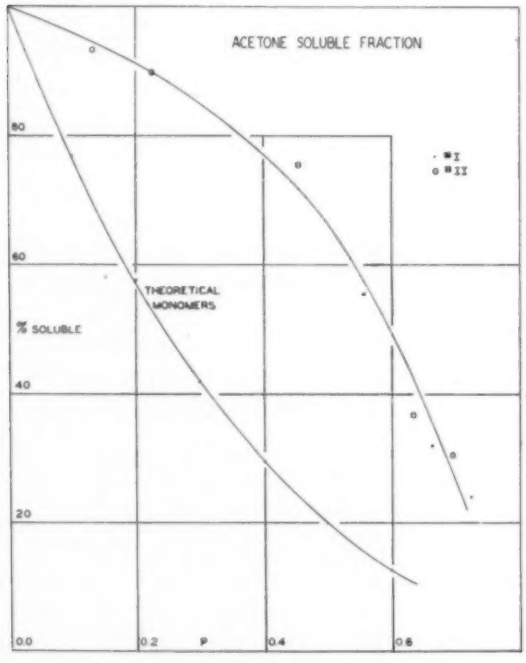

FIG. 12.

The dotted curve in Fig. 11 is given by the equation $p(1-p)$.

Earlier, the assumption was made that the reactive groups all had the same reactivity, that is, both linolenic and linoleic acids were capable of forming only one bond between the glycerides. However, the presence of trimer and higher fatty acids has been reported in the hydrolyzed products of heat bodied oils. This would indicate that one

of the fatty acids, preferably the linolenic acid, was capable of forming more than one bond which would impart a higher functionality to the oil than used in this work. This effect would reduce the magnitude of the difference between the iodine number and molecular weight but would not change materially the shape of the difference curve.

Figure 12 contains a plot of the percentage of oil soluble in acetone against the extent of the reaction as calculated from the iodine number. This is to be compared with the theoretical amount of monomer predicted by Eq. (13). It is assumed that only monomeric material dissolves in the acetone, which fact has been roughly checked experimentally. The results are vitiated somewhat by the mutual solubility effect which has a tendency to dissolve higher molecular weight material and by the difficulty experienced in effecting a separation between two phases. However, at high extents of reaction the amount of acetone soluble material reaches the weight percent of monomers predicted by the theory. This behavior is in agreement with the postulation of the formation of an intermediate compound having a lower iodine number but the same molecular weight as the monomer.

Stockmayer[18] has measured the gel points of the pentaerythritol-adipic acid system in the presence of various quantities of an inert solvent to prove ring formation. Ring formation should be more prevalent at higher dilutions because of the reduced probability of forming a bond between the different molecules. This should increase the ratio of intrapolymer formation to interpolymer formation. Stockmayer extrapolated the results to a fictitious infinite concentration to obtain a value for the extent of reaction free from ring formation and obtained excellent agreement with the theoretical value.

A sample of linseed oil in 50 percent xylene solution and a sample of pure linseed oil have been bodied at 300°C. Physical properties of the resultant bodied oils have been obtained. The iodine numbers of the two samples were identical while the molecular weight and viscosity of the oil bodied in solution were less than those for the oil not bodied in solution, which would indicate additional ring formation in the solution.

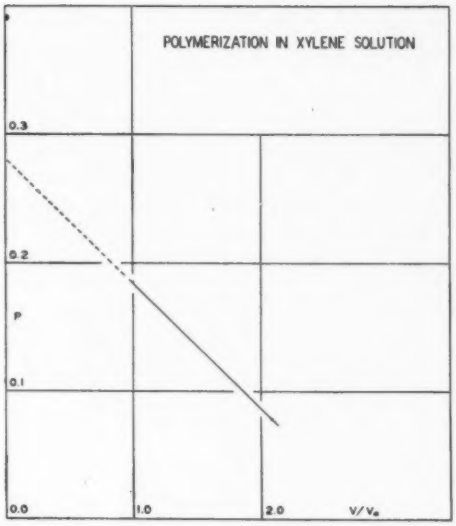

FIG. 13.

Figure 13 shows the extent of reaction as calculated from the molecular weight plotted against the ratio (V/V_0) where (V) is the specific volume of the solution and (V_0) the specific volume of the oil. If one assumes that the points fall on a straight line, a value for the extent of reaction at infinite concentration of $p=0.286$ is obtained. This is to be compared with a value of $p=0.392$ obtained from the iodine number. These results may be within experimental error. More data are necessary to determine whether the extrapolation should be a straight line. Additional work is planned to further study this method.

ACKNOWLEDGMENT

The assistance of Miss Helen I. Yeager, who prepared the graphs, is gratefully acknowledged.

[18] W. H. Stockmayer, *Advancing Fronts in Chemistry*, Edited by S. B. Twiss (Reinhold Publishing Corporation, New York, 1945), Vol. 1, p. 70.

Electrostatic and Tensile Properties of Rubber and GR-S at Elevated Temperatures

R. S. Havenhill, H. C. O'Brien, and J. J. Rankin
Research Laboratories, St. Joseph Lead Company, Josephtown, Pennsylvania

This paper describes a new apparatus for measuring electrostatic contact potentials on various materials at elevated temperatures. In this apparatus, the electrostatic charge, acquired by rolling a steel ball down the surface of a rubber test specimen on a heated inclined plane, is measured when the ball drops into the cup of a suitable measuring device such as our electrostatic modulator. With this instrument the contact potentials of both rubber and GR-S was found to become highly negative at elevated temperatures. This apparent "boiling off" of electrons and resultant disruption of electrostatic attractive forces within the material is much greater for GR-S than for rubber and probably accounts for the much greater decrease in tensile of GR-S over rubber at elevated temperatures, and is further confirmation of the electrostatic contact potential theory of reinforcement. By the further application of this theory suitably dispersed compounding materials, which are in effect highly positive at elevated temperatures such as certain proteins, finely divided silica and sodium silicate, have been found to increase substantially the hot tensile strengths of GR-S compounds.

IN a previous paper[1] a new apparatus was described for measuring the electrostatic contact potential of rubber and GR-S compounds, and a correlation of tensile strength and electrostatic contact potential was observed. This work resulted in the formulation of an "Electrostatic Contact Potential Theory of Reinforcement" in which reinforcement is explained on the basis of electrical contact potentials and resultant electrostatic attractive forces set up between the rubber and the reinforcing agents. For example, when a material which has a (+) positive electrostatic charge such as zinc oxide is added to rubber which has a (−) negative charge, strong electrostatic attractive forces are set up between the zinc oxide and the rubber and give rise to reinforcement. Now since (+) and (−) charges tend to neutralize each other, the electrostatic contact potential or electrical charge on the resulting stock should be more positive (less negative) than it was prior to the addition of the zinc oxide. This was found to be the case; and in general, the more positive the stock, the higher the tensile strength.

On the basis of this theory, we would predict that rubber compounds when heated would become highly negative which would indicate a low hot tensile strength. This was found to be the case.

It is the purpose of this paper to describe a new apparatus for measuring contact potentials at elevated temperatures and to point out that the contact potential of both rubber and GR-S compounds becomes highly negative at 212°F. This increase in negative potential, which may be a "boiling off" of electrons and resultant disruption of electrostatic attractive forces within the material, is much greater for GR-S than for rubber, and probably accounts in part for the much greater decrease in tensile of GR-S over rubber at elevated temperatures and is further confirmation of the electrostatic contact potential theory of reinforcement.

By the application of this theory, materials which maintain their highly positive charge at elevated temperatures should make the GR-S stocks more positive, prevent the release of electrons and increase the hot tensile strengths. This was found to be the case; and certain materials such as proteins, finely divided silica and sodium silicate when added as water dispersions to GR-S latex gave products having considerably improved tensiles at elevated temperatures.

HIGH TEMPERATURE CONTACT POTENTIAL APPARATUS

To measure contact potentials at elevated temperatures, the rubber test specimen must be heated to the desired temperature on an electrically insulated surface, momentarily contacted with a cold reference surface (preferably polished steel), and instantly separated therefrom. The electrical charge or contact potential then can be measured on either the rubber test specimen or

[1] R. S. Havenhill, H. C. O'Brien, and J. J. Rankin, J. App. Phys. 15, 731–740 (1944).

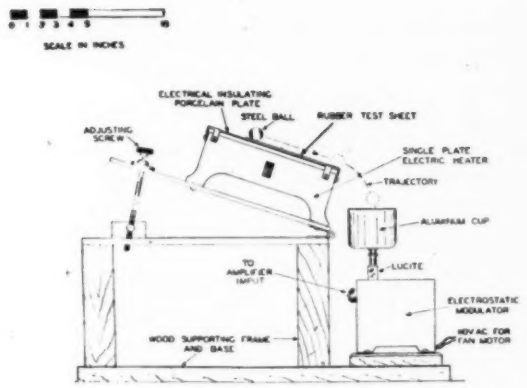

FIG. 1. Rolling ball contact potential apparatus.

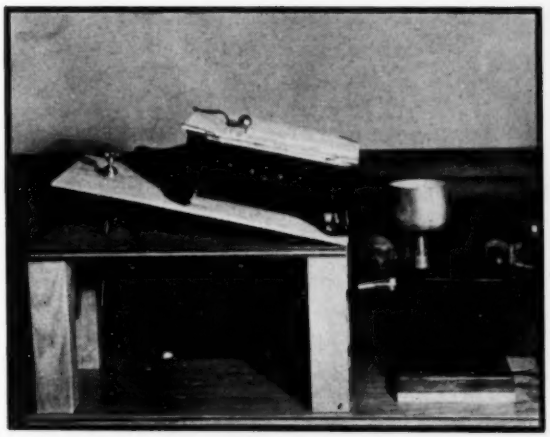

FIG. 2. Rolling ball contact potential apparatus.

on the standard reference contacting surface as the charges are equal and opposite. In our previous apparatus,[1] an insulated steel plunger contacted the test specimen, and the charge was measured on the test specimen which was mounted in a sample holder built into the electrostatic modulator. In this apparatus, it is difficult to build the electrical heater around the sample and provide adequate electrical shielding to prevent the hot a.c. electrical fields around the heater from being picked up on the grid of the audio amplifier. Furthermore, the charged plunger should be out of the test specimen's high temperature electrostatic field when measurements are made. The modulator unit should be isolated from the hot electrostatic field around the sample. To take care of these difficulties, a new apparatus was designed.

ROLLING BALL CONTACT POTENTIAL APPARATUS

In this apparatus (see Fig. 1 and Fig. 2), the electrostatic charge, acquired by rolling a steel ball down the surface of a rubber test specimen on a heated inclined plane, is measured when the ball drops into the cup of a suitable measuring device, such as our electrostatic modulator.

The electrostatic modulator (see Fig. 3) was described completely in our previous paper.[1] Briefly, it consists of a motor-driven fan which cuts the electrostatic field produced by the charged sample and converts it into an alternating-current voltage which easily is amplified and measured by the associated audiofrequency amplifier and built-in output meter. The electrostatic modulator and amplifier were calibrated with an adjustable d.c. high voltage power supply. The power supply leads were attached to the modulator cup and chassis. Amplifier output meter readings were plotted against input volts from the d.c. power supply. The contact potential values reported are all in terms of these input volts. These contact potential values are not the actual contact potentials since they depend on the capacity of sample, capacity of modulator system, and a number of other factors; however, they are proportional to the actual contact potentials of the rubber test specimens.

With this apparatus, the test specimen is both shielded and electrically insulated from the heater by means of the porcelain enameled steel top plate. The charged steel ball which contacts the specimen is isolated from electromagnetic and electrostatic fields when measurements of its charge are made in the shielded electrostatic modulator unit. While this apparatus has a number of advantages over the plunger type apparatus, for high temperature measurements, it also has some disadvantages. The contact area and velocity of the ball as it leaves the sample are not constant for all samples. For example, a soft stock will have a greater contact area than a hard one and a stock with a tacky surface will retard the velocity of the ball which affects the speed of separation of the ball from the test specimen. Since both of these factors affect the contact potential values, they must be taken into account in testing unknown compounds. For similar compounds, these differences usually do not exceed 10 percent error. The relative contact area can be estimated approximately by

FIG. 3. Electrostatic modulator with audio amplifier and output meter.

coating the steel ball with "fingerprint" ink and measuring the length and width of the black streak thus produced. The relative velocity of the ball as it leaves the sample can be estimated from its trajectory. The greater the velocity of the ball, the greater will be the horizontal range on the trajectory curve. This distance can be easily measured from the imprint of the ball on carbon over white paper.

MECHANICS OF ROLLING BALL CONTACT POTENTIAL APPARATUS

The mechanics of the rolling ball apparatus along with the derivation of the formula relating horizontal range (S) to velocity (V) are of theoretical interest and have been calculated by L. E. Carlson of our Research Laboratories as follows. Refer to Fig. 4.

1. Total Area of Contact

Length of Streak = 6 inches
Width of Streak = 1/16 inch
Area = $6 \times 1/16 = .375$ sq. in.

2. Pressure

Weight of ball = .0544 lb.
Diameter of ball = 23/32" = .718 inch
Diameter of contact = 1/16"
Instantaneous area of contact = $(1/32)^2\pi$
Pressure = $.0544/(1/32)^2\pi = 17.8$ lb./sq. in.

3. Velocity

Assume that potential energy of ball at top of incline is converted into rotational and translational kinetic energy by the time it reaches the bottom of the incline of height (h). Thus:

$$mgh = \tfrac{1}{2}mV^2 + \tfrac{1}{2}IW^2.$$

Substituting values of I and W the energy equation reduces to

$$mgh = \tfrac{1}{2}mV^2 + \tfrac{1}{5}mV^2,$$

$$V = \left(\frac{10gh}{7}\right)^{\frac{1}{2}},$$

$$V = \left(10 \times 32.2 \times \frac{.104}{7}\right)^{\frac{1}{2}} = 2.19 \text{ ft./sec.}$$

m = mass of ball,
h = height of incline (.104'),
g = acceleration of gravity,
V = translational velocity (at bottom of incline) parallel to it,
I = moment of inertia,
$= \frac{2}{5}mr^2$ where r is radius of ball,
W = rotational velocity
$= V/r$.

V is the maximum velocity obtainable, assuming the ball rolls and does not slide. Actually, tackiness of the surface and indentation of the surface slow the ball somewhat.

The following is a means of determining actual velocity from horizontal range which is the horizontal distance the ball moves while in the air.

RELATION OF VELOCITY TO DISTANCE (S)

Assuming the ball starts the trajectory path with a velocity V and travels the horizontal distance (S) and the vertical distance .359 ft. in time t, the following equations of motion may be set up.

$$.359 = \tfrac{1}{2}gt^2 + V \sin 12°t,$$
$$S = V \cos 12°t.$$

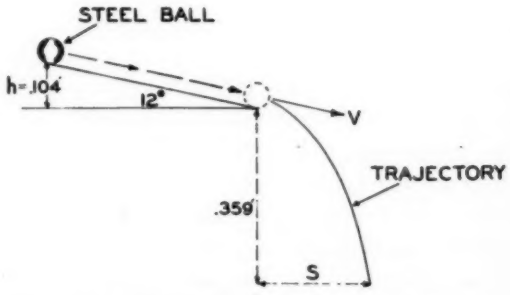

FIG. 4. Mechanics diagram of rolling ball apparatus.

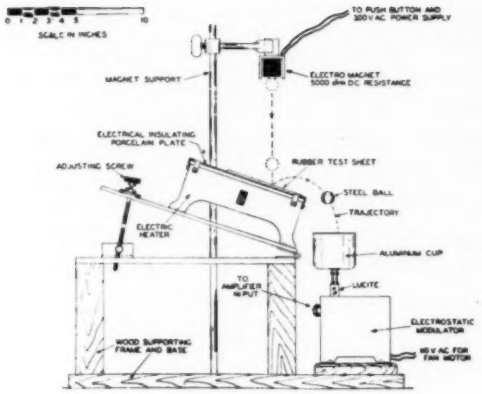

FIG. 5. Bouncing ball contact potential apparatus.

Eliminating t and solving for V,

$$V=\frac{4.11\times S}{(.359-.21265S)^{\frac{1}{2}}}\text{ ft./sec.}$$

Since S can be measured experimentally, V can be calculated using the above formula.

BOUNCING BALL CONTACT POTENTIAL APPARATUS

In order to secure a more intimate contact between the steel ball and the test specimen, the "bouncing ball" type apparatus was designed. Refer to Fig. 5. In this apparatus, which is in part similar to the rebound apparatus described in a previous paper,[2] the steel ball is held above the test specimen by means of an electromagnet and is dropped upon the rubber test specimen which is mounted on a heated inclined plane and the ball bounced into the electrostatic modulator where its charge is measured. With this apparatus, the work done on the sample during a test is so great that there is some evidence that it brings about a structural change in the rubber. In any case, repeated tests on the same spot in the rubber show a progressive decrease in charge (stocks become more positive) which would indicate an increase in tensile strength.

MECHANICS OF BOUNCING BALL CONTACT POTENTIAL APPARATUS

The mechanics of the bouncing ball apparatus are of theoretical interest and are given as follows. Refer to Fig. 6.

[2] R. S. Havenhill and J. J. Rankin, Ind. Rubber World 107, 365–368 (1943).

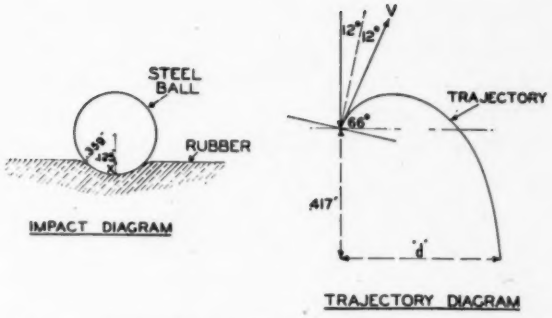

FIG. 6. Mechanics diagram of bouncing ball apparatus.

1. Area of Contact

Diameter of contact spot = .25 inch.
Determined experimentally by coating ball with fingerprint ink.
Area = $(.125)^2\pi$ = .049 sq. in.

2. Pressure

Diameter of ball = .718 inch.
Weight of ball = .0544 lb.
Diameter of contact spot = .25 inch.
Depth of penetration = X.
$X=.359-[(.359)^2-(.125)^2]^{\frac{1}{2}}$.
X = .022 inch.

The ball falls 7.25 inches on to the rubber. It penetrates the surface a depth X. From the law of conservation of energy, it can be shown that the weight of the ball times the distance it falls equals the force exerted on the rubber times the depth of penetration X. Thus:

$$.0544\times 7.25=F\times .022.$$

$$F=17.9\text{ lb.}$$

$$\text{Pressure}=\frac{17.9}{.049}=365\text{ lb./sq. in.}$$

3. Velocity

If the rubber stocks were 100 percent resilient, the velocity of the ball leaving the stock would be equal in magnitude to the velocity of the ball falling 7.25 inches from rest.

$$V=(2gS)^{\frac{1}{2}}=\left(\frac{2\times 32.2\times 7.25}{12}\right)^{\frac{1}{2}},$$

$$V=6.24\text{ ft./sec.}$$

This is the maximum velocity obtainable. Since resilience is proportional to kinetic energy regained after rebound, and kinetic energy is proportional to velocity squared, it can be shown that actual velocity after rebound is as follows:

$$V = .624R^{\frac{1}{2}} \text{ ft./sec.},$$

where R is resilience in percent.

Another means of measuring this velocity is by the use of d, the horizontal distance the ball moves after bouncing. If the ball starts with a velocity V (as shown in Fig. 6) and falls a distance of 0.417 ft. in time t, equations of motion can be set up.

Assuming the angle of impact equals the angle of rebound, these equations are:

$$-V \sin 66°t + \tfrac{1}{2}gt^2 = 0.417,$$
$$V \cos 66°t = d.$$

Solving for V in terms of d

$$V = \frac{10.1d}{(.417 + 2.246d)^{\frac{1}{2}}} \text{ ft./sec.}$$

Values of V obtained from this formula agreed with values obtained from the resiliency-velocity formula within about 5 percent. Hence, the assumption of equal angles has experimental justification.

TESTING PROCEDURE

A 6″×6″×.075″ tensile sheet[3] cured in a clean chromium-plated mold is used for test. The carefully prepared specimen,[1] whose surface should be free from dust, lint, surface bloom, or other foreign matter and free from electrical charge, is placed on the inclined plane and brought to the desired testing temperature by proper adjustment of the Variac supplying the current for the electric heater. Temperature can be measured by means of a thermocouple placed on the stock and another built into the top surface of the inclined plane. A four-minute heating period is usually required to bring the tensile sheet to a testing temperature of 212°F. The steel ball (ballbearing) which is used to contact the sample is first cleaned with c.p. acetone. The ball is then picked up and gently placed on top of the rubber test sheet and allowed to roll freely down the rubber on the incline and drop into the cup of the electrostatic modulator where its charge is measured on the output meter of the audio amplifier. This test is repeated several times, taking care to roll the ball over a fresh uncontacted surface each time. The test specimen should be placed slightly over the lower edge of the inclined plane so that arcing and resultant discharge of the ball cannot take place between the ball and the metal of the heater.

The specimen preparation and test procedure for the "bouncing ball" apparatus are the same as for the "rolling ball" apparatus with the exception that in the former, the ball is released from an electromagnet and bounced instead of rolled into the electrostatic modulator. A thicker test specimen is sometimes desirable with this apparatus, and samples 0.20 inch in thickness were used for certain tests. All contact potential measurements must be made in a constant temperature, constant humidity room; 78°F and 45 percent relative humidity testing conditions have been found to be satisfactory. Like all electrostatic work, results are difficult to duplicate, and a large number of tests must be run.

EXPERIMENTAL DATA

Increase of Contact Potential with Temperature

Our electrostatic contact potential theory of reinforcement predicts that GR-S should become highly negative at elevated temperatures in order to explain the low hot tensiles of GR-S. To check this, contact potentials were run at 78°F and 212°F on a 20-volume zinc oxide loaded GR-S stock and also on a similar rubber stock. Data were obtained with both the "rolling ball" and "bouncing ball" contact potential equipment. Rebound data were also obtained using the St. Joe Inclined Plane Falling Ball Rebound Tester.[2] Hot tensile data were obtained using the St. Joe Electric Heater Attachment[4] for the Scott Tensile Machine (see Fig. 7). These data are shown in Table I. The zinc oxide used in these and all subsequent tests was a

[3] A.S.T.M. D15-41.

[4] Test Method Card No. 66 File S-2 dated 10/23/43—Research Compounding Section, Research and Development Division of the Office of Rubber Director, Washington, D. C.

TABLE I. Comparison of rolling ball and bouncing ball electrostatic contact potentials of rubber and GR-S.

Test	GR-S Formula *A*		Rubber Formula *B*	
	78°F	212°F	78°F	212°F
*Electrostatic contact potential volts				
1. Rolling ball apparatus	116	293	103	140
2. Bouncing ball apparatus	36	89	-28	37
Tensile lb./sq. in.	1000	115	3500	2100
% elongation	930	400	620	625
Modulus @ 400 percent (lb./sq.in.)	125	115	1200	—
% rebound	35	36	44	56
Shore hardness	42	—	51	—
Rex hardness	44	—	53	—

Formulas

A		*B*	
GR-S	100	Rubber	100
Sulfur	2.5	Sulfur	3.5
Captax	1.5	Captax	0.6
ZnO	113.	Stearic acid	1.5
	217.0	ZnO	113.
			218.6
Cure 55′×280°F		Cure 35′×280°F	

* The contact potential values are in terms of negative input volts at modulator. The smaller the value, the more positive (+) the potential.

fine particle size (0.2 micron average diameter), fast-curing type produced by the St. Joe Electrothermic process. It will be noted that the GR-S contact potential increased about 150 percent while the rubber contact potential increased less than 50 percent. This was true for both the "rolling" and "bouncing" ball type apparatus. These data checked the theory, and it was decided to repeat these tests and run additional

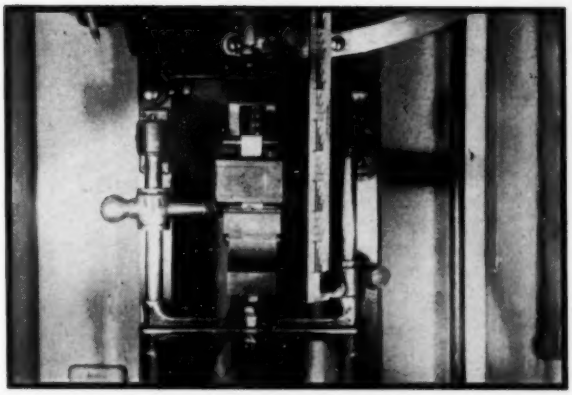

FIG. 7. St. Joe hot tensile apparatus.

ones at different temperatures on both high zinc and pure gum rubber and GR-S stocks. Since the "bouncing ball" apparatus gave such low contact potentials because of small contact area, the results were difficult to check and all subsequent tests were run using only the "rolling ball" apparatus. These contact potential data are shown in Table II. The tensile data are shown in Table III. It will be noted that in all cases there is an increase in negative contact potential as the temperature is increased. This corresponds with a decrease in tensile with temperature and is further confirmation of the electrostatic contact potential theory of reinforcement.

It is interesting to note that the high contact potential values observed at elevated tempera-

TABLE II. Effect of temperature on electrostatic contact potentials of rubber and GR-S.

Formula	Composition	Min. cure @ 280°F	Electrostatic contact potentials rolling ball apparatus volts				% rebound		Hardness 78°F	
			78°F	145°F	212°F	278°F	78°F	212°F	Shore max.	Rex
C	Pure gum rubber	35	100	120	150	250	48	59	42	43
D	Pure gum GR-S	55	150	225	325	450	42	43	35	35
B	20-vol. ZnO rubber	35	85	115	140	185	44	56	51	53
A	20-vol. ZnO GR-S	55	115	200	285	400	35	36	42	44

Formulas

C		*D*	
Rubber	100	GR-S	100
Sulfur	3.5	Sulfur	2.5
Captax	0.6	Captax	1.5
Stearic acid	1.5	Zinc oxide	5
Zinc oxide	5		109.0
	110.6		

See Table I for Formulas *A* and *B*.

TABLE III. Effect of temperature on tensile of rubber and GR-S compounds.

Formula	Composition	Cure min. @ 280°F	78°F Tens. lb./sq. in.	78°F Elong. %	78°F Mod. @ 400% lb./sq. in.	145°F Tens. lb./sq. in.	145°F Elong. %	145°F Mod. @ 400% lb./sq. in.	212°F Tens. lb./sq. in.	212°F Elong. %	212°F Mod. @ 400% lb./sq. in.	279°F Tens. lb./sq. in.	279°F Elong. %	279°F Mod. @ 400% lb./sq. in.
C	Pure gum rubber	35	3350	775	315	2850	675	400	2200	760	275	160	250	—
D	Pure gum GR-S	55	145	450	75	85	250	—	50	150	—	25	160	—
B	20-vol. ZnO rubber	35	3500	620	1200	2850	640	750	2200	625	500	465	400	465
A	20-vol. ZnO GR-S	55	1000	930	125	225	500	150	125	425	100	65	275	—

See Tables I and II for formulas.

tures tend to persist for a short time after the stock is cooled, indicating an alignment or orientation of charges such as a semi-permanent polarization of the stock.

ADDITION OF POSITIVE (+) MATERIALS TO GR-S TO INCREASE HOT TENSILE STRENGTHS

A number of materials having, in effect, a less negative (more +) electrostatic contact potential were added to GR-S to make it less negative (more +) at elevated temperatures and, according to the theory, increase its tensile strength. Some of these materials, such as Flectol H, while (+) and effective in increasing tensile strength at room temperatures, became highly negative at elevated temperatures; and for this reason, neither made the stocks more positive nor increased the tensile at elevated temperatures. A few of these materials when properly dispersed maintained their positive charge at elevated temperatures, making the GR-S less negative and gave increased tensile strength stocks. These materials were finely divided SiO_2, Na_2SiO_3, and certain proteins such as egg white. These materials were not effective when milled into GR-S and did not change appreciably the contact potentials or tensile strengths. A careful examination of the stocks showed poor dispersion of all of these materials. In order to get effective dispersions, these materials were dispersed in water and the water dispersions added to GR-S latex. The procedure was as follows:

LATEX DISPERSIONS

To 1000 grams of Type II GR-S latex (30 percent solids) were added water dispersions of the positive (+) materials in such an amount as to give 20 percent on the GR-S solids. Then, 600 grams of 50 percent Black Label No. 20 zinc oxide dispersed in water with 1 percent of Stablex B were added. Coagulation was carried out by the addition of 100 to 200 cc of 28 percent Epsom Salt solution. Egg white and, especially, sodium silicate are good dispersing agents for zinc oxide and act as stabilizing agents, making it difficult to coagulate the latex. After coagulation, the material is dried at 190°F for approximately twenty-four hours or until the moisture content is under .35 percent. The resulting GR-S master batch contains approximately 50 percent of zinc oxide and 20 percent (on GR-S) of the added (+) material. Compounding then was carried out and regular milling procedure followed in basic Formula *E*. Formula *E* is similar to Formula *A*, except that

TABLE IV. Addition of (+) materials to GR-S latex.

Composition	Cure min. @ 280°F	Electrostatic contact potentials volts 78°F	Electrostatic contact potentials volts 212°F	Original tensiles 78°F Tens. lb./sq. in.	Original tensiles 78°F Elong. %	Original tensiles 78°F Mod. @ 400% lb./sq. in.	Tensiles @ 212°F Tens. lb./sq. in.	Tensiles @ 212°F Elong. %	Tensiles @ 212°F Mod. @ 400% lb./sq. in.	% rebound 78°F	% rebound 212°F	Hardness 78°F shore 15 sec.
Standard	50	100 v	275 v	900	850	225	150	300	—	36	37	40
20% egg white	20	93 v	180 v	1475	538	1000	400	250	—	37	40	49
20% SiO_2	50	95 v	195 v	1325	990	200	300	400	300	33	34	37
20% Na_2SiO_3	40	90 v	175 v	1475	450	1200	400	200	—	36	39	49

Positive (+) materials added
2 egg whites added to 1000 grams of Type II GR-S latex (30% solids)
400 grams of 15% santocel (SiO_2) dispersed in water
120 grams of 50% sodium silicate in water.
Basic Formula *E* (See Text).

Formula *E*.

	Parts by weight
50 percent zinc oxide master batch from GR-S latex (spec.)	200
Sulfur	2.5
Captax	1.5
	204.0

it contains 18 volumes of zinc oxide instead of 20 volumes.

The tensile, rebound, and contact potential data are shown in Table IV. It will be noted that these materials markedly increased the contact potential (made it more positive) and increased both the room-temperature tensile and the hot tensile of GR-S. The hot tensile is more than doubled in case of the egg white (albumen) and sodium silicate stocks. Modulus, hardness, and rate of cure also are increased while rebound data are of the same order. The stocks containing the egg albumen were different from any of the other stocks in that they milled out extremely smoothly and gave a long, plastic, uncured sheet when taken from the mill. They resembled natural rubber more in this respect than any other GR-S material we have observed.

DISCUSSION OF RESULTS

In order to show the relations between temperature, contact potential, and tensile, additional data were obtained at various temperatures on the standard latex compound containing no sodium silicate and on one containing 20 percent sodium silicate. These data are shown in Table V and have been plotted in the form of curves. Refer to Figs. 8 and 9. Figure 8 shows the increase in contact potential with temperature and also that the addition of Na_2SiO_3 greatly decreases the contact potential and makes the stock more positive (+). Figure 9 shows how the tensile drops off with temperature and shows the superiority of the Na_2SiO_3 stock.

In Fig. 10, the contact potential data for all the rubber compounds run at different temperatures have been plotted against the tensile strength values; and it appears that there is a relation between tensile strength and contact potential.

In Fig. 11, the contact potential data for all the GR-S and GR-S latex compounds run at different temperatures have been plotted against the corresponding tensile strength values and again it appears that there is a correlation of contact potential and tensile strength; however, it is a different one from that for rubber as might be expected from the difference in physical and chemical properties of the two materials. These data are all further confirmation of the electrostatic contact potential theory of reinforcement.

SUMMARY AND CONCLUSIONS

A new apparatus has been described for measuring contact potentials of rubber and GR-S compounds at elevated temperatures. In this apparatus, the electrostatic charge, acquired by rolling a steel ball down the surface of a rubber test specimen on a heated inclined plane, is measured when the ball drops into the cup of the electrostatic modulator. This potential, while not the actual contact potential, is, nevertheless, proportional to it. With this apparatus, the contact potential of GR-S at elevated temperatures was found to increase much more (become more negative) than for rubber. The release of electrons (increase in negative contact potential)

TABLE V. Effect of temperature on GR-S containing sodium silicate.

	Contact potential volts		Tensile strength					
			Standard stock no sodium silicate			20% sodium silicate		
Temperature of test	Standard stock	20% Na_2SiO_3 stock	Tensile lb./sq. in.	Elong. %	Mod. @ 400% lb./sq. in.	Tensile lb./sq. in.	Elong. %	Mod. @ 400% lb./sq. in.
78°F	100	85	900	850	225	1475	475	1000
145°F	180	125	500	400	300	890	425	700
212°F	275	185	150	300	—	400	200	—
279°F	410	255	50	150	—	275	225	—

Basic Formula *E*.

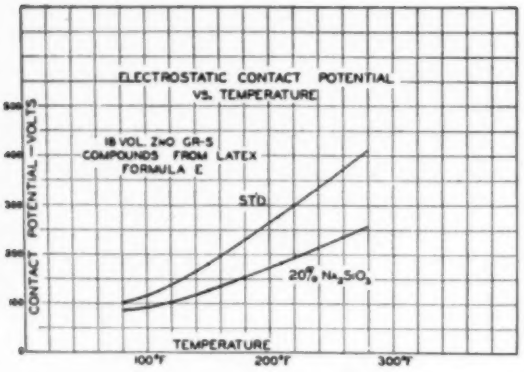

FIG. 8. Contact potential *vs.* temperature for sodium silicate stocks.

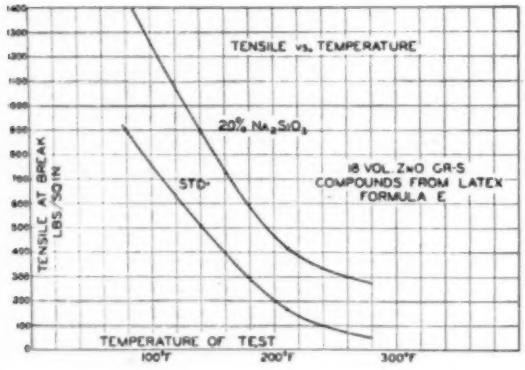

FIG. 9. Tensile *vs.* temperature for sodium silicate stocks.

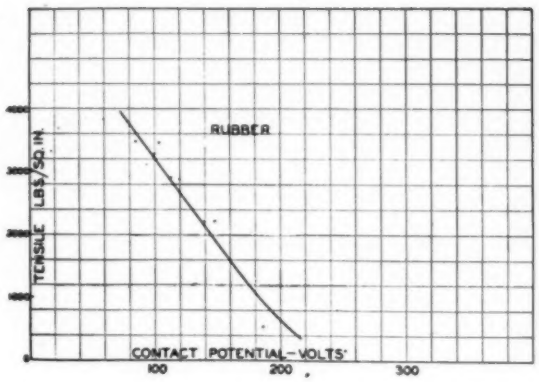

FIG. 10. Contact potential *vs.* tensile strength for all rubber compounds.

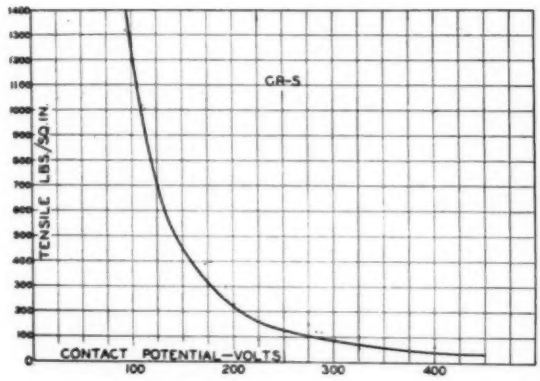

FIG. 11. Contact potential *vs.* tensile strength for all GR-S compounds.

and consequent disruption of electrostatic attractive forces within the material at elevated temperature probably partly accounts for the much greater decrease in tensile of GR-S over rubber and is further confirmation of the electrostatic contact potential theory of reinforcement.

By the further application of this theory, highly positive (+) materials, such as certain proteins, finely divided silica, and sodium silicate, which retain their positive charge at elevated temperatures and make the stocks more positive, have been found to more than double the hot tensiles of high zinc oxide loaded compounds made from GR-S latex.

ACKNOWLEDGMENT

The authors wish to acknowledge the valuable assistance of the Staff of the St. Joe Research Laboratory and particularly that of Mr. G. F. Weaton, Plant Manager, Mrs. D. E. Taylor, Harold Emery, L. E. Carlson, L. A. Cha, and Charles Black, who have contributed to the preparation of this paper.

Significance of the Equation of State for Rubber*

EUGENE GUTH, PAUL E. WACK, AND ROBERT L. ANTHONY
Polymer Physics Laboratory, University of Notre Dame, Notre Dame, Indiana

The physical significance of stress-strain curves and of isometrics obtained by the relaxation method is discussed and clarified. Stress-strain curves taken at various temperatures give the correct dependence of stress upon temperature if they are taken sufficiently fast so that stress relaxation does not mask the temperature dependence. Isometrics obtained after previous relaxation of the sample are shown to depend upon duration and temperature of the relaxation by a numerical factor only. The basis for this behavior is the factorization of the stress into a factor depending upon extension and temperature only which corresponds to the equation of state and another factor depending upon the temperature T^* and the duration of the relaxation process. For simple stress relaxation, the same factorization holds with T^* equal to T. A general theory is formulated for time dependent elastic phenomena by generalizing Boltzmann's theory. The theory explains why factorization does not hold for creep, in agreement with experiment.

1. INTRODUCTION

THE physical significance and the molecular interpretation of equations of state for gases, liquids, and solids are well known. The equation of state for a gas may be given in the form

$$p=p(V, T), \tag{1}$$

where p is the pressure, V the volume, and T the absolute temperature. The equation of state for a solid, which is deformed unilaterally, may be obtained from Eq. (1) by replacing p by $(-Z)$, the (nominal) stress (=force per unit original cross section) and V by ϵ, the strain (=extended length divided by original length minus one)

$$Z=Z(\epsilon, T). \tag{2}$$

A stress-strain curve

$$Z=Z(\epsilon) \tag{2a}$$

is the *isothermal* obtained from Eq. (2) at constant temperature T. A stress-temperature curve

$$Z=Z(T) \tag{2b}$$

is the *isometric* obtained from Eq. (2) at a constant extension ϵ. An extension-temperature curve

$$\epsilon=\epsilon(T) \tag{2c}$$

is the *isotonic* obtained from Eq. (2) at a constant stress Z. Equations (2a), (2b), and (2c) are, of course, equivalent. For certain solids, the isothermals, or the isometrics or the isotonics may be obtained experimentally in a direct way.

For rubber, none of the "iso"-curves may be obtained directly. For instance time is needed to take an isothermal, a stress-strain curve. During this time the stress relaxes by an amount depending upon the conditions under which the curve is taken. The purpose of the present paper is to clarify the role of the time element in the various methods for obtaining the equation of state.

2. STRESS-STRAIN CURVES

Apparently the simplest way of obtaining the equations of state consists in the taking of stress-strain curves at various temperatures. Unfortunately, the time element needed for this procedure may mask or even reverse the correct dependence of stress upon temperature. Stress-

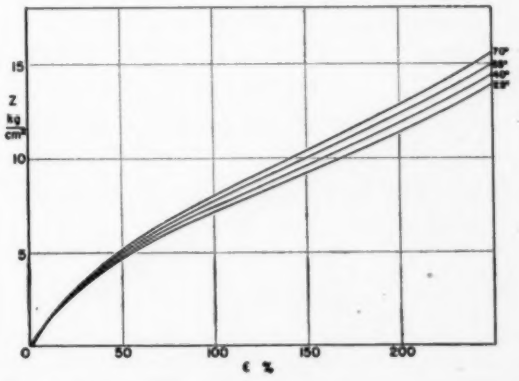

FIG. 1. Stress-strain curves for various temperatures.

* This work was done in 1943, but its publication had to be delayed.

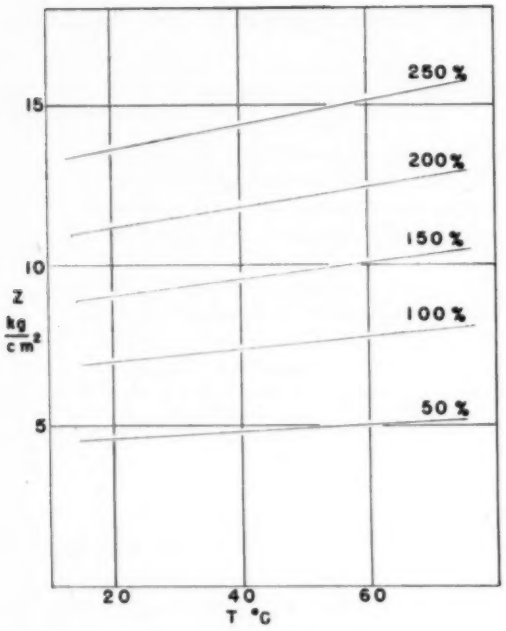

FIG. 2. Isometrics derived from Fig. 1.

strain curves taken at *slow* constant rates of loading or stretching yield on cross-plotting at constant strain a decrease of the stress with increasing temperature, in contradiction to the kinetic theory of rubber electricity.[1]

For *fast* stress-strain curves the correct dependence (i.e., increase) of the stress upon the temperature is obtained. Figure 1 shows stress-strain curves at various temperatures obtained with the fast stress-strain apparatus,[2] developed in the Polymer Physics Laboratory at Notre Dame. Figure 2 shows isometrics which resulted from Fig. 1 on cross-plotting; they exhibit the increase of stress with increasing temperature.

This method alone, however, cannot give a reliable equation of state. For, it is not *a priori* known *how fast*[3] the stress-strain curve has to be taken in order to give the "correct" dependence of the stress upon the temperature. In addition, the adjective "correct" needs further elaboration. At any rate this method would have to be supplemented by a study of the effect of the speed of stretching upon the stress-strain curve.

3. ISOMETRICS BY RELAXATION METHOD

The relaxation method of obtaining isometrics operates as follows: A sample is kept at constant extension at a constant temperature T^* for the time interval t^*. The stress relaxes as shown in Fig. 3. Then the temperature is lowered and the change in stress measured, giving the desired isometrics as indicated in Fig. 4.

The time t^* is chosen so that in the time interval $(t^{**}-t^*)$ (cf. Fig. 3) needed to take the measurements over the temperature interval T^*-T^{**} (cf. Fig. 4) the amount of stress relaxation is within the experimental error.

In earlier work it was customary to take measurements from T^{**} back to T^* also and call the isometrics reversible or equilibrium curves, if

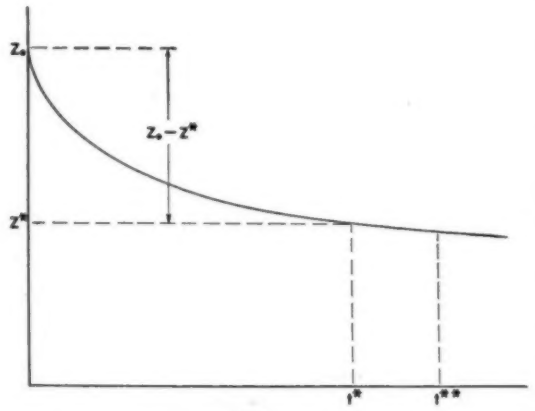

FIG. 3. Illustration of the relaxation method for obtaining isometrics, Z_0 is the initial stress at $t=0$.

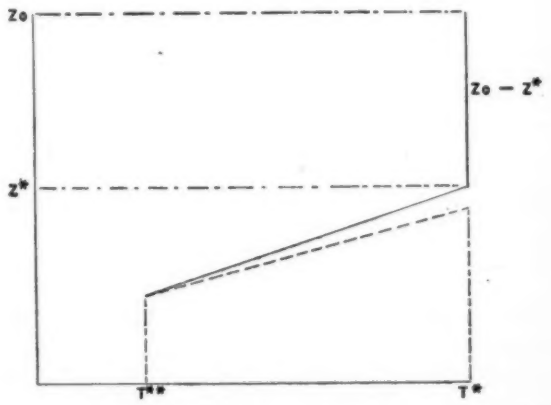

FIG. 4. Isometric obtained after pre-relaxation according to Fig. 3.

[1] H. M. James and E. Guth, J. Chem. Phys. **11**, 455 (1943).

[2] S. L. Dart, R. L. Anthony, and P. E. Wack, Rev. Sci. Inst. **17**, 106 (1946).

[3] Because of the rise of temperature on fast stretching these stress-strain curves are adiabatics in reality. However, the difference between adiabatics and isothermals is within the experimental error for extensions up to crystallization.

the branch coming back coincided with that going down. This is unnecessary, however. Suppose one has chosen t^* so that no measurable stress relaxation takes place going down from T^* to T^{**}, that is, for the time $(t^{**}-t^*)$, but that stress relaxation is not negligible for the interval $2(t^{**}-t^*)$ needed to cover also the return T^{**} to T^*. Then, when coming back, one would obtain the dotted line in Fig. 4. For thermodynamic computations one still may use the branch on going down. This statement will be obvious after considering the theory of the relaxation method of obtaining isometrics in the following sections of this paper.

Apart from the clarification of this item, there were other important points left somewhat obscure. In the actual experiment all rubbers show some (permanent or temporary) set, when the stress is released, after the isometrics are taken. Should one take this *final* unstretched length or the *initial* one (before the experiment started) in computing the extension ϵ? Meyer and Ferri,[4] for instance, have used the final length. Our theory will show that the initial length should be taken instead. In previous work (Meyer and Ferri,[4] our own work,[5] and Wood and Roth[6]) the role of the temperature T^* and of the duration t^* of the pre-relaxation was left somewhat unclear. Also the question of the *absolute value* of the stress was not discussed.

4. STRESS RELAXATION

The importance of the pre-relaxation in the relaxation method for isometrics necessitates a closer study of the laws of stress relaxation.

Our experimental work on the stress relaxation of natural and synthetic gum and tread stocks may be summarized in the factorization relation

$$Z(\epsilon, T; t) = F(\epsilon, T), G(t, T). \qquad (3)$$

Stress relaxation differs from the equation of state in the entering of the time as a new variable. This means, for instance, that it is not possible to derive for all times t the laws of creep ($Z=$const.) from Eq. (3) by solving for ϵ.

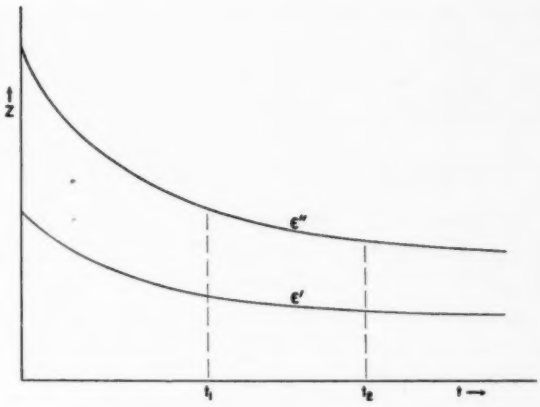

FIG. 5*a*. Similarity of stress-time curves.

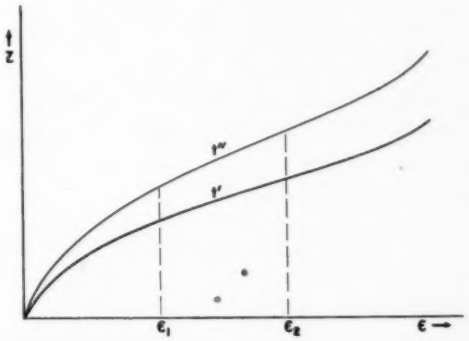

FIG. 5*b*. Similarity of stress-strain curves obtained from stress-time curves of the type shown in Fig. 5*a*.

The Eq. (3) implies the constancy of the following ratios:

$$\frac{Z(\epsilon'', T; t)}{Z(\epsilon', T; t)} = \frac{Z(\epsilon'', T; t_2)}{Z(\epsilon', T; t_2)} = \cdots = \frac{F(\epsilon'', T)}{F(\epsilon', T)}, \qquad (4a)$$

$$\frac{Z(\epsilon_1, T; t'')}{Z(\epsilon_1, T; t')} = \frac{Z(\epsilon_2, T; t'')}{Z(\epsilon_2, T; t')} = \cdots = \frac{G(t'', T)}{G(t', T)}. \qquad (4b)$$

The meaning of the notation in Eqs. (4a) and (4b) is made clear in Figs. 5*a* and 5*b*. These figures exhibit the geometric implications of the factorization. The relaxation $(Z-t)$ curves for various constant extensions ϵ and the stress-

[4] K. H. Meyer and C. Ferri, Helv. Chim, Acta **18**, 570 (1935). Translated in Rubber Chem. Tech. **8**, 319 (1935).
[5] R. L. Anthony, R. H. Caston, and E. Guth, J. Phys. Chem. **46**, 826 (1942). Reprinted in Rubber Chem. Tech. **16**, 297 (1943).
[6] L. A. Wood and F. L. Roth, J. App. Phys. **15**, 781 (1944).

strain (Z—ϵ) curves[7] for various constant times t', t'', . . . are *similar*, i.e., they may all be superposed on each other by multiplication by constant factors.

5. GENERAL THEORY OF TIME ELASTICITY

Time elasticity shall designate any process in which stresses cause deformations with the time element as an important factor. A general formalism may be given in agreement with the factorization (Eq. (3)) by a generalization of Boltzmann's theory of time-elastic processes.

The fundamental integral equation is

$$Z(t)=F[\epsilon(t)]-\beta\int_{-\infty}^{t}\varphi(t-t')F[\epsilon(t')]dt' \quad (5)$$

β is a (small) constant. $\beta\varphi(t-t')$ is the memory function of Boltzmann. Equation (5) reduces to Boltzmann's equation, if the instantaneous stress-strain relation

$$Z=F(\epsilon) \quad (6a)$$

reduces to Hooke's law

$$Z=E\epsilon, \quad (6b)$$

where the constant E denotes Young's modulus.

For *relaxation:*

$$\epsilon(t)=\epsilon(t')=\begin{cases}0, & t<0\\ \epsilon=\text{const.}, & t>0.\end{cases}$$

Equation (5) reduces to

$$Z(t,\epsilon)=F(\epsilon)[1-\beta\psi(t)]=F(\epsilon)G(t), \quad (7)$$

where

$$\psi(t)=\int_{0}^{t}\varphi(t-t')dt'. \quad (8)$$

Equation (7) is identical with Eq. (3). (For simplicity we did not indicate in Eq. (5) the temperature as another variable.)

For *creep* we have to invert our fundamental Eq. (5). For short times this is simple. Then the term with β will be small and terms of order β^2 or higher may be neglected. We obtain

$$\epsilon(t)=F^{-1}\left\{Z(t)+\beta\int_{-\infty}^{t}\varphi(t-t')Z(t')dt'\right\} \quad (9)$$

and for creep

$$Z(t)=Z(t')=\begin{cases}0, & t<0\\ Z=\text{const.}, & t>0,\end{cases}$$
$$\epsilon(t)=F^{-1}\{Z[1+\beta\psi(t)]\}. \quad (10)$$

Equation (10) follows from Eq. (7) by solving for ϵ and yields factorization for creep in the special case of Hooke's law, where $\epsilon=F^{-1}(Z)=Z/E$ but not in the general case of Eq. (6a). We notice that had we assumed factorization for creep, we would have arrived at an equation different from (9) which would have contradicted Eq. (5). Our experiments show that—in contrast to relaxation—factorization does not hold for creep.

All time-elastic phenomena may be derived from the fundamental Eq. (5). For instance, we can obtain the dependence upon time of stress-strain curves obtained at constant rate of loading or of stretching.[8] The *fast* processes of forced or free vibrations may be treated using the same equation as a general frame.

The determination of the memory function from molecular models we shall defer to another paper. The function $Z=F(\epsilon)$ is the stress-strain relation as given by the statistical theory of rubber elasticity.[1]

$$Z=K\cdot T\left[1+\epsilon-\frac{1}{(1+\epsilon)^2}\right]. \quad (11)$$

For *shear* deformations Hooke's law (6b) holds (with ϵ as shear-strain) up to moderate extensions and Eq. (5) reduces to Boltzmann's. For shear there is then factorization for *both* creep and relaxation.

6. THEORY OF ISOMETRICS FROM RELAXATION METHOD

Experimental work at Notre Dame on natural and synthetic gum stock may be summarized in the relation

$$Z(\epsilon,T;T^*,t^*)=F(\epsilon,T),G(T^*,t^*). \quad (12)$$

[7] These stress-strain curves are obtained by cross-plotting from the relaxation curves (Fig. 5a). They differ from stress-strain curves obtained at a constant rate of loading or stretching.

[8] Cf. G. Slomimsky, Acta Phys. Chem. U.S.S.R. **12**, 99 (1940), for the case of Boltzmann's theory.

Here T^* and t^* designate the temperature and duration of the pre-relaxation process which precedes the taking of the isometrics (cf. Figs. 3 and 4). Equation (12) expresses a generalized factorization. Again, as in the case of simple relaxation (to which Eq. (12) refers for $T^*=T$), the constancy of certain ratios is implied in Eq. (12)

$$\frac{Z(\epsilon'', T; T^*, t^*)}{Z(\epsilon', T; T^*, t^*)}=\frac{F(\epsilon'', T)}{F(\epsilon', T)}, \tag{13a}$$

$$\frac{Z(\epsilon, T''; T^*, t^*)}{Z(\epsilon, T'; T^*, t^*)}=\frac{F(\epsilon, T'')}{F(\epsilon, T')}, \tag{13b}$$

$$\frac{Z(\epsilon, T; T_2^*, t^*)}{Z(\epsilon, T; T_1^*, t^*)}=\frac{G(T_2^*, t^*)}{G(T_1^*, t^*)}, \tag{13c}$$

$$\frac{Z(\epsilon, T; T^*, t_2^*)}{Z(\epsilon, T; T^*, t_1^*)}=\frac{G(T^*, t_2^*)}{G(T^*, t_1^*)}. \tag{13d}$$

Again the constancy of these four ratios means geometrically the similarity of certain curves derived from the stress-temperature-time relationships.

The factorization expressed in Eq. (12) shows clearly that all isometrics, for various times t^* or temperatures T^* of pre-relaxation, differ only by a numerical factor $G(T^*, t^*)$. This factor is determined by the form of Boltzmann's memory function as explained in Section 4. Equation (12) also shows that the initial unstretched length should be taken for the computation of the extension ϵ. Thus the functional form of the equation of state may be obtained unambigously from experiment.

The question of the *absolute value* of the stress is connected with the particular form of the memory function, i.e., with the statistical model used to explain the memory function.

Suppose the time elasticity of our material is given by a Maxwell body, i.e., a spring and a dashpot in series, leading to permanent set. Then one should extrapolate the time factor G to $t=0$. On the other hand, if the time elasticity is better described by a Maxwell body in parallel with a spring (leading to temporary set only), then one should extrapolate G to $t=\infty$. We restrict ourselves here to these two examples.

7. LIMITATIONS

The experimental results which yielded similarity for simple stress relaxation and for isometrics using pre-relaxation were obtained in air in the temperature range: 0–70°C.

The interesting work of Tobolsky and his associates[9] at Princeton showed that relaxation and creep of rubber at temperatures above 100°C is caused by chemical changes involving the breaking and formation of primary valence bonds. The similarity law of Eq. (3) is valid. For our temperature range of 0–70°C, however, these processes are less important. In fact, in our experiments there was comparatively little permanent set left after taking the isometrics.

We wish to point out that there is always an observable decay of stress during the relaxation. Figures (6) and (7) of Tobolsky and Andrews[10] are only in apparent contradiction to this statement. The apparent constancy of Z/T in these figures is caused by the small scale employed. Blown up to a larger scale, their results show also a stress decay.

Long duration creep and relaxation tests were carried out by Mooney, Wolstenholme, and Villars[11] at 35° and 70°C. For moderate extensions and duration their data are compatible with similarity.

It is planned to publish in greater detail in the near future the work summarized briefly in this paper. There, among other things, the role of the ordinary thermal expansion of rubber will be discussed.

---

[9] Cf. A. V. Tobolsky and R. D. Andrews, J. Chem. Phys. **13**, 3 (1945).

[10] See reference 9, pp. 9–10.

[11] M. Mooney, W. E. Wolstenholme, and D. S. Villars, J. App. Phys. **15**, 324 (1944).

The Theory of Permanent Set at Elevated Temperatures in Natural and Synthetic Rubber Vulcanizates

R. D. Andrews and A. V. Tobolsky
Frick Chemical Laboratory, Princeton University, Princeton, New Jersey

and

E. E. Hanson
Research Laboratory, The Firestone Tire and Rubber Company, Akron, Ohio

A molecular theory is developed to describe quantitatively the permanent set taking place in thin samples of vulcanized natural and synthetic rubbers held at constant extension at elevated temperatures. Permanent set is considered to be the result of the formation, through the action of molecular scission and cross-linking reactions, of a dual molecular network in the rubber sample, in which the network chains are of two types: chains which are at equilibrium when the sample is at its unstretched length, and chains which are at equilibrium when the sample is at its stretched length. According to the theory the amount of permanent set in a rubber sample is a function of only two quantities: the relative ratio of the number of chains of the two types, and the elongation at which the sample was held. Experimental data on permanent set for various rubber types and under different conditions are presented and are shown to be in good agreement with the theory.

CERTAIN materials, including natural and synthetic rubbers, after being deformed for finite periods of time and then released, do not return completely to their original dimensions. This phenomenon is called "permanent set."

There are many different types of measurements, made under a great variety of conditions, all of which are described as measurements of permanent set. The molecular causes of permanent set are not the same under all of these conditions. For this reason we shall restrict ourselves in the present article to a discussion of the permanent set taking place in thin rubber samples which are maintained at constant extension at elevated temperatures. We shall show that the permanent set occurring under these conditions is due to chemical changes which affect the structure of the rubber network and that a quantitative molecular description of permanent set can be accomplished by the use of concepts already developed concerning the nature of these deteriorative chemical processes.

MOLECULAR SCISSION AND CROSS-LINKING: THEIR MEASUREMENT AND RELATION TO PERMANENT SET

The changes in physical properties that occur in hydrocarbon rubbers at elevated temperatures are due to the simultaneous existence of chain scission and cross-linking reactions induced by oxygen.[1] Depending upon whether chain scission or cross-linking is faster in each individual case, various rubber types soften or harden as a result of exposure to air at elevated temperatures. Butyl vulcanizates tend to soften; butadiene-styrene rubbers (GR-S, for example), butadiene-acrylonitrile rubbers, and Neoprene tend to harden; natural rubber (Hevea) tends first to soften, then to harden. Intermittent measurements of the modulus of a sample maintained in a relaxed state during exposure to the elevated temperature ("intermittent relaxation") provides a method of measuring the *net* rate of scission and cross-linking.

On the other hand it is possible to isolate the scission reaction by measuring the decay of stress in a sample maintained at constant extension at the elevated temperature ("continuous relaxation"). The decay of stress is a direct measure of the cutting of the molecular chains of the network. The cross-linking of chains, which is occurring simultaneously, tends to take place, to a first approximation, in such a way that it causes no increase of stress at constant extension. In other words, new network chains are being formed by a process of oxido-vulcanization which are in equilibrium when the sample is at the

[1] A. V. Tobolsky and R. D. Andrews, J. Chem. Phys. **13**, 3 (1945).

stretched length (by network chains we refer to the portions of chain molecules between contiguous network junctures).

The qualification that the cross-linking has no effect on the continuous relaxation curve "to a first approximation" is added because of the fact that in continuous relaxation experiments carried out for extended times an increase in stress is observed for some rubbers notably GR-S, Butaprene N, and Neoprene, following the initial almost complete decay of stress. This stress increase is reproducible with the same accuracy as the earlier part of the curve in which the stress decreases. A contraction of length has been observed to accompany embrittlement in unstretched thin strips resulting from heat aging. General theoretical considerations suggest that a volume contraction is probably taking place. Such a volume contraction would appear to be the most reasonable explanation of the observed stress increase, although this has not yet been investigated experimentally. It is apparent from the Neoprene-gum curve in Fig. 1 that the increase in stress may eventually become quite appreciable. In the case of Hevea gum the stress first decays completely to zero and later begins to increase as embrittlement of the stock sets in, following the initial softening. In Butyl stocks, which soften progressively, the stress decays completely to zero and no stress increase whatever is observed in the continuous relaxation curves even when they are carried out to very extended times. In the continuous relaxation curves of Hevea and Butyl stocks which appear later in this paper, no error should arise from this source, since in the time intervals to which the Hevea curves were carried out, the stock was still softening, and since the effect is not found at all in Butyl stocks. In the case of the GR-S tread stock, the relaxation curve was not carried out to times where this effect becomes significant. Nevertheless, it is well to mention this effect in any general statement concerning the nature of continuous relaxation curves.

Let us now consider the molecular changes taking place in a rubber sample which is being held at constant elongation at an elevated temperature, in terms of their relation to the phenomenon of permanent set. Immediately after extension the individual molecular chains are all

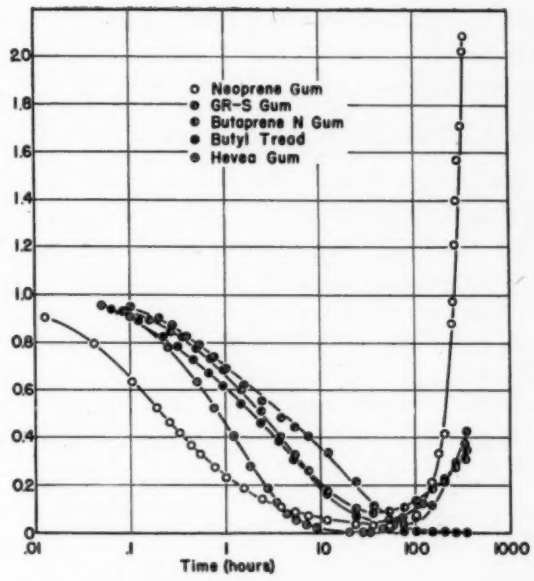

FIG. 1. Continuous relaxation curves for extended periods for various rubber types; 130°C; 50 percent elongation.

stretched and the equilibrium condition for all chains corresponds to the unstretched length of the sample. As the rubber remains at its constant elongation, cutting of the original chains takes place and the stress relaxes; new chains are formed by cross-linking which are at equilibrium when the rubber sample is at that particular elongation, and some of these newly formed chains are cut also. Thus at the beginning, the network chains in the rubber sample were all at equilibrium at the unstretched length; if the stress (due to chains being held out of equilibrium) eventually decays completely to zero, all the chains in the network are at equilibrium at the stretched length. At any intermediate stage between these two extremes, however, the molecular network in the rubber sample is a dual or "hybrid" network, containing chains of two types: (1) chains which are at equilibrium when the sample is at its unstretched length, (2) chains which are at equilibrium when the sample is at its stretched length. When the external constraint holding the sample at constant extension is removed, the chains of the first type tend to pull the sample back to its original unstretched length, whereas the chains of the second type tend to hold the sample out at its stretched length. As a result, the length which the sample actually assumes will be intermediate between its un-

stretched and stretched lengths and its value will be the length at which the stresses on each of the two sets of chains exactly balance each other.

DERIVATION OF PERMANENT SET EQUATION

Having formulated the theory of permanent set in the above qualitative way, it remains only to put the theory into mathematical form. This is done in the following way: For the case of a "homogeneous" network, in which all the network chains are at equilibrium at the same sample length, the equation relating stress and elongation in terms of the concentration of network chains in the rubber, is given as follows:

$$f=skT\left\{\left(\frac{l}{l_u}\right)^2-\frac{l_u}{l}\right\}, \tag{1}$$

where f is stress per unit *attained* cross-sectional area, s is the number of network chains per cc of the rubber, k is Boltzmann's constant, T is absolute temperature, and l and l_u are the attained length and unstretched length (the sample length at which the chains are at equilibrium) of the rubber sample, respectively. This equation is derived from the kinetic theory of rubber elasticity and is equally applicable both to extension and compression, i.e., l may be either greater or less that l_u. A positive value of f indicates a stretching force, and a negative value a compressing force. This equation should apply to both types of chains in the rubber network. Since the equation is derived from the statistics of a single chain, it is not necessary for either type of chain to form a continuous network within the rubber sample; it is thus perfectly applicable when one type of chain is predominant in the rubber network, chains of the other type occurring only here and there, in a relatively isolated way.

Let us denote the unstretched and extended lengths of the rubber sample by l_u and l_x, respectively, and the "set" length by l_s. We may then write for the two sets of chains in the rubber the two equations

$$f_u=s_ukT\left\{\left(\frac{l_s}{l_u}\right)^2-\frac{l_u}{l_s}\right\}, \tag{2}$$

$$f_x=s_xkT\left\{\left(\frac{l_s}{l_x}\right)^2-\frac{l_x}{l_s}\right\}, \tag{3}$$

where f_u is the stress per unit attained cross section on the chains which have their equilibrium position at the unstretched length l_u, and s_u is the number of those chains; f_x and s_x are defined correspondingly for the chains which are at equilibrium (or unstressed) at the extended length l_x. Now the condition for equilibrium in a sample with permanent set, as mentioned before, is that the retractive force exerted by the chains of type "u" is just balanced by the stretching force exerted by chains of type "x"; or, stated mathematically, that

$$f_u=-f_x. \tag{4}$$

Substituting in (4) the expressions for f_u and f_x from Eqs. (2) and (3), we obtain after simplification

$$\frac{s_u}{s_x}\frac{l_x^2}{l_u^2}=\frac{l_x^3-l_s^3}{l_s^3-l_u^3}. \tag{5}$$

Permanent set is generally expressed as the percentage of the deformation retained by the sample; stated mathematically

$$\%\ \text{Permanent Set}=\left(\frac{l_s-l_u}{l_x-l_u}\right)\times 100. \tag{6}$$

This may also be written in the form

$$\%\ \text{Permanent Set}=\frac{(l_s/l_u-1)}{(l_x/l_u-1)}\times 100, \tag{7}$$

which is more satisfactory for the present purpose. It is to be noted that the denominator in (7) is a constant whose value depends on the elongation at which the sample is being held in the experiment. Thus only l_s/l_u must be evaluated to calculate permanent set. We can obtain l_s/l_u from Eq. (5) by algebraic transformation, giving the result

$$\frac{l_s}{l_u}=\left[\frac{(l_x/l_u)^3-1}{(s_u/s_x)(l_x/l_u)^2+1}+1\right]^{\frac{1}{3}}. \tag{8}$$

This expression for l_s/l_u may now be substituted in Eq. (7), giving the following equation for permanent set

$$\%\ \text{Permanent Set}=\left\{\left[\frac{C_1}{(s_u/s_x)C_2+1}+1\right]^{\frac{1}{3}}-1\right\}C_3, \tag{9}$$

where C_1, C_2, and C_3 are constants whose values depend on the elongation of the sample

$$C_1=\left(\frac{l_x}{l_u}\right)^3-1;\quad C_2=\left(\frac{l_x}{l_u}\right)^2;\quad C_3=\frac{100}{(l_x/l_u)-1}.$$

Thus it is to be noted that according to this theory the amount of permanent set in a rubber sample depends upon the elongation of the sample as well as upon the ratio of s_u to s_x.

In order to verify this relation experimentally it is necessary to evaluate the ratio s_u/s_x in terms of continuous and intermittent relaxation curves. This can be done very simply and directly: the value of s_u/s_x at any time t is obtained by dividing the stress value given by the continuous curve at that time by the difference between the stress values of the continuous and intermittent curves. The reason for this is that the stress value given by the continuous curve is proportional to s_u, and that given by the intermittent curve is proportional to (s_u+s_x), by the same factor or proportionality. There are actually no chains of type x in the intermittent sample, of course, but the number of chains of type u is equal to the sum of the number of chains of types u and x in the continuous sample. (The assumption made here, of course, is that the rates of scission and cross-linking are exactly the same in stretched and unstretched samples, so that at any given time the *total number* of chains is the same in both the intermittent and continuous samples.)

The stress data given in this paper are plotted as stress divided by initial stress, f/f_0, rather than

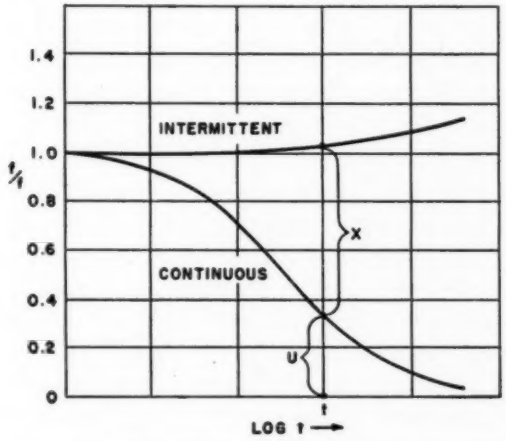

FIG. 2. Evaluation of U and X from continuous and intermittent relaxation curves.

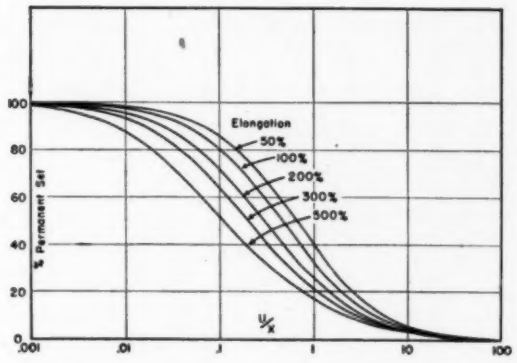

FIG. 3. Permanent set function for various elongations.

as absolute stress. The procedure for evaluating s_u/s_x is not affected by this fact, however. The f/f_0 value given by the continuous curve is designated as U, and the difference in the f/f_0 values of the intermittent and continuous curves as X. This is illustrated in Fig. 2. Thus, according to this notation

$$s_u/s_x=U/X, \tag{10}$$

and U/X may be substituted for s_u/s_x in Eq. (9), giving the following final equation for permanent set in terms of relaxation data

$$\%\ \text{Permanent Set}=\left\{\left[\frac{C_1}{(U/X)C_2+1}+1\right]^1-1\right\}C_3, \tag{11}$$

where the constants have the same values as before. A graph of this permanent set function for a number of different elongations, plotted in the form of percent permanent set *versus* the logarithm of U/X, is shown in Fig. 3.

It might be well to add a few additional remarks at this point concerning the central assumption in the theory of permanent set presented here, i.e., that the cross-linking takes place in such a manner as to form chains which are relaxed when the sample is at the length at which the cross-links were formed. It is not possible to describe satisfactorily a single local cross-linking process mathematically; the effect must rather be considered as a statistical one, and it is necessary to say that the *average effect* of the cross-linking is to form new chains which are relaxed, just as is the case with the cross-linking taking place during vulcanization. Thus there are probably chains under a whole distribution of stress states in a

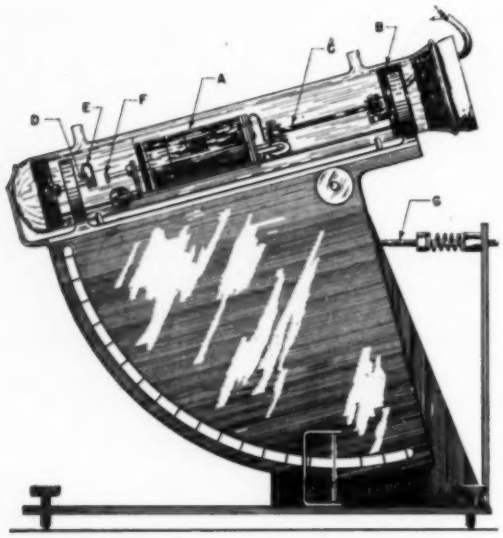

FIG. 4. Tilting relaxometer.

sample held at constant elongation for a period of time at high temperatures. This situation is considered to be equivalent, however, to the case of a network in which there are chains of only two distinct types—chains which are at equilibrium at the original unstretched length of the sample, and chains which are at equilibrium at the stretched length. This model makes possible a mathematically simple calculation of permanent set, just as the same sort of simplification makes possible the calculation of the theoretical stress-strain Eq. (1), obtained from the kinetic theory of rubber elasticity. Therefore, although the picture of a "dual" network employed in the derivation above undoubtedly does not describe exactly the character of the individual chains in the network, it should describe the statistical average behavior of the individual chains.

APPARATUS AND EXPERIMENTAL PROCEDURE

The continuous and intermittent relaxation curves included in this paper were obtained in part on a beam balance type of relaxation apparatus, and in part on an inclined plane type of relaxation apparatus. Duplicate relaxation curves from the two types of apparatus have been found to agree satisfactorily. A description of the beam balance apparatus and its operation has been given in a previous publication.[2]

[2] A. V. Tobolsky, I. B. Prettyman, and J. H. Dillon, J. App. Phys. 15, 380 (1944).

A sketch of the tilting apparatus is shown in Fig. 4. The apparatus consists of two parts: part *A* is a brass cart for carrying as many as five 250 g lead weights, and part *B* is a brass frame which surrounds the weight cart, but is separate from it. The frame and the cart fit inside a glass tube along which the cart is free to roll on its four wheels. The rubber samples (*c*) used in this apparatus are flat rings ($1\frac{7}{8}$ in. O.D., $1\frac{1}{2}$ in. I.D.), died from thin cured sheets (approximately .030 in. thick). Thin samples are used to insure complete penetration of oxygen at elevated temperatures, so that the scission and cross-linking reactions occur homogeneously throughout the samples. These samples are looped around two stainless steel pulleys, one attached to the upper end of the frame and the other to the upper end of the cart, as shown. Projecting from the lower end of the frame is a support post (*D*) with a phosphor bronze spring contact (*E*) at its upper end. The motion of the cart is arrested when a small wooden knob (*F*) fixed to the lower end of the cart touches this support post; this knob also closes the spring contact in touching the post. The support post is replaceable; posts of lengths to give the sample any elongations desired in the range of 0 percent to 200 percent are easily constructed.

The glass tube containing the apparatus is attached by clips to a tilting stand in the manner illustrated in Fig. 4. The apparatus is tilted by a crank shaft (*G*) which extends through the side of the temperature box and is connected with the tilting stand through a worm gear. The entire apparatus, tube and tilting stand, is installed in an air oven with a double glass door. The temperature is thermostatically controlled to 0.3° C, and air circulation is maintained by three small air blowers. The temperature is regulated with reference to a small iron-constantan thermocouple (not shown in sketch) which is attached to the side of the sample with fine thread. The measurement of the test temperature in this way, exactly at the position of the sample, was found to be necessary in order to obtain the most accurate and reliable results.

In carrying out a relaxation experiment the apparatus was first heated thoroughly at the test temperature. The tube was then removed from the oven, the sample (with thermocouple at-

tached) looped over the pulleys, the tube replaced in the oven with the stand at 0° tilt, the electrical leads from the spring contact connected to a neon glow bulb on the outside of the oven, and the oven closed again. When the thermocouple indicated that the sample had reached the test temperature, the sample was extended, and stress readings begun. In taking a stress reading, the angle of tilt was slowly decreased, tapping rapidly on the crank shaft at the same time, (to give the apparatus a slight vibration), until a suitable flicker was observed in the neon signal bulb (a flicker equally on and off was taken as the indication of balance.) The time was noted and the angle of tilt read by means of an indicator on the base of the tilting stand; the scale on the stand is marked in half degree units, and the angle of tilt was read to 0.1 degree. In continuous relaxation experiments (in which the sample is maintained continuously at the specified elongation) the angle of tilt was maintained between readings at some value greater than that necessary to balance the stress in the sample, and was never decreased below the angle of balance, so that there was no opportunity for the sample to contract to an elongation lower than that determined by the support post. In intermittent relaxation experiments (in which the sample remains unstretched at all times, except when a stress reading is taken), the tilt was set at zero degrees between readings, the apparatus being returned to the level position immediately after each stress reading. The time required to take a stress reading on an intermittent sample was generally 15 to 30 seconds.

The weight on the sample is equal to the total weight of the cart (cart plus slotted weights) multiplied by sin α, the sine of the angle of tilt. When it is desired only to calculate f/f_0, the stress at time t divided by the initial stress, as a function of time (as was the case in the present work), this can be directly evaluated from the equation:

$$f/f_0 = \sin \alpha / \sin \alpha_0, \qquad (12)$$

where α and α_0 are the angles of balance at times t and zero, respectively. Zero time was taken as the time of the first stress measurement, for both continuous and intermittent experiments.

Measurements of permanent set were made by

FIG. 5. Permanent set frame.

use of the brass frame shown in Fig. 5. The frame consists simply of square bars at top and bottom held by support rods at the side, and provided with bolt clamps to hold the samples. An idea as to the size of the frame can be gained from the fact that the distance between the inside edges of the top and bottom bars is $6\frac{1}{4}$ in. (Fig. 5 is drawn to scale.) The frame will hold as many as five samples.

The samples used were small strips $\frac{1}{4}$ in. wide and approximately 6 in. long, cut from the thin vulcanized sheets from which relaxation samples are obtained. Two fine silver ink marks were placed on the edge of each sample an appropriate distance apart, and the distance between marks was accurately measured for each sample with a millimeter rule. The samples were then fastened to the frame, stretched to the desired elongation, and the distance between marks again accurately measured. The frame was inserted in an air oven whose temperature was thermostatically controlled to ± 0.3°C, the temperature being indicated by a thermometer with its bulb adjacent to the frame. The frame was suspended from a nail on the back wall of the oven, by means of a small L-bracket attached at the end of the top crossbar of the frame, so that the frame projected sidewise perpendicularly from the oven wall. When it was desired to remove a sample, at

various time intervals, the frame was removed from the oven, the sample quickly cut loose with scissors, and the frame immediately replaced in the oven. After the samples had cooled for 5 min., the distance between ink marks was again measured, and the permanent set of the sample calculated by the equation

$$\% \text{ Permanent Set} = \frac{l_s - l_u}{l_z - l_u} \times 100. \qquad (13)$$

The original distance between marks l_u, the distance when the sample was stretched on the frame l_z, and the distance after removal of the sample from the oven l_s, were each measured to an accuracy of 0.1 mm and the permanent set was calculated to 0.1 percent. Appropriate time corrections were applied for the time required for the oven to reach temperature after inserting the frame and for the time in which the frame was out of the oven to remove samples; the corrections necessary were small in each case.

In one case, i.e., the permanent set measurements on GR-S tread stock at 130°C, a slightly different procedure was followed in cutting the samples from the frame. In these measurements the samples were cut loose at one end without opening the oven, by the use of a razor blade attached to a rod which was manipulated through a small aperture in the back of the oven. One minute later the oven was opened and the sample was cut free from the frame with scissors, without removing the frame from the oven. The permanent set was measured 5 min. after removal of the sample from the oven, as before, and in all other respects the procedure was the same as that used for the other stocks. This modified procedure was used in order to avoid any cooling of the sample before cutting, which would result in the formation of "secondary" interchain bonds in the sample, which in turn would cause an error in the permanent set value. This effect will be discussed in more detail in the section on experimental results.

TABLE I. Recovery at room temperature.

Stock	Percent permanent set after recovery times of: 0 hr.	1 hr.	1 day (22 hr.)	1 week (169 hr.)
Hevea gum	58.3%	57.9%	56.6%	56.0%
Butyl gum	42.9%	42.9%	42.5%	42.3%
Butyl tread	57.3%	57.3%	56.3%	55.5%
GR-S tread	60.9%	60.3%	59.3%	58.9%

The time interval of 5 min. between removal of the sample from the oven and measurement of permanent set was chosen to allow the sample to cool completely to room temperature. The recovery observed on standing of the samples at room temperature was quite small, as can be seen from the data in Table I. Recovery was measured at intervals of one hour, one day, and one week after the original permanent set measurement. Samples of the four different rubber stocks studied in this paper were used, each of which was exposed for two hours at 130°C, at 50 percent elongation. It is seen that the recovery was less than 3 percent in every case after a week had elapsed, being particularly small in the case of Butyl gum.

EXPERIMENTAL RESULTS

Results of permanent set measurements, in which experimental permanent set values are compared with permanent set predicted from continuous and intermittent relaxation curves by means of the permanent set theory developed above, are shown in Figs. 6–10. These experiments were planned to include as many variables as possible: different polymer types, gum and tread type stocks, different temperatures, and different elongations. Four different rubber stocks were used in these experiments: Hevea gum, Butyl gum, Butyl tread, and GR-S tread. The compounding and cure of these stocks is given in Table II.

Permanent set results for Hevea gum stock at 130°C and 50 percent elongation are shown in Fig. 6. The continuous and intermittent relaxation curves are drawn in as solid lines; and the theoretically predicted curve of permanent set as a function of time, calculated from the relaxation curves, is drawn as a dashed line. Experimental permanent set points are shown as circles, each point, of course, being obtained from a separate sample. It is seen that the agreement between experiment and theory is excellent.

Similar data for Butyl gum and Butyl tread at 130°C and 50 percent elongation are shown in Figs. 7 and 8. Although the agreement between

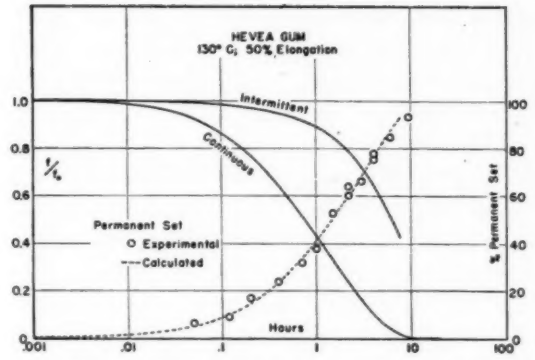

FIG. 6. Permanent set as a function of time for hevea gum stock at 130°C and 50 percent elongation.

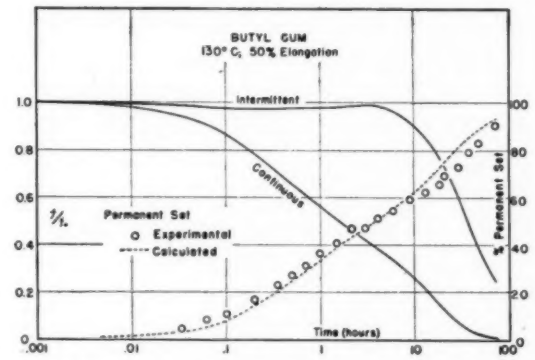

FIG. 7. Permanent set as a function of time for butyl gum at 130°C and 50 percent elongation.

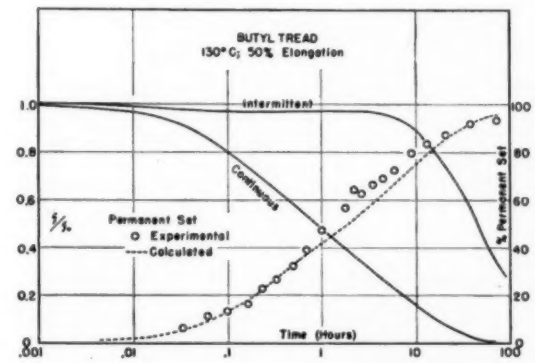

FIG. 8. Permanent set as a function of time for butyl tread; 130°C; 50 percent elongation.

the experimental points and the theoretically calculated permanent set curves is not as precise here as was the case for Hevea gum, the agreement must nevertheless be regarded as satisfactory. Duplicate permanent set points were obtained for Butyl gum at 1.00 hr., 2.20 hr., and 4.10 hr. The agreement between these duplicate samples was so close that it was impossible to

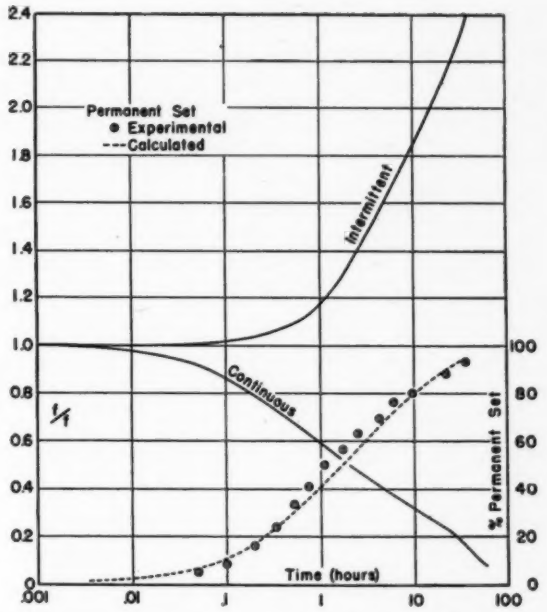

FIG. 9. Permanent set as a function of time for GR-S tread; 130°C; 50 percent elongation.

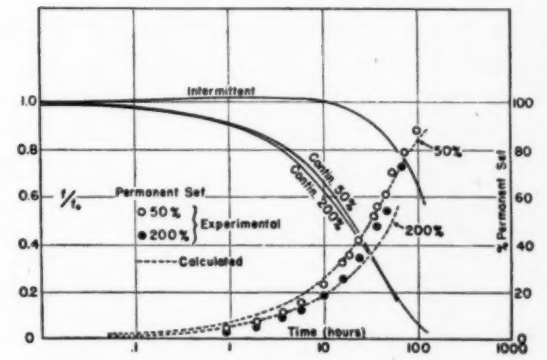

FIG. 10. The effect of elongation on permanent set. Hevea gum at 50 percent and 200 percent elongation; 100°C.

draw two separate points; for this reason these points are indicated by half circles in the graph.

Relaxation and permanent set data are shown for GR-S tread at 130°C and 50 percent elongation in Fig. 9. In this stock molecular cross-linking takes place more rapidly than scission, unlike the Hevea and Butyl stocks, in which the reverse is true. Nevertheless, it is seen that the agreement between experimental and calculated permanent set values is rather good in this case also.

It will be remembered that in this particular experiment the permanent set samples were cut at the test temperature while the oven remained

closed, rather than immediately after removal of the set frame from the oven, as was the case in the other permanent set measurements reported here. This was found to be necessary because of the formation of stable "secondary bonds" in the sample as a result of the cooling which took place on removal of the frame from the oven, before the samples could be cut. These so-called secondary bonds are not primary chemical valence bonds, but rather are weak physical inter-chain bonds (possibly of a dipole-dipole or van der Waals type) which are quite unstable at very high temperatures, but whose stability increases as the temperature is lowered. Since in terms of stress phenomena (such as permanent set) a secondary bond which has not broken has the same effect as a primary valence cross-link, the formation of stable secondary bonds by cooling of a sample at its extended length will be the same as if an increased amount of primary valence cross-linking had taken place; i.e., the observed permanent set will be increased. It is found experimentally that permanent set values obtained from GR-S tread samples cut from the frame immediately after removal from the oven are a few percent greater than the values obtained from samples cut in the oven at test temperature; and when the frame is removed from the oven and the samples allowed to cool a few minutes before cutting, the permanent set values obtained are very markedly greater than the values obtained from duplicate samples exposed for the same length of time to the elevated temperature but cut at test temperature with the oven closed. GR-S tread stock shows large secondary bond effects in general. When permanent set samples of the other stocks were cut at the test temperature in the same way, the permanent set values obtained from Hevea gum and Butyl gum samples did not differ significantly from the results in Figs. 6 and 7; permanent set values of Butyl tread samples were slightly less than the values in Fig. 8, thus slightly improving the agreement between experiment and theory. There was apparently a slight secondary bond error in the case of Butyl tread; in general it is observed that secondary bond effects are greater in tread stocks than in the corresponding gum stocks. It would undoubtedly be best to cut permanent set samples at test temperature as a standard procedure, to avoid any error due to this source.

TABLE II. Compounding of stocks.

Type stock	Hevea gum	Butyl gum	Butyl tread	GR-S tread
Polymer:				
Hevea smoked sheet	100			
GR-I		100	100	
GR-S				100
Sulfur	3	2	2	2
Zinc oxide	3	5	5	5
Stearic acid	0.5	1.5	3	3
Captax	1	0.5	0.5	1.5
Tuads		1	1	
Agerite powder	1			
Bardol				5
Channel black			50	50
Cure	75 min. at 270°F (132.2°C)	75 min. at 300°F (148.9°C)	100 min. at 300°F (148.9°C)	100 min. at 270°F (132.2°C)

In Fig. 10, permanent set data are shown for Hevea gum at 100°C at both 50 percent and 200 percent elongation. Theoretical permanent set curves have been calculated for both elongations from the continuous relaxation curves at the two elongations and the intermittent curve (obtained at 50 percent elongation) which are shown in the graph. The same intermittent curve was used for both calculations since the elongation of the intermittent sample is really 0 percent in both cases and intermittent curves in which the stress is measured at different elongations should give the same f/f_0 curve. It is seen that the experimental permanent set points for 50 percent elongation agree well with the calculated 50 percent curve. The 200 percent elongation experimental points agree satisfactorily with the calculated 200 percent curve at the earlier times, but for some reason rise somewhat above the calculated curve at the later times, having values more nearly like those of the 50 percent points than is predicted from the relaxation curves. The 200 percent experimental points appear to give a smooth curve, just as the 50 percent points do, so that apparently the effect is not fortuitous. The explanation for this deviation is not known. There is a definite difference between the 50 percent and 200 percent experimental permanent set points, however, the 200 percent points being

lower than the 50 percent points, which agrees with the predictions of the theory.

The generally satisfactory agreement of experimental permanent set data with predicted permanent set, calculated from continuous and intermittent stress relaxation curves by means of the permanent set theory developed in this paper, appears to offer a rather good confirmation of the general correctness of the molecular picture of permanent set at elevated temperatures upon which this quantitative permanent set theory is based.

ACKNOWLEDGMENT

This work was done at Princeton University with the cooperation of the Firestone Physics Research Group. The authors wish to thank F. S. Grover for his work in constructing the tilting relaxometer. Valuable suggestions made by Professor H. S. Taylor and Dr. J. H. Dillon are gratefully acknowledged. The permission of the Firestone Tire and Rubber Company, who sponsored this work, to publish these results is appreciated.

Calendar of Meetings

May

6–7 Inter-Society Color Council, New York, New York
6–10 Society of Motion Picture Engineers, New York, New York
10–11 Acoustical Society of America, New York, New York
27–29 American Geophysical Union, Washington, D. C.

June

2–5 American Society of Refrigerating Engineers, St. Paul, Minnesota
10–14 American Society for X-Ray and Electron Diffraction, Silver Bay (Lake George), New York
13–14 Institute of Aeronautical Sciences, Detroit, Michigan
17–20 American Society of Mechanical Engineers, Detroit, Michigan
20–22 American Association of Physics Teachers, St. Louis, Missouri
20–22 American Physical Society, Chicago, Illinois
20–23 Society for the Promotion of Engineering Education, St. Louis, Missouri
24–28 American Institute of Electrical Engineers, Detroit, Michigan
24–28 American Society for Testing Materials, Buffalo, New York

July

12–13 American Physical Society, Berkeley, California
17–19 American Society of Civil Engineers, Spokane, Washington

August

14–15 Institute of Aeronautical Sciences, Los Angeles, California
19–20 Mathematical Association of America, Ithaca, New York

September

9–13 American Chemical Society, Chicago, Illinois
16–20 The Instrument Society of America, Pittsburgh, Pennsylvania
18–21 Illuminating Engineering Society, Quebec, Canada
19–21 American Physical Society, New York, New York
30–October 3 American Society of Mechanical Engineers, Boston, Massachusetts

Crystallization of Unvulcanized Rubber at Different Temperatures

LAWRENCE A. WOOD AND NORMAN BEKKEDAHL
National Bureau of Standards, Washington, D. C.

The crystallization and melting of unvulcanized natural rubber in the unstretched state have been investigated at different temperatures. Change of volume has been used as a quantitative measure of the extent of crystallization, and mercury-filled dilatometers containing the rubber have been used for the volume measurements. Crystallization was observed to occur at temperatures between −50° and +15°C and to be most rapid at about −25°C. The final decrease of volume on crystallization was usually found to lie between 2.0 and 2.7 percent. The melting of the crystalline rubber was found to occur over a range of temperature and to be strongly dependent on the temperature at which the crystals were formed. The temperature at which the beginning of melting occurs is from 4° to 7° above the temperature of crystallization. The range of melting is about 35° at the lowest temperatures and decreases to about 10° at the highest. The same range of temperature of melting is obtained regardless of the extent of the crystallization.

I. INTRODUCTION

CRYSTALS may be formed in natural rubber under quite varied experimental conditions. Different combinations of stretching and cooling have been used to induce crystallization in unvulcanized and in vulcanized rubber. The appearance and disappearance of crystals have been studied by observations of the volume,[5, 8] heat capacity,[6] light absorption,[53] birefringence,[40, 58, 63, 67, 74] x-ray diffraction,[22] and hardness[53] and other mechanical properties.[42] There has, however, been no comprehensive study of the effect of temperature on the crystallization. The present investigation was undertaken in order to explore this field.

In the work reported here it has been the aim to study the crystallization at different temperatures under the simplest possible conditions. The main features of the crystallization of vulcanized rubber have been shown[8] to be similar to those of the crystallization of unvulcanized rubber, the vulcanization causing a decrease in the rate of crystallization. Consequently unvulcanized rubber was selected for study. Stretching obviously adds complication to the experimental conditions, and so was not employed. Of the different methods of measuring crystallization, it seems that change of volume is the simplest and best adapted to yielding quantitative data about the course of the crystallization or fusion. The present work therefore is concerned with a general study of the volume changes in unvulcanized rubber at different temperatures.

II. EXPERIMENTAL PROCEDURE

The volume changes of the specimens were measured by the use of dilatometers with confining liquids. The technique incorporates some improvements over that previously used.[5, 8] The dilatometers were made of Pyrex glass and each consisted merely of a bulb with a capillary tube sealed to it. Changes in volume could be calculated from measurements of changes in the height of the confining liquid in the capillary tube. Mercury was selected as the confining liquid because it seems to have no effect on rubber, even when the two are in contact for periods of several years. Some absorption, swelling, and softening usually occur with other liquids. The specimens were strips cut from plantation smoked sheet rubber.

The construction of the dilatometers and the procedure of filling them were somewhat improved during the course of the work reported here. In the later dilatometers the capillary tubes were about 2 mm in inside diameter and about 500 mm in length. They were specially selected capillaries, but were not of the precision-bore type recently developed. They were graduated in millimeters along their length. The tubes were calibrated by sealing a stopcock to one end, and observing the lengths of weighed amounts of mercury at five or more different points along each tube. The maximum variation in cross-sectional area along a single capillary was found to be about 3 percent in most cases. Each capillary was then sealed to a glass tube about 15 mm

in inside diameter, the other end of the tube being left open. Into the glass tube were inserted a weighed rubber specimen and a hollow glass bulb about 40 or 50 mm long. Finally the open end of the glass tube was sealed off to form the bulb of the dilatometer.

This construction made it possible to avoid heating of the specimen during the sealing operation, without unduly increasing the net volume of the dilatometer bulb. In most cases the volume of the specimen was between two and three times the volume of the mercury in the bulb of the dilatometer. The effect of the insertion of the hollow bulb is equivalent to a mere reduction of the net volume of the dilatometer bulb. Since the inner hollow bulb was made of the same type of glass as the rest of the dilatometer, neither its volume nor its expansivity entered directly into any of the calculations.

The dilatometer was next evacuated for several days to remove gas from the specimen. Mercury was then admitted to the evacuated system through a two-way stopcock, until it filled the dilatometer bulb and stood at a suitable height in the capillary. Occasionally it was necessary to carry out further removal of gas until the height of the mercury in the capillary did not change by more than a few millimeters as the pressure was again raised to that of the atmosphere. Calculation showed that the gas remaining under these conditions would have a negligible effect on the observed specific volume and expansivity. The dilatometer was weighed before and after the addition of the mercury.

The volumes of specimen and mercury at 25°C were determined from their weights and densities. The densities of the rubber specimens at this temperature were measured by the method of hydrostatic weightings. The volume of the dilatometer up to the level of the mercury in the capillary at this temperature was obtained as the sum of the volumes of the mercury and the specimen. At any other temperature the volume up to the same point on the capillary was found from the known expansivity of Pyrex glass. The volume of the dilatometer up to any other point on the capillary could then be calculated from the calibration of the capillary. The volume of the specimen corresponding to each observation was obtained by subtracting from this volume, the volume of the mercury at the temperature of the observation.

After the specimens and dilatometers had been prepared, they were usually placed in a stirred bath of about 6 liters of alcohol cooled by solid carbon dioxide to a temperature of about −39°C, an approximate lower limit set by the freezing of the mercury. Observations of the height of the mercury in the capillary were made as the temperature was raised to +55°C at a rate of the order of 0.5°C per minute. At the lower temperatures the bath was warmed at about this rate by the heat from its surroundings. Beginning at about −10°C additional heat was furnished by means of a knife-type immersion heater controlled by a Variac. The alcohol was usually replaced with water for measurements above room temperature. In this manner the volume-temperature relation of the amorphous rubber was obtained. This relation, which is linear over a considerable range of temperature, will be described and discussed in greater detail later in connection with the melting of crystalline rubber.

It was found in preliminary experiments that at a heating rate of 0.5°C per minute or less no observable differences from the equilibrium values of the volume could be noted. At a heating rate of about 1°C per minute the apparent volume lagged behind the equilibrium value by an amount equivalent to about 1°C. At a heating rate of about 2° per minute, the lag was about 2°C.

The dilatometers were next placed in a small unstirred alcohol bath in a refrigerator at the temperature at which it was desired to crystallize the rubber. Observations of the height of the liquid in the capillary tube were made periodically and usually continued until no further volume change could be noted.

When it was observed in this manner that the rate of crystallization had become inappreciable, the specimens were placed in the stirred bath of alcohol cooled by solid carbon dioxide to a temperature of about −39°C. Observations of the volume were made as before, as the temperature was raised, and the volume-temperature relation of the crystalline rubber was obtained.

In a number of cases, to be described in detail later, there were deviations from this standard procedure for the purpose of studying the effect

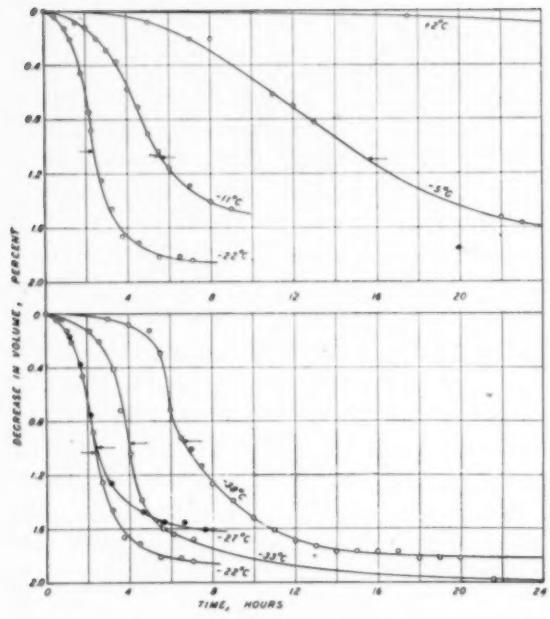

FIG. 1. *Crystallization of rubber at different temperatures as indicated by decrease in volume.* The arrows indicate the estimated values for half the total decrease of volume at each temperature.

of varying some of the experimental conditions, or because the importance of some of the exact conditions was not realized at the time the experiment was performed.

III. EXPERIMENTAL RESULTS

1. Rate of Crystallization

When crystallization was carried out according to the procedure just described it was found that the rate was very low at first, increased to a maximum, and decreased to a negligible value. The volume-time relation at constant temperature thus has the sigmoid shape which has previously been given[5, 8, 69] for crystallization near 0°C. Figure 1 shows two families of such curves, one for crystallizing temperatures of −22°C and above and the other for −22°C and below.

Since the volume is changing very slowly in the final stages, a determination of the time required for completion is somewhat uncertain. The time required for one-half the total volume change is much more precisely determinable since the curves are usually steepest near this point. The time required for half the volume change has been measured at a number of different temperatures. The reciprocal of this time, it can be readily seen, is a measure of the average rate of crystallization during the first half of the process. It is plotted as a function of temperature in Fig. 2.

2. The Melting of Crystallized Rubber

When the volume-temperature relation of crystalline rubber is investigated, as already described, curves of the type shown in Fig. 3 are obtained for increasing temperatures.

It can readily be seen that melting of the crystals occurs over a range of temperature, and that the range is markedly dependent on the temperature at which crystallization has occurred.[7] The temperature corresponding to the beginning of melting is that at which the volume begins to deviate from the curve representing the normal thermal expansion of crystalline rubber. Over the range of temperatures under consideration here the normal expansion curve is linear, and the temperature at which deviation begins to occur can be located within about one-half a degree. Similarly melting is complete when the volume again reaches the nearly linear curve which represents the volume-temperature relation of amorphous rubber and which was evaluated earlier.

There was found to be no evidence of any time lag or delay in melting of the crystals after the establishment of thermal equilibrium. For example, at any constant temperature in the melting range the volume was never observed to increase with time. In this range if the temperature is lowered, the volume-temperature relation is observed to be linear and intermediate between the amorphous and crystalline volumes. Rubber

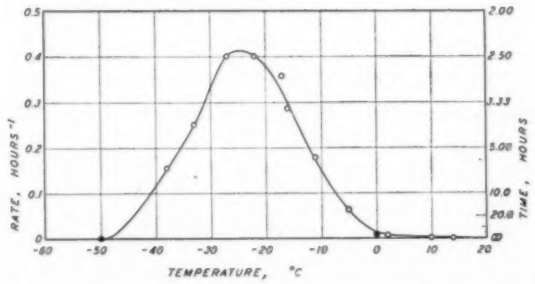

FIG. 2. *Rate of crystallization of rubber.* The rate plotted is the reciprocal of the time required for one-half the total volume change.

in the partially-melted state, however, can undergo additional crystallization with a resulting decrease of volume. If the temperature at which the additional crystallization occurs is the same as that at which the first crystallization has occurred, the melting curve is identical with that obtained from the complete melting of the first crystals. If the additional crystallization occurs at a different temperature from the first crystallization, two different ranges of melting will be observed, corresponding independently to the two temperatures of crystallization. Further discussion of this effect will be given below in the section on stark rubber and is illustrated in Fig. 7 in that section.

The additional crystallization possible in partially-melted rubber mentioned in the preceding paragraph is considered in more detail in the section dealing with recrystallization. At this stage, however, it should be pointed out that the phenomenon may give rise to difficulty in determining the upper end of the melting range itself.

The rate of crystallization at certain temperatures was sufficiently great to permit significant recrystallization during the time that the temperature was being raised through the melting range of the original crystals. Since the recrystallization took place at a higher temperature than the original crystallization, the new crystals melted at a higher temperature than the original crystals, and the apparent upper end of the melting range was displaced upward by an amount which depended on the rate of temperature rise during melting.

When the initial crystallization occurred below 0°C, therefore, the upper end of the melting range was determined from a series of experiments at each temperature of crystallization. A stirred bath was adjusted to the approximate temperature of the upper end of the melting range. The dilatometer was then removed from the bath in which the original crystallization had been taking place and plunged into the stirred bath. The volume of the specimen increased because of both thermal expansion and the melting of the crystals. In less than five minutes, a reasonable time for the establishment of temperature equilibrium, the volume became constant. After an interval of time, the volume began to decrease because of recrystallization at the temperature of the stirred bath.

If the value of the volume when temperature equilibrium had become established and before observable recrystallization had occurred was the same as that originally observed for amorphous

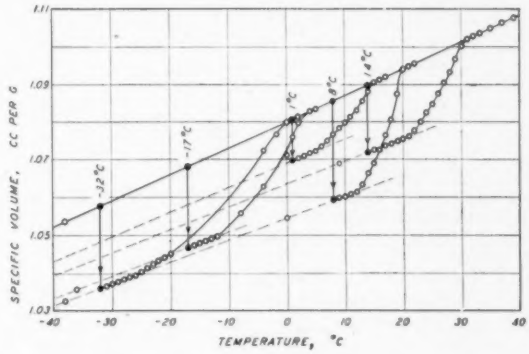

FIG. 3. *Crystallization of rubber at different temperatures and subsequent melting.* The change of specific volume on crystallization is indicated by the vertical lines joining the dark circles.

rubber at the corresponding temperature, it was concluded that the temperature of the stirred bath was at or above the upper end of the melting range. If the volume at equilibrium was less than that of the amorphous rubber at that temperature the conclusion was drawn that the melting was incomplete and that the temperature of the bath was below the upper end of the melting range. As might be expected the volume at equilibrium was never found to be greater than the volume of the amorphous rubber. A series of experiments of this sort served to locate the upper end of the melting range corresponding to a single temperature of original crystallization, and an additional series was required for each other temperature.

If the initial crystallization occurred at 0°C or above, the rate of recrystallization during melting was found to be so small as not to be significant during the time the specimen was in the melting range when the usual heating rates were employed. At these temperatures the range was of the order of 10° or less, and the time required to cover the range was usually between 20 and 30 minutes. The upper end of the melting range was determined from curves of the type shown in Fig. 3 for all cases where the initial crystallization was at 0°C or above.

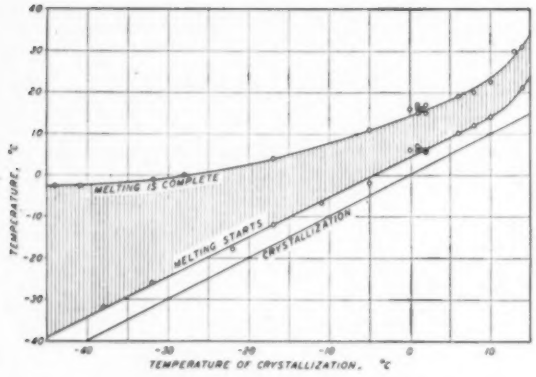

FIG. 4. *Melting range of crystalline rubber as a function of the temperature of crystallization.* The lower line shows the crystallization temperature also as ordinate for easier comparison with the range of melting.

The results of a number of individual experiments of this sort are plotted in Fig. 4 which shows the melting range as a function of the temperature of crystallization.

In one series of experiments a specimen was successively crystallized and melted 16 times. After each melting the temperature was raised by different amounts varying from 1° to 40° above the end of the melting range. In all cases the same melting range was obtained on subsequent crystallization at a fixed temperature.

3. Partial Crystallization

The melting range of partially-crystallized rubber has been found to be the same as that obtained when the crystallization is more nearly complete. Data regarding this point were obtained from a series of experiments in which the specimen was kept at 2°C for different lengths of time, and the melting range of the resulting crystals then measured. In the first experiment after 20 days of crystallization the volume decrease amounted to 2.7 percent. In the second experiment crystallization was interrupted at the end of 9 days when the volume change amounted to only 1.0 percent (or 37 percent of the volume change in the first experiment). In the third experiment by interruption of the crystallization after 1 day the volume change was limited to 0.085 percent (or 3.1 percent of that in the first experiment). The melting range in all three cases was 6° to 16°C within the accuracy of determination. On the basis of these experiments the crystallization in some cases was not carried completely to the point where the volume had ceased to change at a significant rate. Cases of this sort will be observed in Fig. 3.

4. The Recrystallization of Rubber

It will be noted that in the cases previously described the specimens were heated to at least 55°C immediately before crystallization. The purpose of this heating was to destroy centers of crystallization which might have been persisting from previous crystallizations, and which would have altered the rate of crystallization. A study of the rate of recrystallization when the specimen had not received such heating will now be described.

The preliminary crystallization was first carried out overnight at −33°C according to the standard procedure already described. The specimen was then plunged into a bath held at 0°C and observations made of the change of volume with time. It will be noted from Fig. 4 that the melting of crystals formed at −33°C is complete below 0°C. At first there was a volume increase due to thermal expansion and to the melting of the crystals. This change was found to be complete within about 5 minutes, a reasonable time for the establishment of thermal equilibrium. After an interval of time there was a volume decrease due to recrystallization at 0°. The whole procedure was repeated with the preliminary

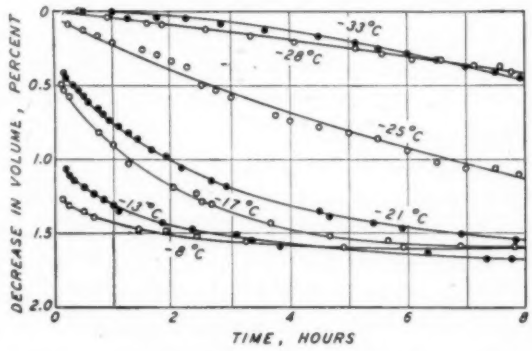

FIG. 5. *Recrystallization of rubber at 0°C.* The curves show the change of volume as a function of time, after preliminary crystallizations at the fixed temperatures indicated on the curves. The zero on the ordinate axis represents the volume of amorphous rubber at 0°C. The zero on the time scale represents the time at which the dilatometer was plunged into the bath at 0°C. Observations taken in the first five minutes, before the attainment of temperature equilibrium, are omitted. The upper ends of the melting ranges as read from Fig. 4, corresponding to the different temperatures of preliminary crystallization are −2°, −1°, +1°, +2°, +4°, +6°, and +9°C, respectively.

crystallization occurring at −28°, −25°, −21°, −17°, −13°, and −8°C, respectively. The results are reproduced in Fig. 5.

Very similar results were obtained when the conditions were altered so that the preliminary crystallization was carried out in each case at −18°C and the recrystallization at temperatures of −8°, −4°, 0°, +1°, and +4°C, respectively. The results are shown in Fig. 6. The significance of these results is discussed in a later section.

5. Stark Rubber

When received in temperate climates, crude rubber is sometimes found to be crystallized[28,29] and to have a melting range above room temperature. For convenience in the present discussion, crystalline rubber having a melting range extending above 25°C will be called stark rubber in accordance with the suggestion of Pickles[51] and Whitby[72] since it is stiff and rather rigid at room temperature. The use of such a term is not intended to imply any essential fundamental difference between stark rubber and that melting at lower temperatures. It is to be presumed on the basis of Fig. 4 that during the formation of the crystals in stark rubber conditions were such that the stark rubber was crystallized at temperatures higher than about 10°C. No cases, other than those in the present paper, seem to have been reported in which the temperature of crystallization was measured (or even estimated, within 10°C) during the formation of stark rubber.

One sample of stark rubber, for which the authors are indebted to Professor H. I. Cramer, formerly of the University of Akron, was found to have a melting range from about 32° to 39°C. When specimens of this stark rubber were placed in a dilatometer and held at a temperature of about 1°C for 48 days considerable additional crystallization occurred, most of it within the first few days. When the specimens were melted in the usual manner the curves shown in Fig. 7 were obtained. The line between 16° and 32°C passes through the points obtained before the stark rubber was held at 1°C for the additional crystallization.

In another experiment one end of a strip of stark rubber was immersed in water at 50°C for a few minutes. The lower end was thereby melted

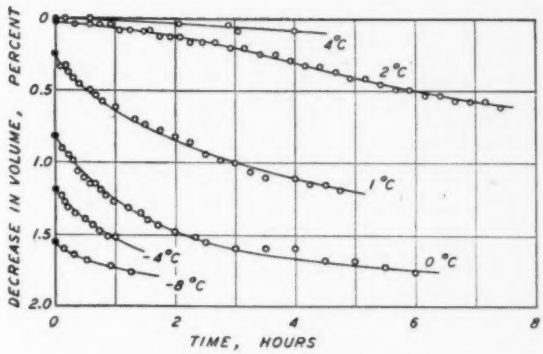

FIG. 6. *Recrystallization of rubber after preliminary crystallization at −18°C.* The curves show the change of volume as a function of time at the temperatures indicated. The zero on the ordinate axis represents, in each case, the volume of amorphous rubber at these temperatures. The zero on the time scale represents the time at which the dilatometer was plunged into the bath at the temperatures indicated. The dark circles represent the volume observed immediately after the attainment of thermal equilibrium. The upper end of the melting range, as read from Fig. 4, corresponding to preliminary crystallization at −18°C is +4°C.

while the upper end remained in the stark condition. When the whole strip was placed in a refrigerator at 1°C for several weeks, the lower end crystallized and could not be distinguished by visual or tactual observation from the upper end. However, when the strip was allowed to come to room temperature, the crystals in the lower end melted, as would be expected from Fig. 4, while the upper end remained stark.

IV. DISCUSSION OF RESULTS

1. The Rate of Crystallization

It should be recognized that the measurements reported here regarding the rate of crystallization were all made on not more than two or three specimens of smoked sheet which had been heated to 55°C immediately before the crystallization. The conditions of preparation of the rubber from the latex undoubtedly have a considerable influence on the rate of crystallization.[42] Uncoagulated latex itself showed no volume change when kept in a dilatometer at 2°C over a period of several months. This behavior confirmed previous observations in this laboratory.[5] Likewise, qualitative observation showed that crystallization was extremely slow in a sheet of evaporated latex. In this case crystallization appeared to take place most readily in certain regions. This effect is similar to the "patchy

crystallization" described by Treloar,[69] who reported that visual observations on a sample of smoked sheet showed that neighboring portions crystallized at widely different rates. No attempt was made in the present work to investigate the exact reasons for such differences. Various factors which have been reported to increase the rate of crystallization are residual stresses remaining after previous mechanical treatment, moderate pressure[40, 65, 66, 77] and exposure to a beam of x-rays.[47] Very high pressures may inhibit crystallization.[18] The effect of previous thermal treatment on the rate of crystallization is discussed in the sections dealing with recrystallization.

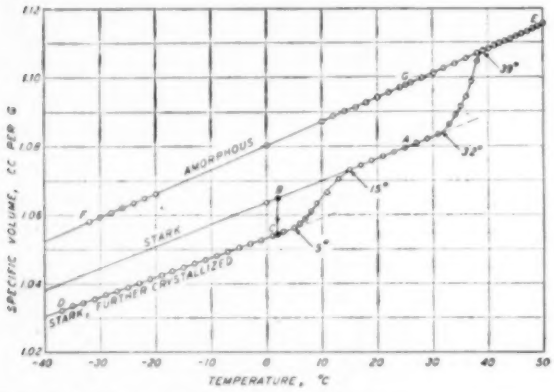

FIG. 7. *Further crystallization and melting of a sample of stark rubber.* The specific volume of the sample as received is shown at *A*. It was cooled to *B*, where further crystallization occurred, reducing the specific volume to *C*. After cooling to *D* the temperature was raised to *E*. The temperature was lowered to *F* and then raised to room temperature at *G*.

It would appear reasonable from theoretical considerations to suppose that an increase of mobility of the atomic chains, brought about for example by mastication of the rubber, would increase the rate of crystallization. Although van Rossem and Lotichius[53] could find only insignificant differences in the rate of crystallization with increasing times of milling, Katz,[35] Gehman,[22] and Cotton[17] all state that masticated rubber crystallizes more readily than unmasticated. The reverse effect, a decrease in the rate of crystallization caused by a decrease in the mobility of the chains on vulcanization has already been described.[8]

The rates of crystallization observed in the present work are in reasonable agreement with observations of density by Bekkedahl[5] and Treloar[69] at 0°C, by Smith and Hanna[56] at −20°C, and by van Rossem and Lotichius[53] at 4°C and −10°C. Likewise a similar rate can be calculated from observations of Young's modulus at 0°C made by Conant and Liska.[16]

2. Lower Limit of Temperature of Crystallization

It has been recognized for some years that rubber does not crystallize at extremely low temperatures. No crystallization was evident in a specimen[5] cooled at −259°C, or in another[52] held at −190°C for 8 days. Other specimens[5, 49] were kept between −50°C and −78°C for 3 weeks without the occurrence of crystallization but did crystallize at −35°C and above. The present work serves to locate more definitely the lower limit of temperature at which crystallization is possible as about −50°C. Figure 2 shows that the rate of crystallization has become negligible below this temperature. Here the mobility is presumably insufficient to permit the orientation necessary for the formation of crystals. The supercooling of rubber is similar in this respect to that of selenium,[45] sulfur, and many organic liquids.

3. Upper Limit of Temperature of Crystallization

Crystallization has not been reported at the room temperatures (usually above 20°C) normally maintained in American laboratories. No evidence of it was noted in the present investigation when dilatometers were kept at room temperature over a period of a year or more. In European laboratories, however, where the temperatures are frequently near 15°C, the crystallization of rubber on storage has been noted on a number of occasions.[38, 44, 46, 52] Cotton,[17] for example, states: "When smoked sheet and crepe rubber have been in storage for some time, they gradually harden and assume a frozen condition. This is due to crystallization." In the present work the highest temperature at which crystallization was observed was 14°C. At this temperature under the experimental conditions described here the time required for crystallization is of the order of years. Crystallization at this temperature was continuing at an approximately constant rate when the experiment was discontinued after 289 days.

The crystallization observed in European laboratories appears to occur at a more rapid rate than this. Quite probably temperatures lower than 15°C during the night initiated the crystallization and the crystals then formed were not melted near 15°C during the day.

It is possible to increase the rate of crystallization by varying the previous thermal or mechanical treatment of the specimen, and thereby forming more centers of crystallization. Consequently, it is likely that the upper limit of temperature of crystallization shown in Fig. 2 may be raised somewhat by the proper previous treatment of the rubber.

4. Temperature at which Crystallization is Most Rapid

The rate of crystallization was found to be a maximum at a temperature near −25°C, as can be seen in Fig. 2. In the production of the form of raw rubber known as "cut sheet" or "patent rubber,"[27] developed in Europe many years ago, rubber is crystallized so that it can be cut into sheets. The rubber is often held at a temperature of about −5° for a few days in order to bring about the crystallization. More recent books[9, 64] state that the rubber should be held between −5° and −10°C for at least six days. No quantitative study of the rates at different temperatures, as in the present work, seems to have been reported previously.

5. Magnitude of the Volume Change on Crystallization

The magnitude of the percentage decrease of volume on crystallization can be noted from curves of the type shown in Fig. 1. The actual specific volume of the amorphous rubber varies with temperature, and can be read from curves like those in Fig. 3. The decrease of specific volume on crystallization is of course found to be the same as the increase of specific volume on subsequent melting. However it might be pointed out that the percentage decrease of volume is not quite the same as the subsequent percentage increase of volume, since they are fractions of different quantities. Furthermore, any comparisons must be made at the same temperature.

In the present work in most cases the decreases of volume on crystallization were found to lie between 2.0 and 2.7 percent. Repeated crystallizations of the same specimen under conditions which were thought to be identical did not always lead to the same volume changes. It seems possible that such variations are statistical fluctuations occasioned by the growth of crystals from different centers in different cases. There was an even greater variation in the decreases of volume when different specimens were studied but in almost all cases the values lay within the limits given. The exact value, within these limits, seems to depend upon factors which were not under control.

Values for this quantity, calculated from measurements of density or specific gravity reported by previous workers[4, 5, 8, 14, 19, 31, 39, 53, 55, 56, 72] generally lie within the same limits, although a few are somewhat lower. Holt and McPherson[32] found a volume change of about 1.85 percent on stretching a specimen of vulcanized rubber to an elongation of 700 percent at 25°C. Treloar[69] by stretching unvulcanized rubber at 0°C, observed a volume decrease of over 3 percent, the highest value reported. With unstretched pale crepe he found a volume decrease of 2.3 percent on crystallization at 0°C.

Observations made in the course of the present work furnish no data from which conclusions may be drawn as to the relative amounts of crystalline and amorphous material in a specimen.

Field[21, 24] has recently conducted x-ray studies of this proportion of crystalline and amorphous components in stretched rubber, and concludes that under favorable conditions about 80 percent of the material is in the crystalline state, in agreement with an earlier study by Meyer and Mark.[43] This value is considerably higher than those estimated by Parks[50] and Wildschut[73] by other methods. If reliance is to be placed on x-ray values, it would be very desirable to conduct several parallel studies of crystallization by means of x-rays and by means of observations of volume change. In this manner the relation between the percentage decrease of volume and percentage of crystalline material could be established.

6. Melting of Crystallized Rubber

The melting of the crystalline rubber is very much dependent on the temperature at which the

TABLE I. Melting temperatures of crystalline rubber previously reported.

Melting						
Lower limit °C	Maximum change °C	Upper limit °C	Crystallization temperature °C	Observers	Technique	Remarks
	43.5			Whitby[72]	Density	
	43			Whitby[72]	Density	
	41			Whitby[72]	Density	
	41			Barnes[4]	Visual	{Flexibility {Transparency
40				Wood, Bekkedahl, and Peters[78]	Linear expansion	
40		50	5 to 15	Feuchter[19]	Density	After 1 year
	up to 37			Katz[36]	X-ray	
	36			Katz[37]	X-ray	"old rubber"
	37			van Rossem and Lotichius[53]	Density, hardness, and light absorption	
35		45		Meyer, von Susich, and Valko[44]	X-ray	
35				Wood, Bekkedahl, and Peters[78]	Linear expansion	
34	36	>40		van Rossem and Lotichius[53]	Density	Stored 13 years
	35			Feuchter and Hauser[20]	Retraction	1 year after racking
		35 to 40		von Susich[60]	X-ray	
31.5		33		Cotton[17]		"Normally frozen"
30		40		Feuchter[19]	Density	Masticated
30		39		Katz[36]	Density	
30	33	35		Pickles (van Rossem)[51]	Density	
28	32	35		van Rossem and Lotichius[53]	Density	
27		29		Katz[36]	X-ray	"Cut sheet"
25		36		Feuchter and Hauser[20]	Retraction	Racked
20		30		Katz[36]	X-ray	
20		30		Bunschoten[14]	Density	

crystals have been formed, as can be seen from Figs. 3 and 4. This conclusion seemed so surprising that it was made the subject of a preliminary communication[7] based upon only a part of the data reported in the present paper.

It can be seen that the higher the temperature of crystallization the higher are the temperatures at which both the beginning and ending of the melting occur. The beginning of melting occurs at a temperature of from 4° to 7° above that at which the crystals have been formed. For all temperatures of crystallization below about −35°C the temperature at which melting is complete is about −2°C.

The range of melting becomes narrower the higher the temperature of crystallization up to about 0°C; for crystals formed at temperatures between 0° and 14°C, the range of melting is about 10°; for crystallization at higher temperatures no direct observations are available, but the range is probably narrower, since it appears that stark rubber has a somewhat narrower range of melting the higher the mean temperature of the range.

The results presented here undoubtedly explain many previously reported discrepancies in the temperatures of melting of crystalline rubber. Unfortunately in only a few cases have previous workers specified the temperature at which crystallization occurred. The variations in the melting have sometimes been thought to be connected with the variety of rubber, or the experimental technique. In most cases no explanation at all was attempted. Table I presents the results of measurements of the melting temperatures of crystalline rubber, as reported by previous observers. In those instances in which the temperature of crystallization was reported the only pronounced deviations from the results of Fig. 4 are in the few instances where the crystals were

TABLE 1.—*Continued.*

Melting						
Lower limit °C	Maximum change °C	Upper limit °C	Crystallization temperature °C	Observers	Technique	Remarks
20	25	30	Cool cellar	Ruhemann and Simon[54]	Specific heat	Smoked sheet
		<30	−5.8	Carson[15]		
20		24		Hock[31]	Retraction	
20		23		Hock[30]	Retraction	
20		23	7 to 10	Thiessen and Kirsch[65]	X-ray	Crystallized under pressure of 10–25 atmospheres
10	18	30	−15	Ruhemann and Simon[54]	Specific heat	"Cut sheets" crystallized at 150 atmospheres
11		13	6	Thiessen and Kirsch[66]	X-ray	Pressure of 30 atmospheres
9.5		11	−58 to −43	Smith, Saylor and Wing[59]	Birefringence	Sol rubber crystallized from solution
8		10		Cotton[17]	Visual	Frozen in refrigerator
		<20	0 to 2	Katz and Bing[38]	X-ray	
		<20	−5 to −10	Katz[34]	X-ray	
		<20	−10	Katz and Bing[38]	X-ray	
6	11	17	2	Bekkedahl and Wood[8]	Volume	Vulcanized rubber
6	11	16	0	Bekkedahl[5]	Volume	
	10			Park[48]	—	
2		14	−10	van Rossem and Lotichius[53]	Density and hardness	
0	5	10		Ruhemann and Simon[54]	Specific heat	
−2		14	−50	Smith and Saylor[57]	Birefringence	Gel crystallized from solution
−5.5		16	−25	Smith and Saylor[58]	Birefringence	
−15	11	17	<0	Bekkedahl and Matheson[6]	Specific heat	
	0			Bunn and Garner[13]	—	
−20		10		Ruhemann and Simon[54]	Specific heat	Beta-anomaly

formed from solution rather than from the bulk material.

A study of the table confirms the conclusion of the present investigation that there are not merely two forms of crystalline rubber, as has sometimes been suggested[5,17] but rather that crystals melting at any temperature between about −40° and +45°C may be formed in rubber by the proper choice of temperature for crystallization. It is rather surprising that such a conclusion has not been already drawn on the basis of the experimental data shown in Table I. The assignment of a definite melting point or melting range to rubber in general is thus seen to be without meaning in spite of the many investigators who have hoped to do so.[5,13,17,30,44,48,66] A recent writer[12] on the subject expresses considerable wonder at the variability of the melting point.

The temperature at which retraction of stretched rubber occurs is sometimes associated with the melting of crystals formed on stretching. Although the scope of the present investigation did not include any measurements on stretched rubber some of the results may probably be safely applied to crystals formed by stretching. For example the influence of the temperature of crystallization on the melting seems to furnish an explanation of certain effects observed by Treloar[68] in the retraction of stretched rubber. He found that the recovery temperature was dependent on the temperature at which stretching was performed. Lacking the results reported here, he said "One would not expect the melting point of the crystals to depend on the temperature at which they were formed."

Some years ago van Rossem and Lotichius[53]

made a rather careful study of the crystallization of raw rubber. In the main, there seems to be no disagreement between their experimental results and those contained in the present paper. In one instance it now seems desirable to give to their results an interpretation different from the one originally given.

This instance, which is one of the best-known of the conclusions of van Rossem and Lotichius, is a statement that the melting temperature of one sample of stark rubber was 31°–33°C in 1919 and had become 35°–37°C in 1927. An examination of the graph giving the specific gravity values which are the basis for discussion shows that the terms "melting temperature" or "melting point" were limited to the steepest portions of the curves. The full melting range of the specimen observed in 1919 appears to extend from 28° to 35°C. The observations made in 1927 show that the melting range began at 34° and extended above 40°C, the highest temperature at which observations were made. Since the specimen measured in 1927 was not completely melted at 40°, its specific gravity did not come down to the value characteristic of the amorphous rubber, as did that of the specimen measured in 1919, where melting was apparently complete at 35°C. No indications were given regarding the temperature at which the specimen was stored from 1919 to 1927. The observed change of melting range could be explained on the reasonable assumption that the temperature, at least part of the time, was between 28° and 34°C. Crystals melting below 34° would then be melted, and re-crystallization at those temperatures would yield new crystals having a higher melting range, as already described in the section on recrystallization.

Thus there seems to be no assurance that van Rossem and Lotichius would have found a rise in the melting range during storage at a constant temperature below 28°C. No such rise was observed in the course of the present work. The actual phenomena observed by van Rossem and Lotichius can then be explained in terms of the results of the present paper, without recourse to speculative assumptions of changes in crystal size or polymerization.

The considerations developed in the present work on the melting of crystalline rubber have already been applied[75] to explain results obtained by Ruhemann and Simon[54] in measurements of specific heat. It has been pointed out that the beta-anomaly which they observed can be explained as a phenomenon of crystallization under the particular conditions of their experiments, without the assumption of an anomaly characteristic of rubber in general. The volume-temperature graphs which they give for rising temperatures are of the same form as those obtained in the present work when the rate of temperature rise was slow enough to permit recrystallization and subsequent melting at higher temperatures.

7. Recrystallization

A number of interesting conclusions may be drawn from the experiments on recrystallization illustrated in Figs. 5 and 6. In the first place the rate of crystallization at a given temperature is much greater than in the instances previously discussed, where the standard procedure called for heating to at least 55°C before each crystallization to destroy possible centers of crystallization. An examination of Fig. 1 shows that at 2°C after such treatment the change of volume in the first 10 hours is about 0.05 percent. On the scales used in Figs. 5 and 6 such a change would hardly be perceptible and the experimental points would lie on an almost horizontal line through the origin. In the second place the effects of the preliminary crystallization in increasing the rate of subsequent crystallization extend at least several degrees above the upper end of the melting range. For example it is clear from Fig. 6 that the melting range does not extend above 4°C, since the initial ordinate is zero for the recrystallization at 4°C. The rate of recrystallization at 4°C is seen to be of appreciable magnitude in comparison with the much lower rate which is observed when the centers of crystallization are destroyed by previous heating to 55°C.

The selection of a temperature of 55°C as being sufficient to destroy centers of crystallization was based on the fact that it was five or ten degrees above the highest temperature at which any crystals have been reported in unstretched rubber, as noted in Table I. In numerous experiments no evidence of any effect of previous thermal history was found persisting in any sample after heating it to 55°C.

Attention should be called to the two different types of crystallization curves shown in Figs. 5 and 6. At temperatures below the upper end of the melting range the rate of crystallization has its largest value at the beginning and decreases with increasing time. At temperatures above the upper end of the melting range the rate of crystallization is small at the beginning, increases with time to a maximum, and, when observations are carried out over a sufficiently long period, decreases again to a negligible value. The latter curves are thus of the sigmoid type shown in Fig. 1. One can therefore conclude from Fig. 5 alone that the end of the melting range would be at 0°C following crystallization at a temperature between −25° and −28°C. From Fig. 4 this temperature is read as −28°C.

In terms of the usual conceptions of crystal growth it is possible to give a simple explanation of the difference between the two types of curves. In accordance with the ideas of Tammann and others[3, 23, 25, 33, 61, 62, 71] a crystal can be initiated only at certain centers or nuclei. The crystal, once initiated, grows from the center at a characteristic rate, called the linear crystallization velocity, until the available crystallizable material between it and the next crystal is exhausted.

In the first instance where crystallization represents merely further growth of crystals already present, no additional centers of crystallization are necessary. The rate of crystallization as measured by volume change is therefore a maximum at the beginning and decreases because of the exhaustion of crystallizable material. In the second instance crystallization at the beginning is slow because of the lack of a sufficient number of centers from which crystals may grow. Crystals start from the available centers, and more centers are formed as time goes on.[3, 26, 76] Thus the rate of crystallization increases at first, reaching a maximum, and then decreases again with the exhaustion of crystallizable material.

At temperatures immediately above the upper end of the melting range there remains of course no crystalline material. However, centers of crystallization must persist at least several degrees above the end of the melting range, since the rate of recrystallization at these temperatures, as shown in Fig. 7, is much greater than is the case when the centers of crystallization are destroyed by heating to 55°C.

8. Nature of the Crystals

The nature of the crystalline regions in long chain high polymers has been the subject of considerable discussion in recent years. Alfrey and Mark,[1, 2, 41] Bunn,[10–12] Treloar,[70] and Wood[76] have summarized some of the ideas. It seems generally agreed, for instance, that the structural units of the crystallites are not whole molecules but rather kinetic units which are segments of chains. Consequently, a single chain may contain segments which are units in two or more different crystallites, joined by segments which are to be regarded as part of the amorphous material.

The scope of the present paper does not include any attempt to extend the detailed conception of the nature of the crystals on the basis of the results obtained here. It has already been pointed out elsewhere[76] that these results cast grave doubts on the acceptibility of several theories proposed to account for the existence of a range of melting. The field is still open for a theory which will logically and satisfactorily explain two experimental observations reported here: (1) that the range of melting is not dependent on the extent of crystallization and (2) that it is definitely determined by the temperature at which crystallization occurs.

Crystals of a lower-melting type can be formed and melted in a specimen already containing crystals of a higher-melting type, as shown in the experiments illustrated by Fig. 7. It is rather remarkable that the presence of crystals of the higher-melting type appears to have so little effect on the formation and melting of the lower-melting crystals. It does appear that the two types must compete for crystallizable material, since the total volume change does not exceed 3 percent in any case.

It cannot be emphasized too strongly that the sole important factor in determining the melting range is the temperature at which crystallization occurs. Other conditions may alter the rate of crystallization by a large factor or the volume change during crystallization, as already discussed, but the melting range remains the same. Even different degrees of vulcanization[8] do not

alter the relation between melting range and temperature of crystallization. Thus, the quantitative results depicted in Fig. 4 are regarded to be of much more general application than the other portions of the present investigation.

The experimental work described in this paper was performed between 1940 and 1942, but war activities prevented earlier publication, except for a preliminary note[7] on the change of melting range with temperature of crystallization.

BIBLIOGRAPHY

(1) T. Alfrey and H. Mark, "Phase transitions in rubber and their connection with the stress-strain curve," Rubber Chem. Tech. **14**, 525 (1941).

(2) T. Alfrey and H. Mark, "A statistical treatment of crystallization phenomena in high polymers," J. Phys. Chem. **46**, 112 (1942); Reprinted in Rubber Chem. Tech. **15**, 462 (1942).

(3) M. Avrami, "Kinetics of phase change," J. Chem. Phys. **7**, 1103 (1939); **8**, 212 (1940); **9**, 177 (1941).

(4) W. H. Barnes, "Diffraction of x-rays by old specimens of 'frozen' rubber." Can. J. Research **15**, 156(1937); Reprinted in Rubber Chem. Tech. **10**, 462 (1937).

(5) N. Bekkedahl, "Forms of rubber as indicated by temperature-volume relationship," J. Research Nat. Bur. Stand. **13**, 411 (1934), RP717; Reprinted in Rubber Chem. Tech. **8**, 5 (1935).

(6) N. Bekkedahl and H. Matheson, "Heat capacity, entropy, and free energy of rubber hydrocarbon," J. Research Nat. Bur. Stand. **15**, 503 (1935), RP844; Reprinted in Rubber Chem. Tech. **9**, 264 (1936).

(7) N. Bekkedahl and L. A. Wood, "Influence of the temperature of crystallization on the melting of crystalline rubber," J. Chem. Phys. **9**, 193 (1941); Reprinted in Rubber Chem. Tech. **14**, 544 (1941).

(8) N. Bekkedahl and L. A. Wood, "Crystallization of vulcanized rubber," Ind. Eng. Chem. **33**, 381 (1941); Reprinted in Rubber Chem. Tech. **14**, 347 (1941).

(9) S. Boström, K. Lange, H. Schmidt, and P. Stöcklin, *Kautschuk und verwandte Stoffe* (Union Deutsche Verlagsgesellschaft Berlin Roth and Company, Berlin, 1940).

(10) C. W. Bunn, "Molecular structure and rubber-like elasticity. I. The crystal structure of *B* gutta-percha, rubber, and polychloroprene," Proc. Roy Soc. London **A180**, 40 (1942); Reprinted in Rubber Chem. Tech. **15**, 709 (1942).

(11) C. W. Bunn, "Molecular structure and rubber-like elasticity. III. Molecular movements in rubber-like polymers," Proc. Roy Soc. **A180**, 82 (1942); Reprinted in Rubber Chem. Tech. **15**, 742 (1942).

(12) C. W. Bunn, "The stereochemistry of the rubber molecule," Trans. Faraday Soc. **38**, 372 (1942); Reprinted in Rubber Chem. Tech. **15**, 704 (1942); **16**, 775 (1943).

(13) C. W. Bunn and E. V. Garner, "The crystal structure of rubber hydrochloride," J. Chem. Soc. **1942**, 654 (1942); Reprinted in Rubber Chem. Tech. **16**, 848 (1943).

(14) E. Bunschoten, Mededeel Rijksvoorlichtingsdienst Behoeve Rubberhandel Rubbernijverheid, Delft, No. 3, 37 (1921).

(15) C. M. Carson, "Effect of storage on milled crude rubber," Ind. Eng. Chem. **23**, 691 (1931); Reprinted in Rubber Chem. Tech. **4**, 417 (1931).

(16) F. S. Conant and J. W. Liska, "Some low-temperature properties of elastomers," J. App. Phys. **15**, 767 (1944); Reprinted in Rubber Chem. Tech. **18**, 318 (1945).

(17) F. H. Cotton, "Rational processing," Trans. Inst. Rubber Ind. **16**, 303 (1941); Reprinted in Rubber Chem. Tech. **14**, 762 (1941).

(18) R. B. Dow, "Inhibition of crystallization of rubber by high pressure," J. Chem. Phys. **7**, 201 (1939); Reprinted in Rubber Chem. Tech. **12**, 496 (1939).

(19) H. Feuchter, "Concerning racked rubber, its 'melting line,' and its density," Kautschuk **2**, 260 and 282 (1926).

(20) H. Feuchter and E. A. Hauser, "Concerning aging, hysteresis, and melting point as well as work capacity and work power of progressively racked rubber," Kautschuk **5**, 194, 218, 245, and 276 (1929).

(21) J. E. Field, "An x-ray study of the proportion of crystalline and amorphous components in stretched rubber," J. App. Phys. **12**, 23 (1941); Reprinted in Rubber Chem. Tech. **14**, 555 (1941).

(22) S. D. Gehman, "The contribution of x-ray research to the knowledge of rubber," Chem. Rev. **26**, 203 (1940).

(23) S. D. Gehman and J. E. Field, "An x-ray investigation of crystallinity in rubber," J. App. Phys. **10**, 564 (1939); Reprinted in Rubber Chem. Tech. **12**, 706 (1939).

(24) S. D. Gehman and J. E. Field, "Observations on the x-ray structure of rubber and the size and shape of rubber crystallites," J. App. Phys. **15**, 371 (1944); Reprinted in Rubber Chem. Tech. **17**, 640 (1944).

(25) A. Goetz and S. S. Goetz, "Vitrification and crystallization of organic cells at low temperatures," J. App. Phys. **9**, 718 (1938).

(26) F. von Goler and G. Sachs, "The kinetics of crystallization phenomena," Zeits. f. Physik **77**, 281 (1932).

(27) K. Gottlob, *Technology of Rubber*, Translated into English by J. L. Rosenbaum (Maclaren Sons. Ltd., London, 1927), p. 319.

(28) E. A. Hauser, M. Hunemorder, and P. Rosbaud, "New x-ray studies on rubber and related substances," Kautschuk **3**, 228 (1927).

(29) E. A. Hauser and P. Rosbaud, "X-ray studies on rubber and similar substances," Kautschuk **3**, 17 (1927).

(30) L. Hock, Chapter on "Physics of Rubber" in Memmler's *Science of Rubber*, Translated by R. F. Dunbrook and V.-N. Morris (Reinhold Publishing Corporation New York, New York, 1934), p. 421.

(31) L. Hock, "Theory of the Joule effect in rubber," Zeits. f. Elektrochemie **31**, 404 (1925).

(32) W. L. Holt and A. T. McPherson, "Change of volume of rubber on stretching; effects of time, elongation, and temperature," J. Research Nat. Bur. Stand. **17**, 657 (1936), RP936; Reprinted in Rubber Chem. Tech. **10**, 412 (1937).

(33) W. A. Johnson and R. F. Mehl, "Reaction kinetics in processes of nucleation and growth," Trans. Am. Inst. Min. Met. Eng. **135**, 416 (1939).

(34) J. R. Katz, "X-ray spectrographic investigations of stretched rubber and their possible significance in the problem of the elastic properties of this material," Naturwiss. **13**, 410 (1925).

(35) J. R. Katz, "Crystal interferences in rubber and other polyprenes," Gummi-Ztg. **41**, 1 (1927).

(36) J. R. Katz, "The freezing of raw rubber. X-ray part," Kautschuk **5**, 6 (1929).

(37) J. R. Katz, "X-ray spectrography of polymers and in particular those having a rubber-like extensibility," Trans. Faraday Soc. **32**, 77 (1936); Reprinted in Rubber Chem. Tech. **9**, 357 (1936).

(38) J. R. Katz and K. Bing, "Is raw rubber partially crystalline?," Zeits. f. angew. Chemie **38**, 439 (1925).

(39) F. Kirchhof, "Raw rubber—a fibrous material," Kautschuk **2**, 151 (1926).
(40) W. Kirsch, "Equilibria between crystals and melts in rubber and their dependency on temperature and pressure," Dissertation (Trillsch and Huther, Berlin, 1937).
(41) H. Mark, "Phase transitions and elastic behavior of high polymers," Ind. Eng. Chem. **34**, 449 (1942); Reprinted in Rubber Chem. Tech. **15**, 452 (1942).
(42) T. H. Messenger and J. R. Scott, "Softening and freezing of crepe," J. Research Assn. Brit. Rubber Mfrs. **5**, 64 (1936); Reprinted in Rubber Chem. Tech. **10**, 7 (1937).
(43) K. H. Meyer and H. Mark, "Rubber," Ber. d. d. chem. Ges. **61**, 1939 (1928).
(44) K. H. Meyer, G. von Susich, and E. Valko, "The elastic properties of the organic high polymers and their kinetic significance," Kolloid Zeits. **59**, 208 (1932).
(45) P. Mondain-Monval, "Investigations of the allotropy and the crystallization of vitreous materials," Ann. de chim. **3**, 5 (1935).
(46) E. Ott, "Concerning the molecular size of rubber and gutta percha," Naturwiss. **14**, 320 (1926).
(47) E. Ott, "X-ray investigations on rubber," J. Am. Chem. Soc. **52**, 4612 (1930); Reprinted in Rubber Chem. Tech. **4**, 82 (1931).
(48) C. Park, "On the crystallization of crude rubber," Memoirs of College of Science, Kyoto Imperial University **A22**, 13 (1939). J. Soc. Rubber Ind. Japan **12**, 462 (1939) (in English); Reprinted in Rubber Chem. Tech. **12**, 778 (1939).
(49) C. Park, "Second report of the investigation of the crystallization of crude rubber," Memoirs of the College of Science Kyoto Imperial University **A22**, 259 (1939) (in English); Reprinted in Rubber Chem. Tech. **13**, 539 (1940).
(50) G. S. Parks, "The amorphous and crystalline forms of rubber hydrocarbon," J. Chem. Phys. **4**, 459 (1936); Reprinted in Rubber Chem. Tech. **10**, 135 (1937).
(51) S. S. Pickles, "The consistency of rubber and rubber compounds," India Rubber J. **67**, 69 (1924).
(52) R. Pummerer and G. von Susich, "Crystallized rubber," Kautschuk **7**, 117 (1931), Translated in Rubber Chem. Tech. **5**, 245 (1932).
(53) A. van Rossem and J. Lotichius, "The 'freezing' of raw rubber," Kautschuk **5**, 2 (1929), Translated in Rubber Chem. Tech. **2**, 378 (1929).
(54) M. Ruhemann and F. Simon, "A contribution to the knowledge of the physical properties of rubber," Zeits. f. physik. Chemie **A138**, 1 (1928).
(55) H. Sachse, "The thermal effects accompanying the spontaneous density increase in raw rubber," Gummi-Ztg. **43**, 2216 (1929).
(56) W. H. Smith and N. P. Hanna, "Comparison between the observed density of crystalline rubber and the density calculated from x-ray data," J. Research Nat. Bur. Stand. **27**, 229 (1941), RP1416; Reprinted in Rubber Chem. Tech. **15**, 265 (1942).
(57) W. H. Smith and C. P. Saylor, "Ether-insoluble or gel rubber hydrocarbon, its solution, crystallization, and properties." J. Research Nat. Bur. Stand. **13**, 453 (1934), RP719; Reprinted in Rubber Chem. Tech. **8**, 214 (1935).
(58) W. H. Smith and C. P. Saylor, "Optical and dimensional changes which accompany the freezing and melting of Hevea rubber," J. Research Nat. Bur. Stand. **21**, 257 (1938), RP1129; Reprinted in Rubber Chem. Tech. **12**, 18 (1939).
(59) W. H. Smith, C. P. Saylor, and H. J. Wing, "Preparation and crystallization of pure ether-soluble rubber hydrocarbon: composition, melting point, and optical properties," Bur. Stand. J. Research **10**, 479 (1933) RP544; Reprinted in Rubber Chem. Tech. **6**, 351 (1933).
(60) G. von Susich, "The fusion curve of natural rubber," Naturwiss. **18**, 915 (1930), Translated in Rubber Chem. Tech. **4**, 211 (1931).
(61) G. Tammann, *Der Glaszustand* (Leopold Voss, Leipzig, 1933).
(62) G. Tammann and E. Jenckel, "The crystallization velocity and the number of nuclei in glycerine and their dependence on temperature," Zeits. f. anorg. allgem. Chemie **193**, 76 (1930).
(63) W. E. Thibodeau and A. T. McPherson, "Photoelastic properties of soft vulcanized rubber," J. Research Nat. Bur. Stand. **13**, 887 (1934), RP751; Reprinted in Rubber Chem. Tech. **8**, 183 (1935).
(64) F. Thiele and E. Wurm, "Chapter on Patentgummi" in E. A. Hauser's *Handbuch der Gesamten Kautschuktechnologie* (Union Deutsche Verlagsgesellschaft, Berlin, 1935), Vol. II.
(65) P. A. Thiessen and W. Kirsch, "Crystallization of rubber by pressure," Naturwiss. **26**, 387 (1938), Translated in Rubber Chem. Tech. **12**, 12 (1939).
(66) P. A. Thiessen and W. Kirsch, "The crystallization of weakly-vulcanized rubber by pressure," Naturwiss. **27**, 390 (1939), Translated in Rubber Chem. Tech. **13**, 48 (1940).
(67) P. A. Thiessen and W. Wittstadt, "Forced and spontaneous changes in the arrangement of the molecules in stretched rubber. Crystals and fused phase in stretched rubber," Zeits. f. physik. Chemie **B41**, 33 (1938), Translated in Rubber Chem. Tech. **12**, 736 (1939).
(68) L. R. G. Treloar, "Elastic recovery and plastic flow in raw rubber," Trans. Faraday Soc. **36**, 538 (1940); Reprinted in Rubber Chem. Tech. **13**, 795 (1940).
(69) L. R. G. Treloar, "Crystallization phenomena in raw rubber," Trans. Faraday Soc. **37**, 84 (1941); Reprinted in Rubber Chem. Tech. **15**, 251 (1942).
(70) L. R. G. Treloar, "The structure and elasticity of rubber," *Reports on Progress in Physics* (Physical Society, London, 1943), Vol. 9, p. 113.
(71) M. Volmer and M. Marder, "The theory of linear crystallization velocity of undercooled melts and undercooled solid modifications," Zeits. f. physik. Chemie **A154**, 97 (1931).
(72) G. S. Whitby, Chapter 2 "Physical properties of raw rubber" in Davis and Blake's *Chemistry and Technology of Rubber* (Reinhold Publishing Corporation, New York, 1937), p. 102.
(73) A. J. Wildschut, "On the proportion of crystalline and amorphous components in stretched vulcanized rubber," J. App. Phys. **17**, 51 (1946).
(74) W. Wittstadt, "External influence and the internal state of rubber," Kautschuk **15**, 11 (1939), Translated in Rubber Chem. Tech. **12**, 488 (1939).
(75) L. A. Wood, "The beta-anomaly of Ruhemann and Simon in rubber," J. Chem. Phys. **10**, 403 (1942).
(76) L. A. Wood, "Crystallization Phenomena in Natural and Synthetic Rubbers," chapter in Mark and Whitby's *Advances in Colloid Science* (Interscience Publishers, Inc., New York, 1946), Vol. 2, p. 57.
(77) L. A. Wood, N. Bekkedahl, and R. E. Gibson, "Effect of pressure on the melting of crystalline rubber," J. Chem. Phys. **13**, 475 (1945); J. Research Nat. Bur. Stand. **35**, 375 (1945), RP1677.
(78) L. A. Wood, N. Bekkedahl, and C. G. Peters, "Application of the interferometer to the measurement of dimensional changes in rubber," J. Research Nat. Bur. Stand. **23**, 571 (1939), RP1253; Reprinted in Rubber Chem. Tech. **13**, 290 (1940).

Tackiness of GR-S and Other Elastomers

W. F. Busse, J. M. Lambert, and R. B. Verdery
General Aniline and Film Corporation, Easton, Pennsylvania

The deficiency of GR-S in "tackiness" resulted in a great deal of work in the rubber industry to improve this complex property, but practically all the work had to be evaluated by qualitative "hand tests" because quantitative tests were not available. An analysis of the factors involved in the "tackiness" of various materials showed that different factors were critical in the so-called "tackiness" of rubber, paints, and varnishes, printing inks, adhesive tapes, etc. A quantitative test was developed to measure the effects of rate of removal on the adhesion or "tackiness" of pressure-sensitive adhesive tapes over a 10^6-fold range of rates. This showed why the results of standard "adhesion tests" of tapes do not predict the relative behavior of the tapes under small forces acting for long times. Another test was developed for the measurement of the "tackiness" of GR-S rubber which correlates well with the judgment of tackiness by hand tests and it even works reasonably well with rough samples taken from a laboratory mill. With this test, the effects of mastication conditions, aging, and of the addition of softeners and tackifiers on "tackiness" of GR-S (with and without carbon black) were studied. The German tackifier "Koresin," which is now manufactured in this country, was found to be far more effective than rosin and similar materials formerly used, and gave a tackiness approaching that of natural rubber.

I. INTRODUCTION

TACKINESS usually is measured by hand tests which are very simple to apply but which are very complex because they involve an unconscious integration of a great many factors. The particular combination of properties which produces tack in one system, such as printing inks, may be quite different from the combination producing tack in another system such as rubber, even though the over-all effect as measured by hand tests may be the same. Hence it is not surprising that there is little agreement as to the factors involved in producing tackiness of different materials and that very few quantitative methods of measuring tackiness have been developed.

This paper presents an analysis of the operation of measuring tack, to make explicit some of the detailed factors involved, both in the materials and in the testing operation. Methods of measuring the effects of some of these different factors have been developed and applied to the study of the "tackiness" of such materials as pressure-sensitive adhesive tapes and various elastomers, including polyvinyl ethers and natural and synthetic rubbers.

The magnitude of the "tackiness" of a material (as measured by the resistance to the separation of two surfaces which have been brought in contact), depends on the geometry or roughness of the surface of the sample, as well as on the surface adhesive forces and the visco-elastic properties of the material, and the relation of these factors to the time of application and magnitude of the force pressing the surfaces together. Hence, the results of quantitative tests of "tackiness" are not in any sense absolute properties of the material. However, they do give better measures of tackiness than can be obtained by hand tests, and they make possible more precise studies of the effects of some processing conditions and compounding agents on the tackiness of GR-S and natural rubbers.

II. HISTORY

Studies of the properties that produce "tack" in viscous liquids were made as early as 1847 by J. Stefan[1] and somewhat later by O. Reynolds.[2] Both considered the tackiness to be measured by the force required to separate, at a given rate, two flat disks immersed in the liquid, and they developed equations for relating the applied force to the times of separation, assuming the laminar flow of Newtonian liquids. Later similar formulas were developed,[3] some of which[4] were modified to take account of the yield value of the materials. Recently it has been shown[5] that tack of printing inks correlates well with the viscosity measured at high rates of shear.

[1] J. Stefan, Ber Kais. Acad. Wiss. Wien **69**, 713 (1847).
[2] O. Reynolds, Phil. Trans. Roy. Soc. London **177**, 157 (1886).
[3] Haley, Trans. Inst. Rubber Ind. **1**, 334 (1926).
[4] J. R. Scott, Trans. Inst. Rubber Ind. **17**, 169 (1931).
[5] H. Green, Ind. Eng. Chem. Anal. Ed. **13**, 632 (1941).

Little work has been done relating tackiness to molecular properties, but it was pointed out[6] that tackiness as well as "stickiness" and the ability of polymeric materials to be drawn into fibers, seems to be correlated with a relaxation time of 10^{-7} to 10^{-4} second, or a viscosity of 10^2–10^4 poise, and a linear chain length of about 100 links.

It has been emphasized[7] that in the case of rubber "autohesion" or the sticking together of two like surfaces when brought in contact is an important factor in tackiness. The relations of various fundamental properties to the tackiness of paints, inks, rubbers, etc., were discussed by a number of authors at a recent meeting of the British Rheologists Club.[8] In this discussion Scott emphasized two factors which are important in producing a bond between the two surfaces:[9]

(1) getting the two surfaces into contact; and

(2) mutual "fusion" of the surface layers.

Phase (1) of the process is greatly influenced by the roughness of the rubber surfaces. Phase (2) for rubber-like materials is thought to involve a rapid interpenetration, i.e., self-diffusion of at least parts of the long rubber molecules composing the two surface layers.

The rheology of the rubber is of great importance since it must deform readily (at least on the surface) under small stresses in order to produce close contact of the two surfaces. It is interesting that this requirement of ease of deformation for good tack is just opposite to the requirement for so-called tacky adhesion between the two plates separated by a layer of viscous or plastic material considered by Stefan and Reynolds.

Experience with GR-S shows that the addition of resinous materials and various other softeners to the rubber often makes it "sticky" to mill rolls, liners, etc., without giving it the combination of surface and bulk properties required for good autohesion or "tack." Extensive studies have been made and published in this country[10] on the effect of various softeners and "extenders" on the physical properties of GR-S without finding materials which gave synthetic rubber the tack of natural rubber. All measurements of tack were based on hand tests.

The report of the committee investigating the German Rubber Industry[11] indicates that one of the few worthwhile advances made by the German Rubber Industry during the war was the development of Koresin as a tackifier of butadiene-styrene rubber. This was reported to give the rubber excellent tack, but no quantitative data were obtained.

III. ANALYSIS OF "TACKINESS"

Before trying to measure quantitatively the tackiness of synthetic rubbers, it is helpful to analyze in detail the operation of measuring tack, to determine some of the different kinds of factors which are involved. This operational method of analyzing the process leads to a recapitulation and organization of many of the factors which have been suggested in the literature and to the recognition of some additional factors.

Expressed in the simplest terms, the operation of determining tackiness consists of:

(A) *Producing contact between two surfaces for a short time by the application of a force, and*

(B) *Separating the surfaces and noting the force required.*

The force applied to separate the surfaces is the "tackiness" under the particular test conditions used. Since most tack tests have been made by hand, this implies that the magnitude of the adhesion force on the area tested (usually of the order of 1–10 sq. cm) should be great enough to be detected by the tactual sensations of the hand. Mechanical tests, however, can extend the concept to a much wider range of values. Further consideration shows that each of these operations can be broken down into a number of simpler factors, as follows.

[6] D. Josefowitz and H. Mark, Ind. Rubber World **106**, 33 (1942).

[7] Zhukov and Talmud, J. Rubber Ind. U.S.S.R. **12**, 1005 (1935).

[8] Rheology Bulletin **16**, 70 (1945); Paint Technology **9**, 211–221 (1944).

[9] J. R. Scott, Paint Technology **9**, 218 (1944).

[10] L. E. Ludwig, D. V. Sarback, B. S. Garvey, and A. E. Juve, Ind. Rubber World **111**, 180 (1944), and **112**, 731 (1945).

[11] Summary Report, Rubber Bureau WPB, and Office of Rubber Reserve, Washington, D. C., August, 1945.

A. ***Producing contact between two surfaces.***

The amount of surface brought into "molecular contact" in a given area depends on:

1. Initial roughness of the surface. This determines the magnitude of the deformations required to bring the surfaces into "contact," i.e., within the range of the molecular forces in the surface, or within say about 10^{-5} cm.

2. Forces acting to bring the surfaces together. These include:

(a) External forces applied to the material. These usually range from about 1 g to 1 kg/cm^2 of nominal area and they may act for times ranging roughly from a few seconds to a minute. Occasionally we are interested in the behavior of a material when surfaces are brought together under pressure for times up to weeks or months, as when bales or sheets of a plastic are piled together in storage. Sealing of the surfaces under these conditions is sometimes called "blocking."

(b) Molecular forces at the surface of the material. These short range forces come into play only when the surfaces are in very close contact. They are usually greatest for polar materials, as indicated by the fact that such materials have the highest surface tension in the liquid state. While many of the most tacky materials are polar (asphalt, (warm) rosin, paint, polyvinyl ethers, etc.), the presence of polar molecules is neither necessary nor sufficient for tackiness. Some materials such as polyisobutylene are not polar but are very tacky while rosin in the solid state is hard and brittle, rather than tacky. In multi-component systems the tackiness may be determined by the molecular forces of the component that diffuses or blooms to the surface in the highest concentration.

3. Resistance of the material to the deformation required to bring the two surfaces into molecular contact. This involves the visco-elastic properties of the material for deformations of both:

(a) a relatively large scale, required to overcome the gross surface roughness of the material, and

(b) a very small scale, required to produce molecular contact between even smooth surfaces. Since the molecular forces have such short range, the presence of even a small amount of dust may prevent large fractions of the surfaces from coming close enough to be within the range of their cohesive force unless these small scale deformations can be made very easily.

It should be noted that the modulus, or the resistance to deformation, for these very small scale deformations at the surface may be very much higher or very much lower than the modulus for large deformations of the whole sample. A very thin layer of hard oxidized material might greatly increase the modulus of the surface layer, while the blooming of a small amount of liquid component to the surface might reduce the modulus of this layer. It is possible that the presence of small regions of rigid gel structure at the surface of GR-S might tend to prevent the molecular contact needed to produce good tack.

The relaxation times of material in the surface layer and the bulk material determine the length of time the forces must act to produce the required deformations.

B. ***Separating the surfaces and noting the force required.***

This factor will depend on:

1. The magnitude of the molecular forces per unit area of molecular contact, and on the total area of such contact.

2. The ultimate tensile strength of the material for the particular kind and rate of applied stress.

It is this factor which keeps liquids such as water from being tacky. The water is easily deformed, makes good molecular contact with other surfaces brought into contact with it, and it has high surface forces, but it does not have sufficient tensile strength or viscosity to resist separation, even at high speeds. In the case of viscous liquid materials like tars, printing inks, etc., the "tensile strength" may in effect be merely the viscous resistance to deformation. Here the "tensile strength" depends very much on the rate of deformation.

3. The distribution of the applied stress and resultant elongations. This determines the magnitude of the force which must be applied to stress the material to its "tensile strength" at the line of separation. This depends on:

(a) The geometry of the sample, i.e., the thickness, area, and shape, and the position and direction of application of the applied force.

This may be applied normal or parallel to the surface, or to produce pealing apart of the materials along a line, producing various kinds of stress gradients.

Since in tack tests the separating force is applied in such a way as to produce a stress gradient in the sample, the total force will depend very much on the ultimate elongation of the material, for this affects the total volume of material that must be stretched.

It should be noted that under some conditions, the force applied to remove the samples may result in two- or even three-dimensional tensile stresses in the sample. The behavior of the sample to such stresses may be quite different from its behavior under a one-dimensional tensile stress, just as is the case in tensile and tear tests of cured rubber.[12] As a rule, the most tacky materials react to this complex stress pattern by forming irregular "teeth" or "legs" in the region of separation.

(b) The stress-strain-relaxation properties of the material.

General experience suggests that the differences in apparent tack which are found by varying the conditions under which the surfaces are separated (e.g., at different rates of separation, temperature, etc.) probably are due to the changes in the stress distribution in the region of separation, resulting from the differences in the apparent effective visco-elastic properties of the medium.

Two sheets of milled rubber, for example, which are stuck together so firmly that they tear along new surfaces when pulled apart slowly, can sometimes be separated along the original surfaces by a very quick pull. This in effect makes the rubber much stiffer and stronger, and thus puts relatively more stress on the bond between the surfaces.

IV. MEASUREMENT OF TACKINESS

(1) Effect of Testing Conditions on Tack of Adhesive Tapes

The properties which affect the tack (or resistance to separation) such as the modulus, elongation, and plastic deformation, vary with both time of application of force, and temperature of the material. Therefore, a complete description of the tackiness of a material should include data for a wide range of time of contact of load and rate of separation of surfaces, preferably also over a wide range of temperatures.

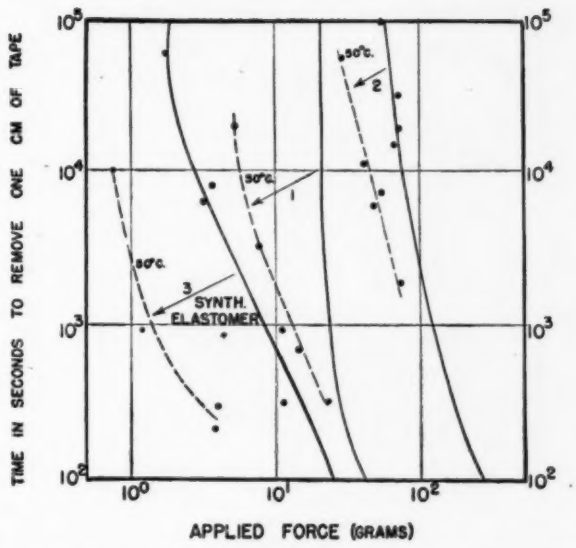

FIG. 1. Relation of applied force to rates of removal of adhesive tapes.

To get some quantitative data on the importance of the rate factor, measurements were made of the relation between the applied load and the rate of removal of pressure sensitive adhesive tapes from glass surfaces, since this makes the factor of surface roughness small and constant.

The simplest method used to measure this relation was to put a number of strips of adhesive tape ½ in. wide by about 12 in. long (1.25 cm ×30 cm) on the bottom of a 10 in. by 15 in. (25 cm×37 cm) plate of glass held horizontally in a rack, hang known loads from the free ends of each tape to pull it away from the glass. This method had the advantage that it could be used in an oven to get data at elevated temperatures, and a number of tapes and loads could be tested at any one time. It had the disadvantage that, particularly at low loads, non-uniformities in the tape might make the rate of removal irregular, or even stop it altogether. However, the test gives considerable more information about the adhesive properties than a test which measures only the force required to remove the tape at one rate.

Data obtained with this test for three samples of experimental pressure-sensitive adhesive tapes

[12] W. F. Busse, J. App. Phys. 9, 438 (1938).

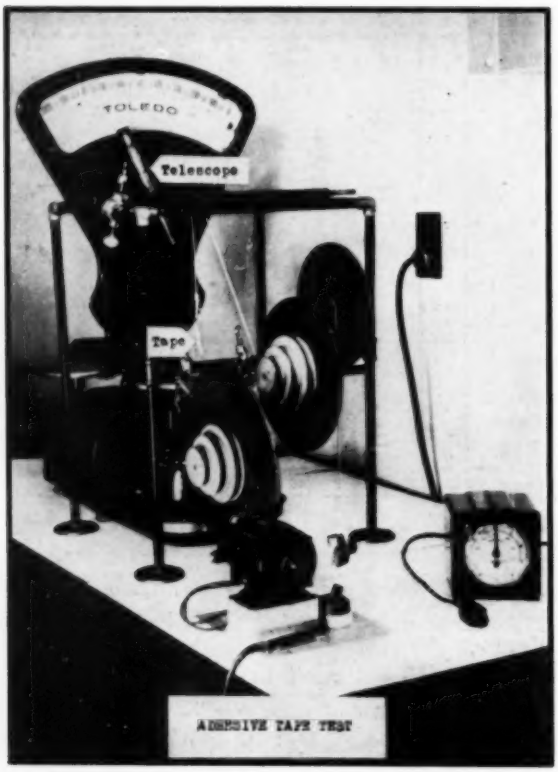

FIG. 2. Adhesive tape test.

at room temperature and 50°C are shown in Fig. 1. Tape No. 1 is made using GR-S, No. 2 has natural rubber, and No. 3 has an experimental synthetic elastomer base.[13] Since each tape has various amounts (not necessarily the optimum) of plasticizer and tackifier, the results illustrate the physical properties that can be obtained in tapes, rather than the fundamental properties of specific elastomers. Because of the long times involved, the removal of the tapes are expressed as reciprocal rates, or seconds/cm.

At room temperature tape No. 3 will support a load of 1.8 g indefinitely (10^5 sec. to remove 1 cm) but it requires about 27 g or a 15-fold increase to remove it at the rate of 10^2 sec./cm. The tape made with natural rubber will hold a load of 20 g indefinitely, but 40 g will remove the tape at 10^2 sec./cm, or a range of only two-fold, which is very desirable. The GR-S tape will support larger loads, but about a fivefold range of loads is required to change the reciprocal rate of removal from 10^5 sec./cm to 10^2 sec./cm.

[13] These were supplied through the courtesy of Industrial Tape Corporation, New Brunswick, New Jersey.

The loads required to remove the tapes at a given rate at 50°C are seen to be only about one-half to one-fifth those required at room temperature, but not enough data are available to draw any theoretical conclusions from the temperature coefficient.

To avoid some of the difficulties of this first test, equipment was built by Mr. F. E. Wetherill of this laboratory to remove the tapes at definite rates over nearly a 10^6-fold range and measure the force applied. This was done by fastening the glass plate to the pan of a direct reading scale that read from 1 to 1000 g. The adhesive tape, 1.2 cm (0.5 in.) wide by about 25 cm (10 in.) long, was fastened to the top of the glass plate, and the free end of the tape was pulled normal to the surface by means of a cord which passed over a roller about a foot above the tape, and then went around another pulley which was driven at the desired speed.

The wide range of driving speeds which were required were obtained very simply by a train of multiple pulleys made from wood and fiber board. They were mounted so that, for example, the large pulley of each unit could be driven by friction from a smaller pulley of the preceding unit. By changing the number and diameter of the pulleys used in the train, and using a motor with built-in speed reducer, the speed of removal of the tape could be varied from about 10^{-1} to 5×10^4 sec./cm.

The amount of tape removed in a given time interval was read with a small telescope from a metal scale placed on the balance pan beside the tape. A picture of the equipment is shown in Fig. 2.

Typical results from this test are shown in Fig. 3 which gives data on experimental tapes. The elastomers are No. 1, natural rubber, No. 2, GR-S, No. 3, and No. 4, two other synthetic elastomers. Again the data illustrate only the behavior of the particular tapes rather than fundamental properties of the elastomers.

It is apparent that tapes Nos. 1, 3, and 4 have about the same properties if tested at relatively high rates of removal—say, from 0.1 to 5 sec./cm removed (10 to 0.2 cm/sec.). At very low rates of removal, however, they are quite different. Tapes Nos. 3 and 4 are removed slowly at loads above about 3.3 g, while the rubber base tape

does not start to be removed until the load is over 10 g. The behavior at these low rates of removal is important wherever pressure-sensitive tapes are used to seal packages, or to hold objects on a wall, etc., as they are then subject to small stresses for long times, and their performance in service may be determined by this factor. Tapes such as No. 3 and No. 4 failed on such service tests while No. 1 was satisfactory. The tape No. 2 had good adhesion to the glass, but other properties made it less satisfactory than No. 1.

(2) Tackiness Test for Natural Rubber and GR-S

a. Discussion of Test

The test used in this work was designed primarily to give a quantitative measure of the effect of various materials on the tackiness or resistance to separation of sheets of GR-S under conditions approximating those of the hand test. The method could easily be modified to study the effects of varying the magnitude and time of application of the compression force, the rate of separation of the surfaces, etc. However, this was not found necessary for the evaluation of compounding ingredients and milling conditions on the tackiness of GR-S.

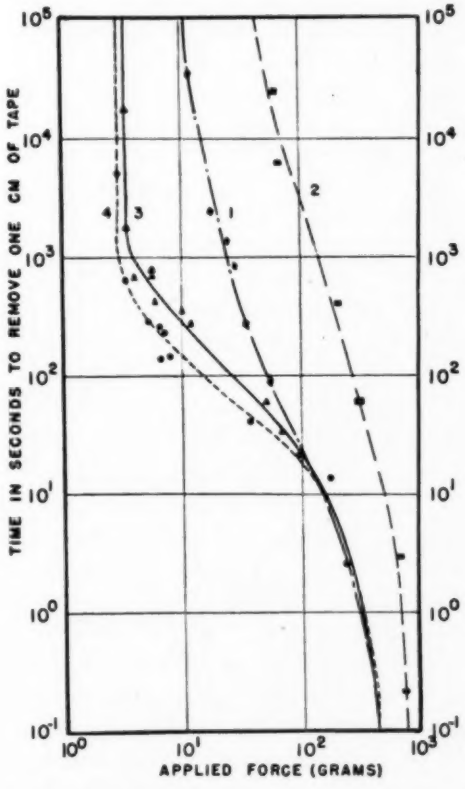

FIG. 3. Relation of applied force to rates of removal of adhesive tapes.

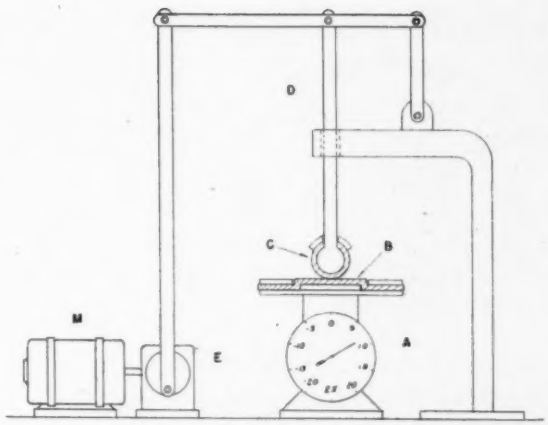

FIG. 4. Schematic diagram of tackiness tester.

An obvious difficulty in developing a quantitative test of the tackiness of rubber is to get samples with reproducible smooth, uniform surfaces. A number of ways of doing this have been suggested, including molding smooth samples, depositing the rubber from solution, calendering the rubber onto fabric, etc., but they all have the disadvantage of changing the rubber that is to be tested.

A closer examination of the problem shows, however, that surface roughness is not necessarily as serious a problem as it first appears. Since it has been possible in practice to ignore this factor in hand tests, it is evident that by standardized preparation of the sample, surfaces of at least approximately reproducible roughness can be obtained. It was found possible to use rubber samples 2–3 mm thick prepared by milling sheets on a small (2″×6″) laboratory mill (made by Wm. R. Thropp and Sons). Uncompounded GR-S gave the most irregular samples, but on adding 45 parts EPC black to 100 parts GR-S the magnitude of the irregularities was reduced, and the sheets appeared more uniform. However, even the uncompounded GR-S could be prepared in fairly reproducible sheets.

To measure the tackiness, the equipment shown schematically in Fig. 4 was used. One strip of the rubber to be tested, *B*, at least

TABLE I. Effect of milling on tack of pale crepe.

Sample	Treatment	Temp. °C	Time, min.	Separating force-g after 1–2 hr.	Separating force-g after 24 hr.	Appearance of sample after milling
I	Initial milling	60	8	525	185	Smooth
Ia	I remilled	25	7	115	—	Creped-rough
Ib	I remilled	60	7	405	—	Smooth
II	Initial milling	25	3	30	35	Creped-rough
IIa	II remilled	25	3	35	—	Creped-rough
IIb	II remilled	60	5	330	—	Smooth
III	Initial milling	25	15	105	110	Creped-rough
IIIa	III remilled	25	15	600	—	Smooth

3×5 cm (1.2×2 in.) is fastened to the pan of a pre-loaded spring scale, *A*, which reads compression and tension loads directly. Another sample, *C*, of the rubber is put around a mandrel 3.4 cm (1¼ in.) in diameter and 2.5 cm (1.0 in.) wide and lowered by the motor *M* through the drive *B*, in a 2.4-sec. cycle.

The sample *C* is pressed against *B* with a force of 565 g (20 oz.) at the bottom of the stroke and then pulled away. The maximum position of the scale pointer on the return stroke is read. This value, when corrected for the inertia effects of the system, is a measure of the force required to separate the samples, or the "tackiness," for "instantaneous" loading. At least five tests are made at different places on the surface and averaged for the "instantaneous tack" values.

The motor driving the mandrel can be stopped at the bottom of the cycle to leave the samples in contact under load for any desired time, and the motor then re-started. The force required to separate the samples after the load is applied for 10 sec. is called the "10-sec. tack." Five readings of this are taken and averaged.

Usually the "instantaneous tack" and the "10 sec. tack" values changed more or less parallel with each other, so the two values are averaged in this report unless otherwise noted. In a few cases, where the samples sealed and could not be separated after the load was on for 10 sec., only the instantaneous values are given. The average tack values for any one sample are reproducible to within about ±30 grams.

TABLE II. Effect of milling temperature on relative tack of GR-S.

Temperature −°C	15	30	50	70
Separating force (g)	155	85	30	10

Because the initial rubber and the details of processing were different in different series of tests, the absolute values of tackiness in different series cannot be compared. Within each series, however, the data are comparable.

b. Effect of Some Processing Conditions on Tack of Natural Rubber and GR-S

It is known that natural rubber breaks down (due to oxidation) and becomes soft and plastic more rapidly when milled on a cold mill (20°C) than when milled on a warm or hot mill[14] (100°C) so it might be expected that cold milling would make the rubber more tacky than hot milling. The following test (Table I) shows that this result is not always obtained.

TABLE III. Effect of mastication time on tackiness and plasticity of GR-S.

Composition	Mast. time, min.	Separating force (g) when mast. Hot	Separating force (g) when mast. Cold	Williams plasticity (100°C) when mast. Hot	Williams plasticity (100°C) when mast. Cold
GR-S	5	215	160	2.9	3.0
	10	285	200	2.7	2.8
	20	425	285	2.3	2.7
	30	525	300	2.1	2.5
	45	640	315	1.8	2.4
GR-S and EPC black	20	115	55	4.4*	4.1
	30	115	55	4.2*	3.8
	45	140	85	3.9*	3.7
	60	170	85	3.8*	3.5

* Plasticity values after 9 days.

Samples of pale crepe were milled at 25° and 60° on a 2″×6″ mill, the temperatures of the rubber being measured by a thermocouple. The tack values or separating force (grams) were measured within 1–2 hr. and after 24 hr. Samples given the initial hot milling were then remilled at 60° and at 25°C. Some of the samples were so tacky that the surfaces sealed when pressed together for 10 sec., so all of the tack values of Table I are for the separating force in grams after the "instantaneous" load.

The results shown in Table I agreed qualitatively with the hand tests of the tack of these samples. They suggest that the difference in tack of the hot- and cold-milled samples is largely due to the physical state of the surface. The samples

[14] W. F. Busse, Ind. Eng. Chem. **24**, 140 (1932); Proc. Rubber Tech. Conf. London, May 1938, p. 288; Cotton, Inst. Rubber Ind. Trans. **6**, 487 (1931).

which were cold milled for a short time had rough creped surfaces which prevented intimate contact over large areas, so gave low values for the tackiness. The hot-milled samples, and the samples cold milled for 30 minutes had smooth surfaces which allowed good contact and so gave very high tack values. The decrease in tack of sample I on standing 24 hr. may be due in part, at least, to the development of surface roughness on standing.

The results show that the tackiness measured in this test is not an absolute property of the material. However, it does appear to measure a combination of properties of the material and the sample geometry which is important both in the hand tack test, and in "adhesion" of plies in actual factory processing.

When GR-S was milled on the small mill the tack was low for all milling temperatures from 15 to 70°C, as shown in Table II. The tack is somewhat higher for samples milled cold, but varying the milling time from 5 to 15 min. had little if any effect on the tack. Samples of GR-S from different sources gave some variation in tack values, but none were very tacky.

When GR-S and a stock containing GR-S 100 parts and EPC black 45 parts were masticated for various times in a Midget Laboratory Banbury mixer the results shown in Table III and Fig. 5 were obtained. The samples marked "hot" were run with steam (100°C) through the jacket and cold water through the rotor, and

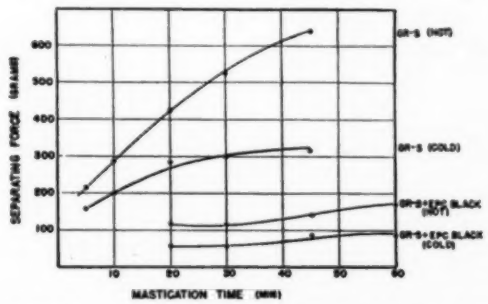

FIG. 5. Effect of mastication time on tackiness of GR-S.

those marked "cold" were run with cold water (20°C) circulating through the jacket and rotor. 250 g of rubber were used and 30-g samples were removed for test after various times of mastication. For the stock containing carbon black the rubber was broken down for 5 minutes and the carbon black was then added and mixed 15 minutes when the 20 minute sample was removed. Each sample was then milled 2 minutes on the 2″×6″ mill to sheet out, the rubber samples being milled at 20°C and the black samples at 600°C. Tack tests and Williams plasticity tests at 100°C were made after 24 hr., except for one group of plasticity tests made after standing for a longer time. The plasticity figures are the thickness in mm of the 2-cc sample after being subject to the 5 kg load for 3 min. The tack values are the average of "instantaneous" and "10-second" tests for each of two independent series of mastication tests.

It is seen that in these tests the hot Banbury mastication consistently gives somewhat tackier and more plastic samples than the cold mastication, even with the stock containing 45 parts EPC black. Increased mastication time increases the tack readings, in part because it makes the samples softer. This method of increasing tackiness may not be practical, however, because of the excessive time of mastication required and the deleterious effects of high temperature on the properties of the cured compounds.[15]

TABLE IV. Effect of polyvinyl isopropyl ethers on tackiness of GR-S.

Sample	Specific viscosity*	Separating force (g)
1	0.05	50
2	0.13	160
3	0.63	330
4	0.84	310
5	2.13	280
Control (GR-S only)	—	30

* In 1 percent benzene solution.

c. *Effect of Vinyl Ethers on Tackiness of GR-S*

Since some of the polyvinyl ethers are extremely tacky materials themselves, it was thought that they might improve the tackiness of GR-S. A series of polyvinyl ethers[16] of different molecular weights (viscosities) was tested by milling 10 parts each into 100 parts GR-S on the 2″×6″-mill run hot (60°C). The results are shown in Table IV.

[15] W. B. Wiegand and H. A. Braendle, Ind. Eng. Chem. 36, 699 (1944).

[16] Prepared by Drs. F. Grosser and C. E. Schildknecht of this laboratory.

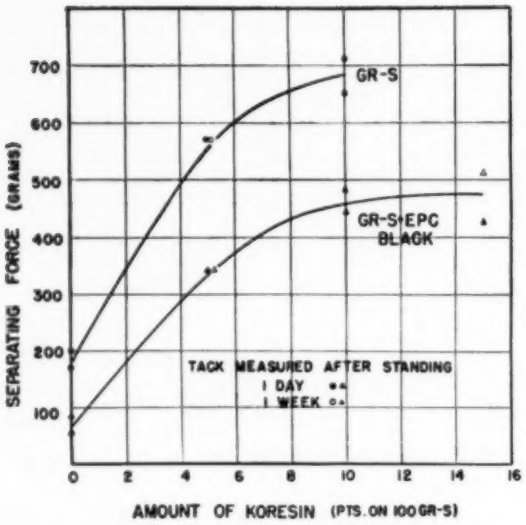

FIG. 6. Effect of mixing Koresin into GR-S.

The results show that within the proper molecular weight range, these vinyl ethers do produce tackiness in GR-S but the lower molecular weight ethers were not effective. On the same test, 10 parts of rosin oil in 100 parts GR-S did not produce a measurable increase in the tackiness.

The vinyl ethers are not very compatible with the GR-S rubber, so they probably tend to bloom to the surface and thus make the surface tacky. Compounded stocks containing vinyl ethers can be plied up and cured satisfactorily to a solid piece. However, if two samples are *painted* with a solution of vinyl ether, and pressed together during cure, they will not fuse together, and the cured samples can easily be separated.

d. Effect of Koresin and Other Tackifiers on GR-S

When reports reached this country that Germany had developed a product that was a very effective tackifier of their Buna S, the Rubber Reserve took steps to find its composition and to get a source of supply in this country. The material was found to be a reaction product of acetylene and *p. ter* butylphenol. Rubber Reserve made arrangements to have this product, known as Koresin, made in this country[17] and samples supplied to the rubber industry.

[17] By General Aniline and Film Corporation, USP 2,337,464.

The results obtained when various amounts of Koresin were mixed in GR-S and in a stock containing GR-S 100 parts and EPC black 45 parts are shown in Table V and Fig. 6. The mixing was done for 5 minutes in the small Midget Laboratory Mixer run hot, and the samples were then sheeted out for 5 minutes by milling on a warm (60°C) 2″×6″ mill. The tackiness was measured after the samples stood various times up to a week in an air-conditioned room 75°F-30 percent R.H.

It is seen that 5–15 parts Koresin on 100 GR-S are very effective in increasing the tack of both straight GR-S and of GR-S containing 45 parts black and that the tack decreases only slightly on standing for one week. However, if the samples are stored at high humidities or where water gets on the surface, the tack drops more rapidly. The addition of the Koresin has no deleterious effect on rate of cure, or tensile properties of the cured GR-S compounds.

When Koresin is applied as a solution or cement to the surface of a stock containing GR-S 100 parts and EPC black 45 parts, the results depend very much on the concentration used. Table VI and Fig. 7 show the results of two series of tests—one studying the effect of various concentrations of Koresin solution in hexane, and the other comparing Koresin with other materials when applied as solutions in hexane.

TABLE V. Effect of mixing Koresin into GR-S.

Stock	Parts Koresin	Separating force (g) after standing for 1–2 hr.	24 hr.	1 week
GR-S	0	200	170	200
	5	540	570	570
	10	650	710	650
GR-S and EPC black	0	55	55	85
	5	395	340	340
	10	455	480	455
	15	595	425	510

There is a definite optimum at around 3–4 percent concentrations of Koresin solution. This tends to confirm the view that the Koresin increases the tack of GR-S in part, at least, because of its tendency to bloom to the surface, forming a layer of high Koresin concentration. When a large excess of Koresin is present, how-

ever, the Koresin seems to form a "lacquer" on the surface which is dry, hard, and non-tacky.

If the solutions are applied in atmospheres of very high humidity, where moisture can condense on the surface, the tackiness is very much reduced. The mechanism of this action is not known, but a similar effect is noted with rubber cements.

A comparison of a number of different softeners and tackifiers added in the Midget Banbury Mixer to a stock containing GR-S 100 parts and EPC black 45 parts is shown in Table VII. The plasticity values are taken after 24 hr., on the Williams Plastometer at 100°C.

It is seen that 10 parts Koresin gives the most tack of any material tested. A mixture of equal parts of Koresin plus the petroleum derivative (Circosol 2XH) (10 parts total) is almost as effective as 10 parts Koresin, even though 10 parts of the petroleum derivative alone has little effect on the tackiness. The tackiness of the Koresin stocks does not decrease markedly in a week when stored in an atmosphere at 75°F and 30–35 percent relative humidity.

CONCLUSIONS

The analysis of tackiness shows that it is a complex property which depends on a balance between a large number of different factors, including the geometry of the sample as well as the surface forces and the visco-elastic properties of the material itself.

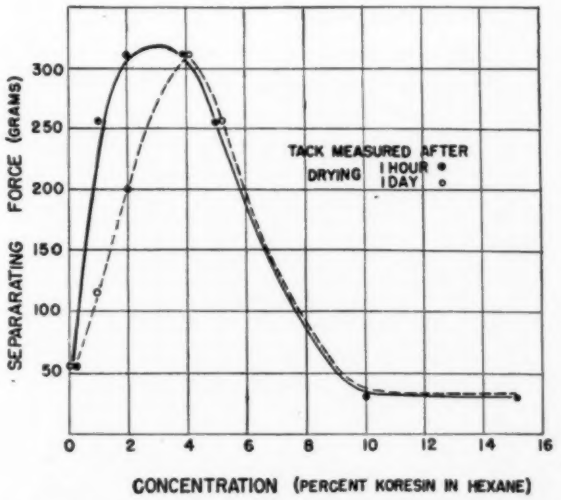

FIG. 7. Effect of painting Koresin solutions (Hexane) on surface of GR-S carbon black compound.

TABLE VI. Effect of painting various materials on surface of GR-S carbon black compound.

Material	Conc. %	Separating force (g) after 1 hr.	3 hr.	24 hr.	1 week
Series 1.					
Solvent only	—	55	—	55	—
Koresin	1.0	255	—	115	—
Koresin	2.0	310	—	200	—
Koresin	4.0	310	—	310	—
Koresin	5.0	255	—	255	—
Koresin	10.0	30	—	30	—
Koresin	15.0	30	—	30	—
Series 2.					
Koresin	3	255	225	255	140
Koresin (German)	4	225	170	140	140
GR-S	4	115	85	85	85
Natural rubber	4	370	225	170	55
Dehydro abietic acid	4	170	140	85	55

TABLE VII. Effect of various materials on the tackiness of GR-S EPC black compound.

Material added	Amount added (on 100 pts. GR-S)	Separating force (g) after standing for 1–2 hr.	1 day	1 wk.	Williams plasticity 100°C
Control (GR-S comp. only)	—	55	55	85	4.3
Koresin	5	395	340	340	3.9
Koresin	10	455	480	455	3.6
Koresin and petroleum deriv.(1:1)	10	480	455	455	3.7
Koresin and coal tar fractions (1:1)	10	425	340	425	3.7
Dehydrogenated rosin	10	370	255	200	3.7
Petroleum derivative	10	170	85	115	4.1
Coal tar fraction	10	170	115	85	3.8
Rosin oil	10	200	115	115	3.7
Stearic acid	10	55	30	55	3.8

The quantitative measurements of the effect of the rate of removal on the apparent tackiness of pressure-sensitive adhesive tapes show that significant differences are found at very slow removal rates (10^5 sec./cm) which do not show up at much higher removal rates (10 sec./cm). These differences may affect the performance of the tapes in service.

A simple quantitative test is described which can be used to study the effects of various processing treatments and various softeners, tackifiers and other compounding ingredients on the tackiness of GR-S and other rubbers. Koresin was the most effective tackifier found for GR-S.

The authors wish to acknowledge the continued interest of Dr. W. E. Hanford, Director of the Laboratory, and the helpful discussions of tackiness measurements with Dr. C. E. Schildknecht. Miss Ruth Sellers and Miss J. L. Nuver helped in taking much of the data. The first Koresin samples were prepared in the laboratory by Drs. C. E. Schildknecht and A. O. Zoss before the commercial material was available.

Applications of Infra-Red Methods in the Structural Examination of Synthetic Rubber

J. E. Field, D. E. Woodford, and S. D. Gehman
Research Laboratories, The Goodyear Tire & Rubber Company, Akron, Ohio

The physical properties of a synthetic polymer are associated with variations in molecular structure which are dependent on the conditions of the polymerizing reaction and the monomers used. In some cases, structural differences of significance for physical properties cannot be detected by infra-red methods because the relative number of chemical linkages affected is too small. An important structural detail which can be followed by infra-red analysis is the relative amount of 1,2 and 1,4 polymerization occurring in polymerization reactions of butadiene. Absorption curves are reproduced to show the wide range in the relative amounts of these two structures. A description is given of an attempt to obtain a quantitative measure of this ratio by means of a calibration curve derived from known mixtures of pure octene 1 and octene 2. For polyisoprene, variations in the proportions of 1,4 and 1,2 or 3,4 structure also occur depending upon the type of polymerization. Comparison with Hevea rubber and Balata fails to disclose definite evidence of *trans*-isomerism in synthetic polyisoprene. Structural differences due to oxidation of polymers may be readily apparent in infra-red spectra, hydroxyl and carbonyl groups being especially prominent. The effectiveness of anti-oxidant in preventing structural changes caused by oxidation is shown in a series of absorption curves for samples of GR-S with and without anti-oxidant. When the samples were heat-treated in air, pronounced structural changes occurred for the sample without anti-oxidant, but no perceptible changes were evident for the sample with anti-oxidant. On the other hand, the anti-oxidant used (phenyl-β-naphthylamine) was ineffective for stabilizing the structure toward ultraviolet light.

INTRODUCTION

INFRA-RED absorption spectra have been long recognized as a convenient means for studying the structure of organic molecules. The interpretations of the spectra are based on the energy interactions of the molecule and the radiations which arise from the vibration of the constituent atoms and molecular rotations. For simple or highly symmetrical molecules, the determination of the normal modes of vibration and the calculation of the absorbing frequencies are relatively simple and straightforward. For more complicated organic molecules, this becomes increasingly difficult because with each additional atom, the number of degrees of freedom is increased by three and the determination of the normal modes of vibration becomes practically impossible. However, interpretations can be made to a useful extent through empirical comparisons with the absorption spectra of simpler known structures.

The data that have been accumulated by investigators in this field have made it possible to assign rather definite absorption frequencies to some of the chemical linkages and functional groups. These correlations which have appeared in numerous places in the literature are partially reproduced in Table I.

Organic compounds generally have strong absorption bands below 1300 cm^{-1} to which few definite assignments can be made with certainty because the vibrations of many of the atoms of the molecule may be involved rather than a specific part of it. It is quite clear that such empirical relationships must be relied upon in studying the structural variations of the long chain, complex molecules which occur in butadiene and isoprene polymers and copolymers and other synthetic rubbers. This procedure has been applied to determine the effects of oxidation and of variations in monomers and polymerizing conditions on the structure of synthetic rubber. It is practically certain that physical deficiencies of synthetic rubber are due principally to the structure of the long chain molecules rather than to the chemical nature of the monomers used.

Table I.

Frequency range	Chemical linkage
3000–4000 cm^{-1}	CH, OH, NH
2000–2500 cm^{-1}	C≡C, C≡N
1350–2000 cm^{-1}	CH_3, CH_2, CH, C=C, C=O
900–1000 cm^{-1}	C=C

EXPERIMENTAL PROCEDURE

A conventional Littrow type rocksalt prism spectrometer of our own design and construction, shown in Fig. 1, was used for obtaining the absorption records. The refracting faces of the 60-degree prism are 15 cm long by 10 cm high. The current from the vacuum thermocouple is conducted to a galvanometer the deflections of which actuate a photo-cell amplifier. The absorption curves are automatically recorded by a Leeds and Northrup Speedomax which operates from the amplifier. These curves show the absorptions (not percent absorption) by the varying galvanometer deflection recorded as a function of the wave number setting of the Littrow mirror.

The samples were prepared, in most instances, by evaporating the solvent from polymer solutions poured on rocksalt plates, thus leaving a thin film of polymer for examination. The thickness of the film was adjusted for about 10 percent transmission of the 1450 cm^{-1} band. This was rather easily accomplished by controlling the concentration of the solution and by the use of successive layers of film. The latex samples were prepared by placing a few drops in a closed glass frame floating on a mercury surface. In order to prevent undue oxidation, these films were first dried in a nitrogen atmosphere and then in a vacuum desiccator. Since the film thickness of the various samples was maintained essentially the same, a fair estimate of the intensity of the absorption of a particular band can be made relative to a corresponding one of another sample without transforming the absorption curves into terms of percent transmission.

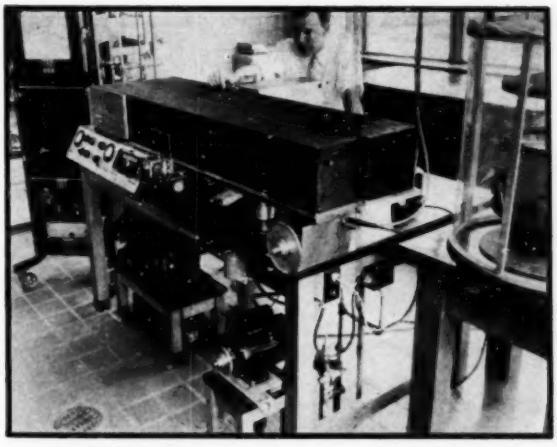

FIG. 1. Spectrometer and recorder.

ABSORPTION SPECTRA OF VARIOUS POLYMER CHAIN STRUCTURES

The chemistry of polymerizing reactions is rather complex in character. Any discussion concerning the general principles and mechanisms of such reactions need not be entered into here. However, in order to understand the absorption spectra of polymers of butadiene and isoprene, which have played such an important role in the development of synthetic rubber, it is necessary to point out the various ways in which polymerization of these diolefinic monomers can proceed. These are diagramatically shown in Fig. 2. The structures appearing at the double

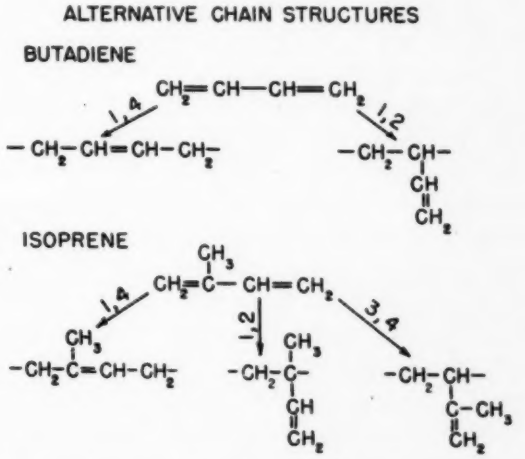

FIG. 2. Alternative chain structures for polybutadiene and polyisoprene.

bonds may be typified in the manner shown in Table II. Compounds which can be differentiated according to the above classification are known to have characteristic absorption frequencies which will be of considerable value in the interpretation of the absorption spectra to be discussed.

TABLE II.

Polybutadiene	
1,4 addition	$R_1CH=CHR_2$
1,2 addition	$RCH=CH_2$
Polyisoprene	
1,4 addition	$R_1R_2C=CHR_3$
1,2 addition	$RCH=CH_2$
3,4 addition	$R_1R_2C=CH_2$

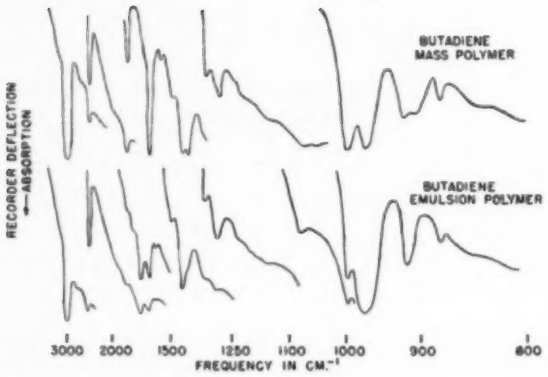

FIG. 3. Absorption curves for sodium and emulsion polymers of butadiene.

POLYBUTADIENE AND GR-S

The absorption curves for sodium and emulsion polymers of butadiene are shown in Fig. 3. The differences appearing in the two spectra are quite significant. That a high degree of 1,2 polymerization occurs in the sodium polymer has been previously deduced from ozonolysis and infra-red work.[1–4] This is recognized by the appearance of the very strong band at 996 cm^{-1} which is characteristic of compounds of the type $RCH=CH_2$.[2,3,5] A relatively weak band appears at this frequency for the emulsion polymer. Absorptions are present in both polymers at 967 cm^{-1} which is characteristic of compounds of the type $R_1CH=CHR_2$. The bands at 914 cm^{-1} and 1450 cm^{-1} appear to be split into doublets in the sodium polymer, evidently because of the influence of the large number of terminal double bonds.

In the development of synthetic rubber of the GR-S type, it was found that emulsion polymers possessed the more desirable physical properties and processing qualities. Since the product of a reaction of this type for butadiene leads predominately to the 1,4 structure, it is thought that the relative amounts of these two structures in the copolymer has some bearing on these physical characteristics because butadiene is the principal constituent in the GR-S type of synthetic. Accordingly, methods have been sought to obtain quantitative determinations of relative amounts of 1,2 and 1,4 structure in polymers and the GR-S copolymer. Infra-red methods afford a positive and direct way of carrying out such analyses. The following procedure has been found to be convenient for this purpose. Referring to Fig. 4, which illustrates the resultant band due to the two overlapping bands at 996 and 967 cm^{-1}, it is evident that the ratio A/B can be used for characterizing the band structure. If this ratio can be calibrated in terms of known relative amounts of the two structures, the infra-red absorption spectrum immediately becomes applicable as a method of determination. In order to do this, absorption spectra were obtained for two compounds, one having a terminal double bond and the other an internal double bond. Pure samples of octene-1 and octene-2 were used for this purpose. The spectra of known mixtures of these hydrocarbons were obtained and the ratio A/B was determined from the absorption curves. This ratio was then plotted as a function of percent octene-1 shown in Fig. 4. It is then assumed that this curve applies for the butadiene polymers and copolymers. This assumption may not be entirely valid since other structural effects on these bands are not considered, but it seems reasonable to believe that a very close approximation can be reached with this method. Following the procedure outlined above, the results for several typical polymers are given in Table III.

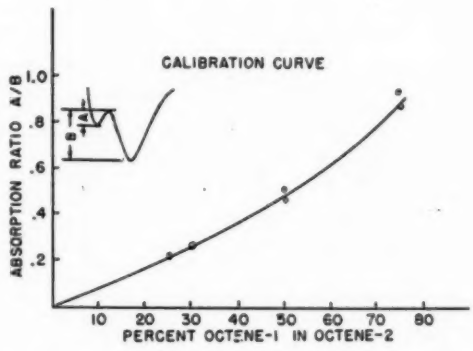

FIG. 4. Calibration curve for determining the amount of 1,2 structure in polymers and copolymers of butadiene.

[1] E. N. Alekseeva, Rubber Chem. Tech. **15**, 693, 698 (1942).
[2] Unpublished work of M. W. Swaney, J. U. White, and P. J. Flory. Esso Laboratories Standard Oil Development Company.
[3] H. W. Thompson and P. Torkington, Trans. Faraday Soc. **41**, No. 279, 246 (1945).
[4] Unpublished work of R. S. Rasmussen and R. R. Brattain, Shell Development Company.
[5] M. Tuot, J. Lecomte, and S. Lorillard, Comptes rendus **211**, 586 (1940).

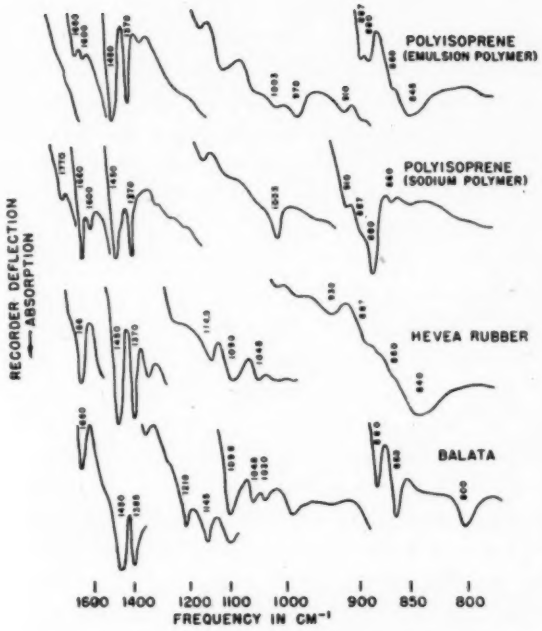

FIG. 5. Absorption curves for comparing the structure of Hevea rubber, Balata, and the emulsion and sodium polyisoprenes.

The GR-S sample included in the above table was a typical production sample. It is of interest because it shows that the amount of 1,2 structure determined by this method is within reasonable agreement with estimates obtained by other methods. The extremely high percentage shown for the sodium polymer may not be so accurate since the method appears to be less sensitive for mixtures with such high ratios.

POLYISOPRENE

The absorption spectra for the emulsion and sodium polymers of isoprene are shown in Fig. 5. The structural study of this polymer is of particular interest because the monomer unit is the same as for natural rubber and yet the structure and physical properties of the latter cannot be reproduced in the synthetic product. The absorption spectra for Hevea rubber and Balata are included in this figure for the purpose of comparison.

If the isoprene is polymerized by 1,4 addition, the structure type would be $R_1R_2C=CHR_3$ which corresponds to the structure of Hevea rubber. Compounds of this general type have a characteristic band around 840 cm^{-1}. A band does appear here for the emulsion polymer indicating that this structure is present. In comparing this spectrum with the one for Hevea, it is observed that, although there are some striking similarities, the structures of the two are not identical. However, they do have more in common than do the sodium polymer and Hevea. On this basis, it is reasonable to believe that the emulsion product of polyisoprene is chiefly of the 1,4 structure.

If the polymerization reaction proceeds by 1,2 addition, the resulting compound would fall in the $RCH=CH_2$ class. This is the same general type as the 1,2 addition of butadiene, and strong bands would be expected to appear around 996 cm^{-1} and 914 cm^{-1}. Rather weak bands do appear in these regions for the emulsion polymer while relatively stronger ones are present in the spectrum of the sodium polymer. Thus, a small amount of this structure is indicated in both of these polymers.

TABLE III.

Type of polymer	Ratio A/B	% 1,2 addition
Polybutadiene (emulsion)	.187	21
Polybutadiene (sodium)	1.1	80
GR-S (production)	.180	19

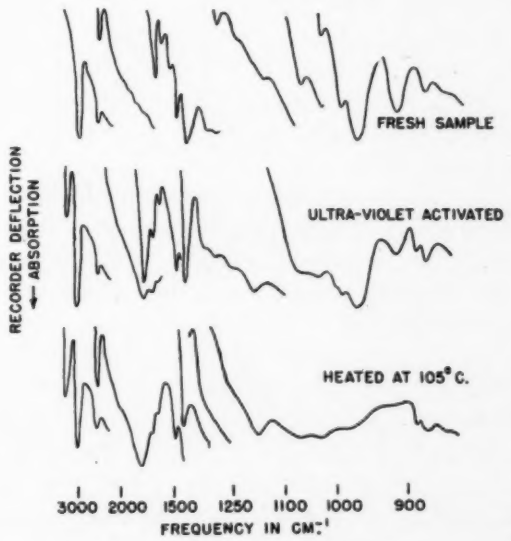

FIG. 6. Absorption curves showing oxidation of GR-S in the absence of anti-oxidant.

The absorption spectrum for the sodium polyisoprene shows a very strong absorption band

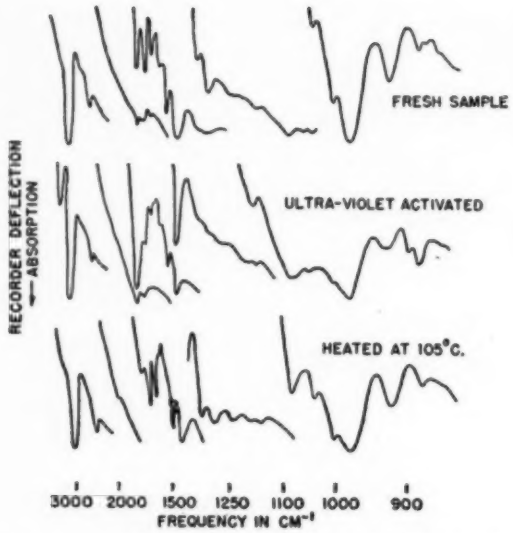

FIG. 7. Absorption curves showing oxidation of GR-S in the presence of anti-oxidant.

at 881 cm^{-1}. Compounds having the general structure $R_1R_2C=CH_2$ are known to have absorption bands in this region. Accordingly, this type of compound would correspond to the 3,4 addition of the polyisoprene structure. The absence of the bands at 840 cm^{-1} and 970 cm^{-1} and the intense absorption at 881 cm^{-1} lead to the belief that the structure of this polymer is predominantly of the 3,4 type.

Balata, the absorption spectrum of which is included in Fig. 5, is generally presumed to be a *trans*-isomer of Hevea rubber. This *cis-trans*-isomerism causes distinctive differences in the infra-red absorption spectra.[6] Comparison of the spectra for these natural products with those for synthetic polyisoprenes does not disclose the presence of any appreciable amount of the *trans*-isomer in the synthetic polymers. This is particularly interesting because there has been speculation that the inferiority of the synthetic polymers to Hevea rubber might arise from the fact that a mixture of *cis*- and *trans*-structure occurs in the synthetic polymers.

EFFECTS OF OXIDATION

The effects of exposure of GR-S films to air under conditions such as to accelerate oxidation are shown in the absorption curves appearing in Fig. 6 and Fig. 7. The samples were all prepared from a master solution of production GR-S in benzene from part of which the anti-oxidant (phenyl-β-naphthylamine) was removed by reprecipitation. Films with and without anti-oxidant were exposed to ultraviolet light (Atlas Fadeometer, violet arc) for at least twenty-four hours at a constant temperature of 40°C. Similar films were heated for twenty hours in air at 103°C. The absorption curves resulting for films without antioxidant are shown in Fig. 6. The control or untreated sample is represented in the top curve. The structural changes initiated by exposure to the ultraviolet light are apparent in the middle curve. New bands appear at approximately 3500 cm^{-1} and 1720 cm^{-1} which are definitely due to O−H and C=O linkages, respectively. These groups have been identified chemically in oxidized natural rubber.[7,8] Increased absorption is also noted in the 1050 cm^{-1} range. The relative intensities of the 996 and 967 cm^{-1} are difficult to interpret. The absorption in the vicinity of the 996 cm^{-1} band is increased but the significance of this is confused by the generally increased absorption over this whole region. The decrease in the intensity of the 914 cm^{-1} band probably is indicative of a definite decrease in the total number of double bonds, which would be expected with oxidation reactions.

When a similar sample was heated for twenty hours in air at 105°C, a number of differences appear in the absorption record when compared with that for the ultraviolet activated sample. This is represented in the bottom curve of Fig. 6. The intensity of the O−H band has increased

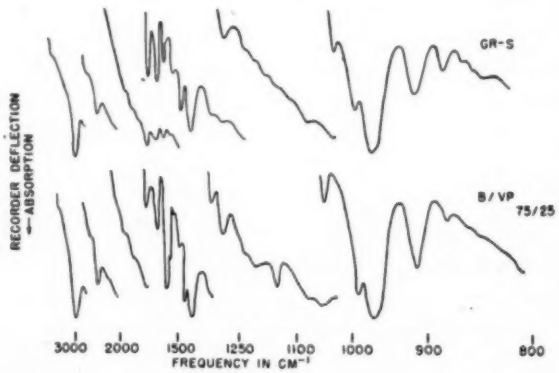

FIG. 8. Absorption curves comparing the structure of GR-S and a copolymer of butadiene and vinyl pyridine.

[6] S. B. Hendricks, S. G. Wildman, and E. J. Jones, Arch. Biochem. **7**, No. 3. (Sept. 1945).

[7] R. F. Naylor, Trans. I.R.I. **20**, 2, 45 (1944).
[8] G. F. Bloomfield, Ind. Rubber J. **108**, 495 (1945).

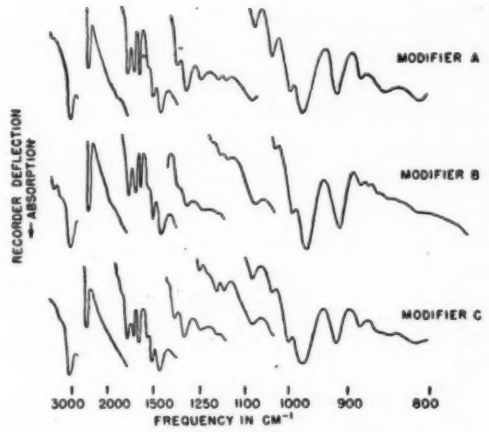

FIG. 9. Absorption curves showing the effect of modifiers on the structure of GR-S.

noticeably. The carbonyl band at 1720 cm^{-1} has broadened considerably. Since the absorptions for the various carbonyls occur at slightly different frequencies, it is possible that the broadening of this band might be due to additional types of carbonyls. The absence of the 914 cm^{-1} band indicates a rather complete saturation of the double bonds. There is a general region of heavy absorption extending from about 900 cm^{-1} to 1300 cm^{-1}, probably indicating heterogeneity in the structure brought about by oxidation. The structure responsible for the occurrence of the 890 cm^{-1} band upon oxidation is not definitely known but its position would suggest the type $R_1R_2C=CH_2$.

In examining the absorption curves of Fig. 7 corresponding to samples with anti-oxidant, it appears that ultraviolet activation is the only agency that has produced any appreciable structural changes. These changes are similar to the ones which occurred for the sample without anti-oxidant. With the anti-oxidant present, twenty hours exposure in air at 105°C produced no noticeable structural changes. It is very interesting that structural changes due to heat treatment are inhibited by the anti-oxidant whereas this anti-oxidant has little influence on the effects caused by ultraviolet activation. Apparently, the mechanisms of oxidation are different in the two cases.

MISCELLANEOUS POLYMER STRUCTURES

An absorption curve for a typical butadiene-vinyl pyridine copolymer is reproduced in Fig. 8 together with one of GR-S for comparison. Although many of the bands are very similar in character, there are several differences that can be observed. One is the relative increase in the intensity of the 1590 cm^{-1} band in the vinyl pyridine copolymer. This band is usually attributed to aromatic double bonded carbons but the presence of the nitrogen in the aromatic group becomes evident with an additional absorption at 1570 cm^{-1}. There is a shift toward the longer wave-lengths of the aromatic CH bending frequencies around 1490 cm^{-1} and a characteristic band at 1150 cm^{-1}. Hence these two synthetic rubbers can be readily distinguished by their infra-red spectra. It is noteworthy that the overlapping bands at 996 cm^{-1} and 967 cm^{-1} are so very similar for the two types of rubber.

Absorption curves are shown in Fig. 9 for samples of GR-S in which different mercaptan

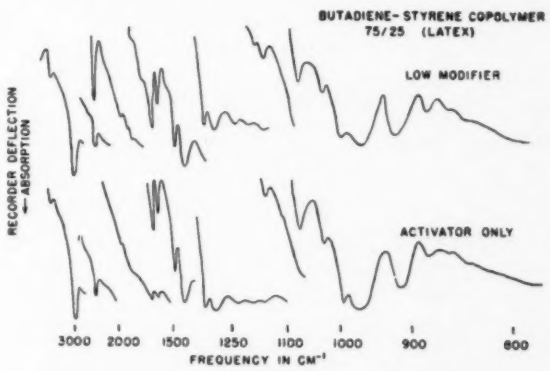

FIG. 10. Absorption curves showing the structure of GR-S in the absence of modifier.

type modifiers were used in the polymerization. These films also contained phenyl-β-naphthylamine as anti-oxidant. Since the presence of modifiers during polymerization influences the physical properties of the product, it was thought that structural differences might be detected in these absorption spectra. However, the absorption curves for polymers made with these three modifiers are strikingly similar. Since the 996 cm^{-1} band shows no evident difference in the number of side vinyl groups present and other differences in the spectra are insignificant, it can be concluded that these three modifiers influence the structure in much the same way, at least as far as can be detected by infra-red methods. In this case, there appears to be little hope that

these methods will detect such differences, since the fundamental structure is so similar. The differences in physical properties evidently result either from a variation in a relatively small proportion of the chemical linkages, as might readily be the case for cross linking, or in variations which do not give rise to unique absorption bands. The amount of modifier present is so small that it does not appear directly in any of the absorption curves.

Since unmodified copolymers of butadiene and styrene are generally insoluble in organic solvents, films were made from latices of the copolymers containing little or no modifier. The absorption curves for these are shown in Fig. 10, respectively for samples containing .1 percent mercaptan activator-modifier and .1 percent mercaptan activator. The latter activator is considered to have little or no modifying action. The increased number of side vinyl groups as compared to GR-S becomes apparent from the increased absorption of the 996 cm^{-1} band. This increase is more pronounced for the slightly modified sample than for the one which contained activator only. This evidence is far from conclusive as the effect of the modifier and activator on the amount of 1,2 polymerization but indications are that when the normal amount of modifier is used there are less side vinyl groups formed than if no modifier or only a very slight amount of modifier is present.

We wish to express our appreciation to Dr. L. B. Sebrell and The Goodyear Tire & Rubber Company for permission to publish this work, to Dr. A. M. Borders and Dr. J. O. Cole of the Research Staff for preparing the polymers used, and to Dr. M. R. Fenske for supplying the samples of octene-1 and octene-2.

A Photoelectric Instrument for Light Scattering Measurements and a Differential Refractometer

P. P. DEBYE*
General Aniline and Film Corporation, Central Research Laboratory, Easton, Pennsylvania

The method of determining particle sizes and molecular weights by light scattering measurements on solutions is finding increasing fields of application. In order to obtain the necessary data quickly and conveniently, an instrument has been developed which allows the required light scattering measurements to be taken on a routine basis. This apparatus is described. It measures transmission and the scattering of light at 90°; two different schemes can be employed to obtain the angular intensity distribution of the scattered light. A description is also given of a compensating refractometer which is used to determine the difference in refractive index of solvent and solution. The instrument, which is simple in design, gives a direct reading of the refractive index difference and has an accuracy of better than 10^{-5}. The light scattering instrument has been tested using polystyrene of known molecular weight, and has been applied to study the change of apparent molecular weight (or particle size) of a series of polyvinyl ethers as a function of concentration in some cases, also a number of solvents. For a series of polyvinyl *n*-butyl ether samples which was studied, the relation between the intrinsic viscosity $[\eta_i]$ of the benzene solutions and the weight average molecular weight M determined by light scattering is $\eta_i = .365 \times 10^{-7} M^{1.48}$.

IN 1944, P. Debye[1] described a method for determining by light scattering measurements on solutions the molecular weight and particle size of the solute. Since then this procedure has become an important tool in the field of high polymers, and it seemed desirable to have special instruments to make the necessary measurements more conveniently.

The fundamental concepts of the theory show that the diameter of particles larger than about 1/20 of, but still comparable to, the wave-length of the light can be determined if the angular intensity distribution of the scattered light is known. To illustrate this Fig. 1 shows the intensity of the scattered light as a function of the angle; the family of curves is drawn for varying ratios d/λ, where d is the particle diameter and λ the wave-length of the light in the solution. This particular angular intensity dis-

* Now at Bell Telephone Laboratories, Inc., Murray Hill, New Jersey.
[1] P. Debye, J. App. Phys. **15**, 338 (1944).

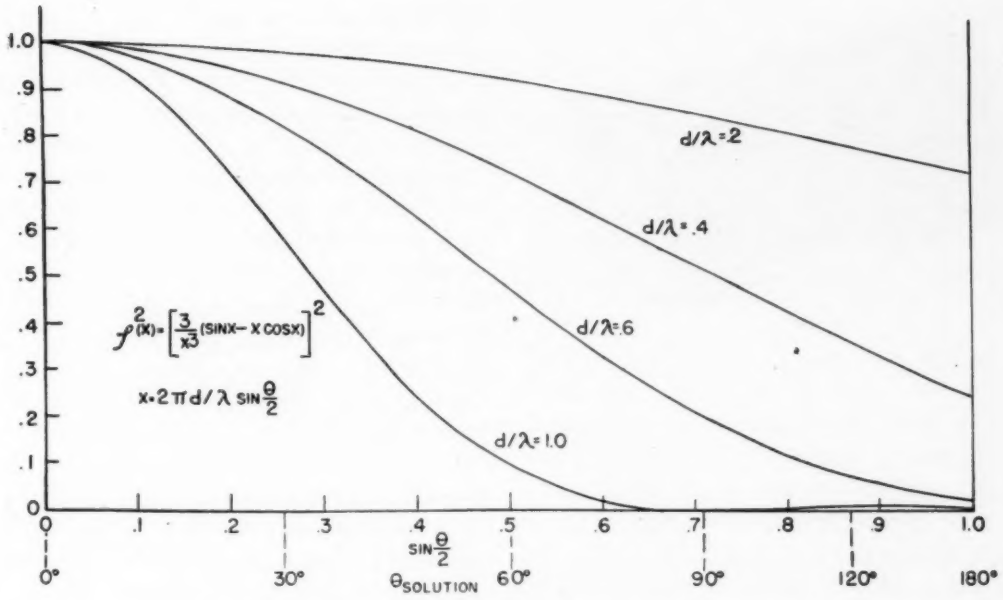

FIG. 1. Theoretical angular distributions for spherical particles.

tribution has been calculated for spherical particles and the angular intensity variation due to the polarization effect has been omitted.

In case the particles are smaller than approximately 1/20 of the wave-length and the solution scatters as much in the forward as in the backward direction, P. Debye's formula for the turbidity (τ) of the solution (in the limit for infinite dilution) is applicable:

$$\tau = \frac{32\pi^3}{3}\,\frac{\mu_0^2(\mu-\mu_0)^2}{\lambda^4}\,\frac{1}{n},$$

where μ_0 and μ are the refractive indices of solvent and solution, respectively, λ is the wave-length of the light in vacuum and n the number of particles per cc. For practical purposes Avogadro's number (N), the molecular weight (M), and concentration (c) in g/cc can be introduced leading to the relation

$$Kc/\tau = 1/M,$$

$$K = \frac{32\pi^3}{3}\,\frac{\mu_0^2}{N\lambda^4}\left(\frac{\mu-\mu_0}{c}\right)^2.$$

From this the number (n) of solute particles per cc can be calculated. The turbidity in practical concentrations and solvents is for many materials quite small. In most cases it is therefore easier to measure the amount of scattered light, for example as 90° scattering, instead of the small difference in intensity of the primary light beam before and after it passed through the solution. The quantity of $\mu-\mu_0$ also requires careful measurement; its magnitude is in general approximately .001 for a 1 percent solution. The useful lower molecular weight limit of the method is determined by the refractive index difference that can be obtained for a given polymer-solvent system. It lies roughly in the neighborhood of a molecular weight of 10,000. The weights as determined are weight average molecular weights.

The two instruments[2] presently to be described were developed in order to measure (a) the angular intensity distribution, (b) turbidity by the measurement of transmission, (c) turbidity by measurement of 90° scattering, and (d) the refractive index difference ($\mu-\mu_0$) of solution and solvent. The photoelectric instrument is adapted for measurement of a, b, and c and the differential refractometer reads $\mu-\mu_0$ directly.

The light scattering unit with its amplifier is shown in Fig. 2. The unit contains four separate

[2] Both instruments were built by Mr. H. Bush, Chemistry Department, Cornell University, Ithaca, New York.

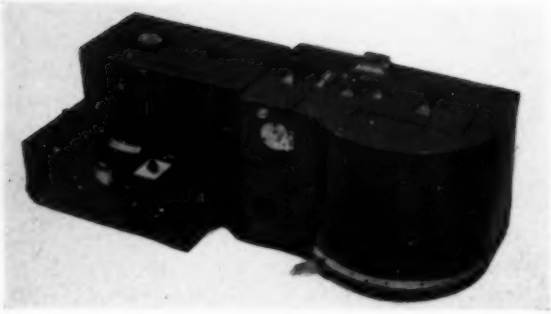

FIG. 2.

photo-tubes of the type RCA 929 which can be connected interchangeably to a special d.c. amplifier.[3] The light intensities are read on a built-in taut suspension galvanometer, which is shunted in order to have a variable sensitivity range of 1:2:5:10:20:50. The linearity of this arrangement has been checked on a photometer bench and has been proved satisfactory. Before and after each series of measurements the primary light beam intensity is obtained by reflection on a magnesium carbonate block under 45 degrees with respect to the primary light beam and with an additional dark glass filter interposed. In this way long term fluctuations of the light source as well as of the amplifier can be eliminated.

The light scattering unit has three separate and easily interchangeable lamp houses; one house containing a high intensity tungsten filament bulb, the other a water-cooled high pressure mercury arc (H-6), and the third a medium pressure-forced air cooled mercury arc of the AH4 type. Almost all measurements are taken with this latter lamp. It has been found that a simple electrical stabilizing circuit makes the light output of the AH4 bulb quite satisfactorily constant. The circuit used is shown in Fig. 3; it consists of a voltage regulating autotransformer (T_1), a current regulating ballast lamp (B), a step-up transformer (T_2) to compensate for the voltage drop in the ballast, and the auxiliary transformer (T_3) which is always necessary to operate the AH4 bulb from line current.

The arrangement of the optical parts is shown schematically in Fig. 4. The light of the mercury arc illuminates an opal glass (O) situated in front of a slide (A), having various interchangeable apertures of different sizes; then it passes a monochromatic glass color filter (F) and a stationary lens (L_2) with iris diaphragm (D). The parallel beam of light which leaves the lens can then be intercepted by a Polaroid (P) and/or an extra plain glass slide (G). The latter is used to calibrate the electrical parts by decreasing the primary light intensity by small but known amounts. This is useful in the case of transmission measurements where the zero of the galvanometer is suppressed by electrical means. Between the aperture slide and the color filter there is a removable additional lens (L_1) which on account of its higher numerical aperture gives greater light intensities. It focuses the first aperture in the center of the solution cell (S).

As shown in Fig. 4 one photo-tube is situated close to the solution cell for measuring turbidity by 90° scattering. The other photo-tube is used for transmission measurements but it can also be applied to measure angular distribution; the latter is done by moving the tube in a semi-circle around the solution cell. The perpendicular axis of this motion extends through the bottom of the unit and is connected to an indicator arm on the outside of the case where a pointer shows the position of the tube in degrees with respect to the primary beam. The motion covers an angle interval from 0 to 125 degrees.

In an arrangement like this it is necessary to employ a circular solution cell unless one applies corrections for the varying reflection and absorption, which is at least time consuming. In order to avoid this a suggestion by P. Debye has been followed. The same support which carries the photo-tube for transmission measurements carries in addition another photo-tube which moves on a semi-circle underneath the solution cell. This tube receives its light from a mirror (at 45° to the horizontal) which travels suspended from

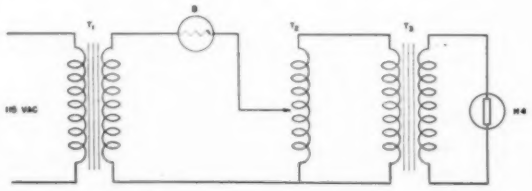

FIG. 3. Light source stabilization circuit.

[3] Photovolt Corporation, 95 Madison Avenue, New York, New York.

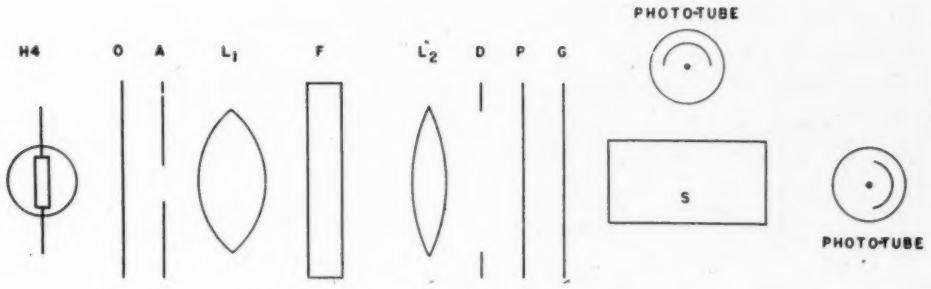

FIG. 4. Schematic arrangement of optical parts in the light scattering unit.

the outside but within the solution on the same semi-circle as the photo-tube. A sketch of this arrangement is shown in Fig. 5. By this method the scattered light always leaves the solution cell perpendicularly to the interface solution-air and the corrections otherwise necessary are avoided.

A fourth photo-tube not shown in the diagram is used to measure independently the intensity of the light source; it receives the light from a plain glass which is placed under 45 degrees in the primary beam.

The apparatus has been calibrated with a solution of polystyrene of which the weight average molecular weight had been determined as 409,000±7 percent. This figure has been arrived at by J. McCartney[4] who used an instrument of special design to measure the turbidity. The reported number average molecular weight by osmometry for this polystyrene was 240,000.

The differential refractometer (Fig. 6) allows the measurement of $\mu-\mu_0$ with great convenience and an accuracy of about 0.000,003. This is appreciably better than can be achieved with the ordinary type of refractometer and not quite as good as the accuracy possible with an interferometer. However, the great simplicity of the instrument and the ease with which it performs makes this refractometer a great asset if a number of refractive index differences have to be obtained every day. The original design was developed in the course of work for the Rubber Reserve Corporation at the Chemistry Department, Cornell University, in 1943; the instrument as described here is an improved copy of the Cornell refractometer.

A schematic drawing is shown in Fig. 7. An adjustable precision slit (S) is illuminated by monochromatic light from a mercury arc (AH-4) and an image (I) of this slit is formed at a distance of about 190 cm in the field of a filar micrometer. A rectangular glass cell (C) containing the solvent is placed between the two lenses (L_1 and L_2) in the parallel light beam. Suspended in the solvent cell (C) is a hollow prism glass cell (P) containing the solution. The refraction angle of the prism is approximately 125 degrees. If there is any difference of refractive index of solvent and solution, the image of the slit which can be observed in the eyepiece of the filar micrometer will undergo a deflection. If the

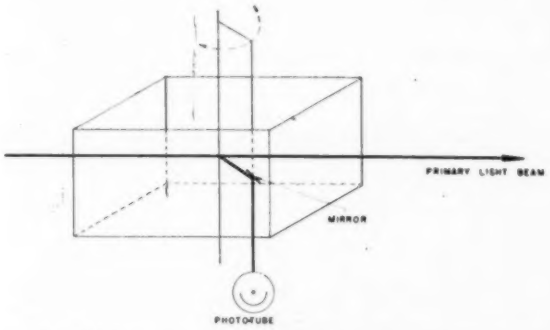

FIG. 5. Schematic arrangement for the measurement of the angular intensity distribution.

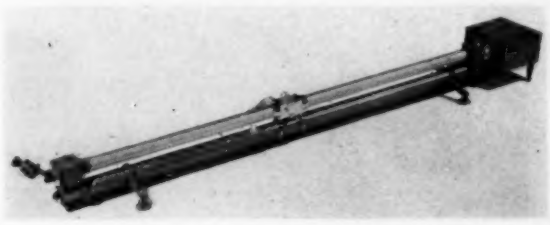

FIG. 6.

[4] J. McCartney, Chemistry Department, Cornell University, Ithaca, New York.

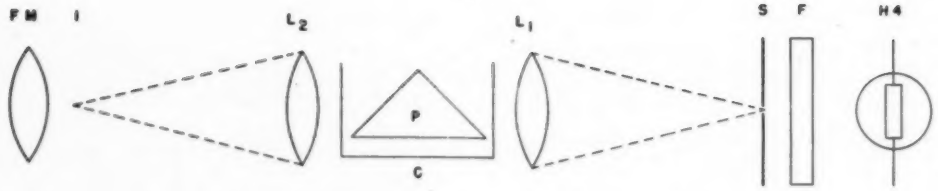

FIG. 7. Schematic arrangement of the differential refractometer.

difference in refractive index $(\mu-\mu_0)$ is not too large, the image deflection will be proportional to the refractive index difference. For this instrument the full scale deflection is still in the linear range.

The image deflection can be calculated by the following equations. If the top angle of the prism is A, the angular deflection α and prism and cell have the refractive indices μ and μ_0, respectively, then

$$\alpha=2(\mu-\mu_0)\tan A/2.$$

With a lens of focal length (f) this gives an image deflection X

$$X=\alpha f=2f\tan A/2(\mu-\mu_0).$$

The relation shows that the image deflection X depends linearly on the refraction difference $\mu-\mu_0$ only in first approximation (for small deflections).

The equation for the image deflection (X) also shows that X is independent of the refractive index of the solvent (μ_0). The instrument can therefore be calibrated with, for instance, an aqueous sucrose solution and then be used for any other solvent-solute system.

The differential method employed in this instrument holds the great advantage of being fairly insensitive to small temperature changes. On this account a good enclosed type mercury regulator will work well for the temperature control of the water which is pumped through the jacket surrounding the cells (Fig. 8). In practice the temperature equilibrium of prism and cell is attained in 5–7 minutes.

The refractometer has been calibrated with dilute sucrose solutions of known refractive index. The calibration (Fig. 9) is shown to be linear.

Since the completion of these instruments, a great number of materials have been tested. Some of the experimental results on polystyrenes are shown in Fig. 10. The data for Kc/τ have been linearly extrapolated (by the method of least squares) to zero concentration, at which point the ordinate corresponds to the reciprocal of the actual molecular weight. The scale in Figs. 10–12 is drawn in arbitrary units.

Another group of polymers which has been of great interest has been that of the polyvinyl ethers. Figure 11 shows the experimental curves for various polyvinyl normal butyl ethers. It is interesting to note that the plotted data for these materials show a definite downward curvature.

FIG. 8.

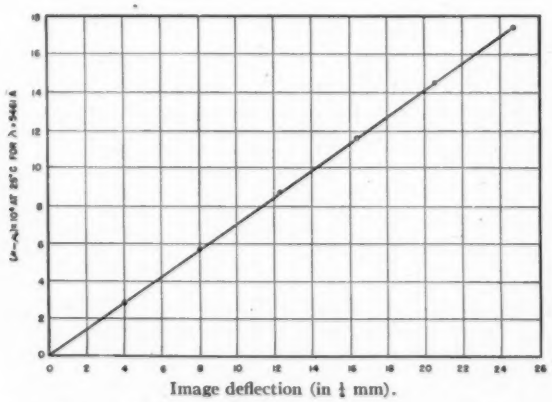

FIG. 9. Calibration of differential refractometer.

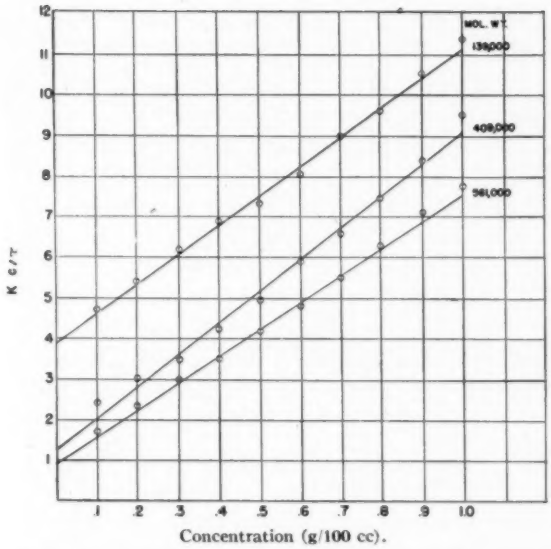

FIG. 10. Experimental data on polystyrenes in toluene.

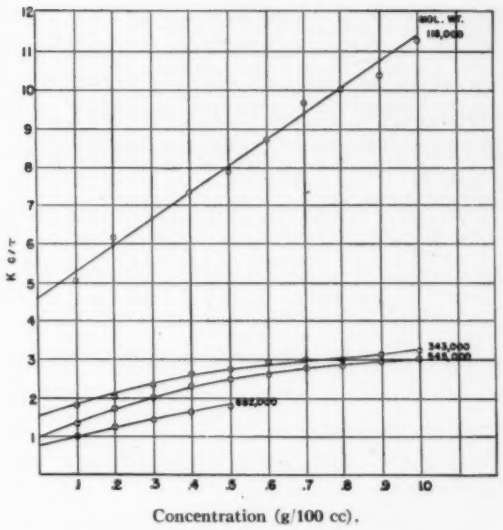

FIG. 11. Experimental data on polyvinyl *n*-butyl ethers in benzene.

This might be explained by agglomeration of particles at increased concentration. A very broad particle size distribution also would show a similar effect. In this case the purpose of the investigation was to connect molecular weights with viscosity values in order to obtain the constants in the familiar expression

$$\log \eta_i = A + \alpha \log M.$$

The intrinsic viscosities were determined in benzene solution at 25 C. The flow times were measured in tubes of the modified Ostwald-Fenske design. The constants for the polyvinyl normal butyl ether were determined as $A = -7.14$ and $\alpha = 1.36$.

Another interesting case was found in a preliminary study of the effect of milling (at 25–30 C) on a sample of polyvinyl isobutyl ether. Figure 12 shows that the slopes of the Kc/τ *vs.* concentration data were very much decreased by milling the polymer. Considering the experimental error involved, however, this procedure did not seem to affect appreciably the weight average molecular weight of the materials under the conditions of this experiment. This might indicate that the homogeneity of the sample increases by milling, which necessitates not only a breaking down of the high molecular weight fraction but also at the same time a building up of larger units from the lower molecular weight fraction. The smaller slope of the milled samples could also be explained by a decreased solubility. The milled polymer may have been oxidized during the milling process resulting in a less soluble material. At present this question is being studied with polymers that have been milled in inert atmosphere.

TABLE I.

Material	η sp/concentration in benzene at 25 C for conc. = .2 g/100 cc	Molecular weight by light scattering
Not milled	1.75	219,000
10 min. milled	1.01	233,000
45 min. milled	.68	240,000

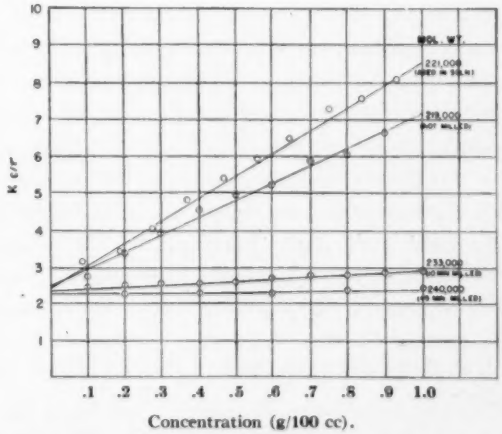

FIG. 12. Experimental data on polyvinylisobutylether in benzene.

The relatively small change in the average molecular weight is surprising if one considers the decrease in specific viscosity/concentration. A comparison of viscosity data and the molecular weight as determined by light scattering is shown in Table I.

Figure 12 also shows as another example the experimental data for the unmilled material after it has been "aged" in solution for 48 hr. at about 65 C. Again the molecular weight is essentially unchanged. However, the greater slope seems to indicate a wider particle size distribution or a change in solubility. Further work should be done to extend these experiments.

Thermal Expansion and Second-Order Transition Effects in High Polymers III. Time Effects

R. S. Spencer and R. F. Boyer
Physical Research Laboratory, The Dow Chemical Company, Midland, Michigan

It has been suggested that the so-called second-order transition in high polymers is not an equilibrium phenomenon, i.e., a true thermodynamic singularity, but rather a rate effect. Confirmation of this point of view has been obtained by determining the equilibrium volume-temperature curve of polystyrene. Such equilibrium curves exhibit no transition within the range of from 20° to 140°C, whereas the same material shows a transition at about 82°C for rates of heating usual in thermal expansion measurements. Two facts appear in agreement with the viscous flow interpretation of the thermal expansion process: First, two mechanisms were found to operate, at markedly different rates. One gave almost instantaneous expansion, even at room temperature, whereas the other was quite temperature-dependent in this region, being extremely slow at room temperature. Second, the activation energy for the slower mechanism was found to be of the order of magnitude of that for viscous flow, considerably lower than the activation energy for rubber-like elasticity. Volume-temperature curves at finite rates of heating are discussed in light of these findings.

INTRODUCTION

THE thermal expansion of high polymers exhibits features quite different from the usual behavior of simple organic liquids. The volume-temperature curve is characterized by the presence of a temperature, or interval of temperature, which separates the curve into two portions corresponding to two markedly different expansion coefficients.[1] This temperature has been known as the second-order transition temperature, so-called because of the fact that there is an apparent discontinuity in the secondary thermodynamical quantities, such as expansion coefficient, heat capacity, etc., at that point.[2] As the temperature is raised through this point, there appears to be a change of state, without latent heat, resulting in a larger value of thermal expansion coefficient and heat capacity and a change in the general physical properties of the material. The polymer softens and acquires rubber-like elastic properties. Significantly enough, however, there is no discontinuity of first- or second-order in the viscosity.[3]

Several interpretations of this phenomenon have been suggested, with no very conclusive evidence appearing, as yet, to confirm any one of them completely. The second-order transition might be a true thermodynamical singularity of the type discussed by Ehrenfest[4] and Mayer and Streeter.[5] Justi and Laue[6] have pointed out that Ehrenfest's conditions for a second-order transition are not sufficient, and the further condition

[1] R. F. Boyer and R. S. Spencer, J. App. Phys. **15**, 398 (1944).
[2] R. F. Boyer and R. S. Spencer, J. App. Phys. **16**, 594 (1945). The first two references present a brief survey of second-order transition phenomena and give a number of references to earlier work.
[3] G. S. Parks, *et al.*, Physics **5**, 193 (1934).
[4] P. S. Ehrenfest, Comm. Leiden, Suppl. 75b (1933).
[5] J. E. Mayer and S. F. Streeter, J. Chem. Phys. **7**, 1019 (1939).
[6] E. Justi and M. Laue, Zeits. f. tech. Physik **12**, 521 (1934).

they proposed would lead to something which should perhaps more properly be termed a third-order transition. Pines[7] has extended the thermodynamical treatment to the case in which the transition appears to take place over a temperature interval rather than at a single point. The authors have suggested elsewhere[8] the possibility that the apparent transition in high polymers might consist of a series of λ-transitions, of the type encountered in some simpler molecules,[5] occurring at temperatures spaced quite close together. In this way the general features of the heat capacity-temperature curve may be accounted for.

The other viewpoint, which is now rather widely accepted, is to assume that there is no thermodynamical singularity at the second-order transition and to ascribe all attending phenomena to the temperature dependence of the time-rate of whatever internal mechanism is operating to give the macroscopic property under observation. Thus Alfrey, Goldfinger, and Mark[9] interpret the apparent second-order transition as the point where the rate of attainment of equilibrium is of the same order of magnitude as the time-scale of ordinary physical experiments. In the case of the change of volume with temperature, they distinguish between two mechanisms of expansion: (1) an over-all increase in intermolecular distances due to enhanced thermal vibrations, as in the case of a crystalline solid, and (2) the diffusion of "holes" through the material.

The rate of the second process is strongly temperature-dependent and is taken to account for the transition phenomena observed. The authors have proposed[2] a similar scheme in which more emphasis is placed on the viscous flow of chain segments necessary to create new "holes" and thereby increase the volume. The second-order transition then begins at the lowest temperature at which an observable volume change is produced by viscous flow of the segments under the expansive forces acting on the segments, within the time limits of the experimental technique employed. This introduction of the concept of viscous flow into the thermal expansion process has proven very fruitful in interpreting and correlating the effects of various external variables, such as applied stresses, plasticizers, and experimental time scale, on the transition temperature. It has also served to explain the origin of the second-order transition observed in heat capacity measurements, which will be discussed in more detail in a later paper in this series.

Available data seem to favor regarding apparent second-order transitions as rate effects rather than thermodynamical singularities. Jenckel[10] was able to lower the transition temperature of selenium glass 7°C by extending the heating time from several hours to several days. Alfrey, Goldfinger, and Mark[9] also reported a 7°C variation of the transition temperature of polystyrene as the rate of heating or cooling was varied. Richards[11] has pointed out that the transition temperature of glucose glasses varies over a much wider interval, from 7° to 77°C, as the rate of observation is speeded up in the sequence heat capacity-thermal expansion-1000 c.p.s. dielectric constant.

On the other side of the picture it should be pointed out that no one has, as yet, reported data extending the volume-temperature curve found above the transition temperature (supposedly representing a state of equilibrium) below the transition temperature observed at usual heating rates. Winter's work on glass[12] suggests that a similar anomaly in refractive index is not entirely a rate effect, but rather that the transition persists even under conditions of equilibrium. She selected several temperatures in the transition region and at each temperature determined the isothermal refractive index-time curve with the glass initially in the state above the transition region and also with the glass initially in the state below the transition region. The limiting refractive index defined by these two curves was found to be identical and was taken as the equilibrium refractive index at the specified temperature. In this way the equilibrium refractive index-temperature curve was

[7] B. J. Pines, J. Exp. and Theo. Phys. (U.S.S.R.) **9**, 963 (1939).
[8] R. F. Boyer and R. S. Spencer, *Advances in Colloid Science* (Interscience Publishers, Inc., New York, 1946), Vol. II.
[9] T. Alfrey, G. Goldfinger, and H. Mark, J. App. Phys. **14**, 700 (1943).
[10] E. Jenckel, Zeits. f. Elektrochemie **43**, 796 (1937).
[11] W. T. Richards, J. Chem. Phys. **4**, 449 (1936).
[12] A. Winter, J. Am. Ceram. Soc. **26**, 189 (1943).

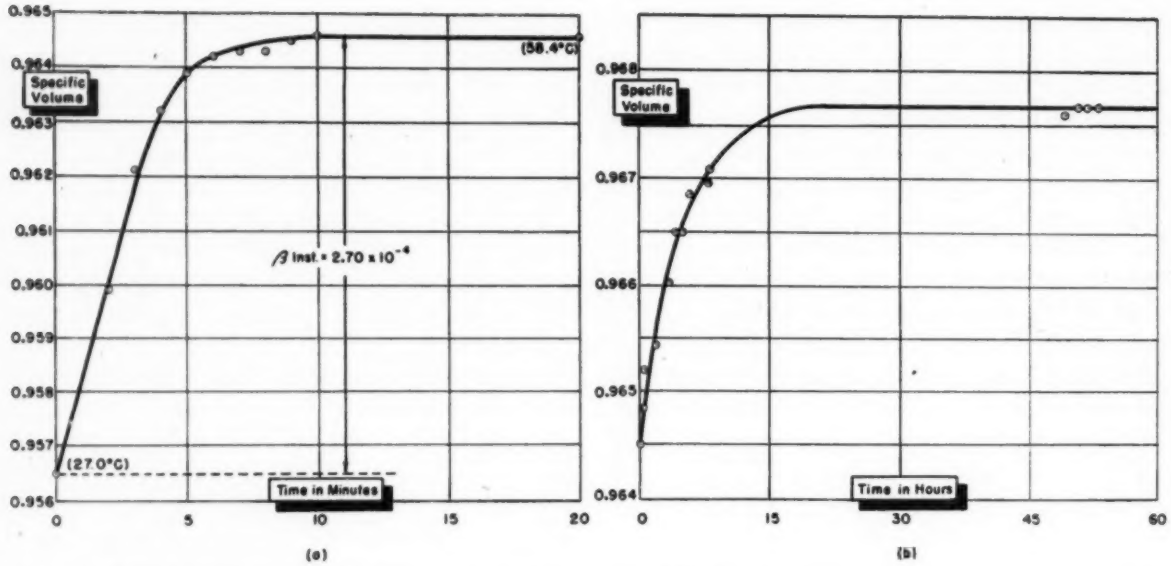

FIG. 1. Isothermal expansion of polystyrene at 58.4°C. (a) Thermal lag in dilatometer and "instantaneous" expansion. (b) Slow approach to equilibrium.

obtained, and it was found that the transition did not disappear but remained, even at equilibrium. For glass, therefore, the second-order transition seems to be an essential singularity with superposed rate effects. This conclusion prompted the following work on polystyrene, in which the equilibrium volume-temperature curve was determined.

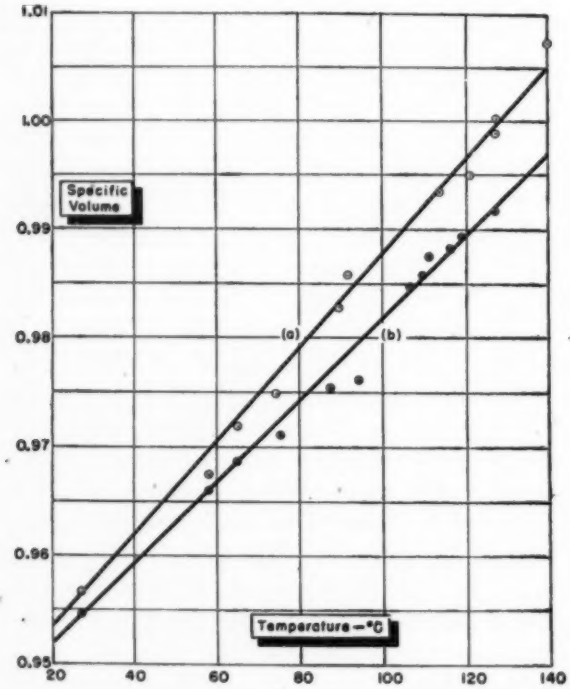

FIG. 2. Equilibrium volume-temperature curves of two samples of polystyrene. (a) β inst. $=2.70\times10^{-4}$ per °C, β eq. $=4.53\times10^{-4}$ per °C. (b) β inst. $=2.83\times10^{-4}$ per °C, β eq. $=3.98\times10^{-4}$ per °C.

EQUILIBRIUM VOLUME-TEMPERATURE CURVE OF POLYSTYRENE

The polystyrene used in this study was in pellet form, had a molecular weight of 300,000, and had been stored at room temperature for approximately two years. This made it seem reasonable to assume that this material was very close to its equilibrium volume at room temperature. The technique of handling samples was similar to that described in an earlier paper.[1] A weighed sample of polymer was placed in the bulb of a Pyrex dilatometer, followed by a hollow glass plug, and the bulb was sealed off. The dilatometer was then evacuated and filled with a known amount of mercury through the capillary tube. The position of the mercury in the capillary tube at room temperature was noted.

The dilatometer was next transferred to a constant temperature glycol bath and the height of the mercury in the capillary tube recorded as a function of time, over a period of several days. When it was evident that equilibrium had been reached, the dilatometer was transferred to a bath held at a higher temperature and the process

repeated. Occasionally, after the highest desired temperature had been reached, some of the points were re-checked on cooling.

It was found that when a polymer sample was suddenly raised in temperature, it expanded to a new volume almost instantaneously, being slowed down somewhat, of course, by thermal lag; after this initial expansion the material continued to expand, isothermally, at a slow rate until equilibrium was reached, within the limits of observation. If the sample were cooled, instead of heated, the same thing happened, except that the material contracted instead of expanding. The length of time necessary to reach equilibrium was dependent on the temperature, higher temperature resulting in shorter time.

This behavior is shown in Fig. 1, which is typical of the results obtained. In 1(a) we see the rapid change in volume associated with the thermal lag in the dilatometer bulb; and in 1(b) we see the much slower drift of volume toward equilibrium, following the attainment of thermal equilibrium. The pseudo-equilibrium attained in 1(a) corresponds to the "instantaneous" expansion of the sample, whereas that of 1(b) is a true equilibrium volume.

The equilibrium volumes of a polystyrene sample were determined at different temperatures and plotted as the equilibrium volume-temperature curve. Figure 2 shows such equilibrium volume-temperature curves for two different samples of polystyrene. It may be seen that from room temperature upwards the volume is essentially a linear function of the temperature, there being no discontinuities or transitions. The instantaneous (β_i) and equilibrium (β_e) cubical expansion coefficients (referred to the volume at 0°C) were slightly different for the two samples. They correspond roughly in magnitude to the expansion coefficients reported by Wiley[13]

TABLE I. Half-times for isothermal expansion and contraction of polystyrene.

Temperature	Half-time
30.0°C	13.6 hours
58.7	2.9
65.4	1.32
74.5	0.94
90.0	0.41

[13] F. E. Wiley, Ind. Eng. Chem. **34**, 1052 (1942).

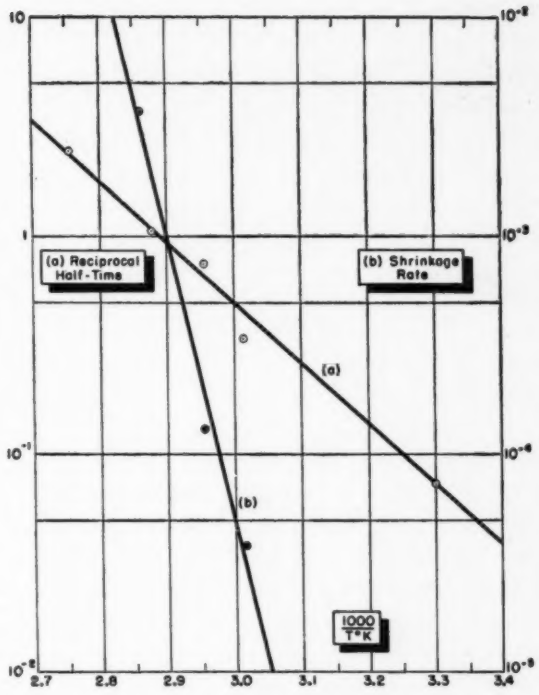

FIG. 3. Effect of temperature on the rates of two molecular processes in polystyrene. (a) Half-times of isothermal volume changes. Activation energy = 12 kcal. (b) Shrinkage rate of an oriented specimen. Activation energy = 61 kcal.

and by Alfrey, Goldfinger, and Mark[9] for polystyrene below and above its transition temperature, respectively. The points represented include those obtained by both isothermal expansion and contraction. No hysteresis was observed.

An unsuccessful attempt was made to carry out the same type of study on polymethyl methacrylate and a copolymer of styrene and divinyl benzene. The polymethyl methacrylate appeared to release gas upon heating, which rendered it impossible to use the dilatometer method. The styrene-divinyl benzene copolymer seemed to have residual strains at room temperature, which gradually released upon heating, resulting in anomalous volume-time curves.

NON-EQUILIBRIUM PHENOMENA

The authors have suggested[2] the relationship

$$\tanh\left[\alpha(V-V_e)/2\right]=Ce^{-kt} \qquad (1)$$

for isothermal volume changes in high polymers, where V is the volume at time t, V_e is the equilibrium volume, and α, C, and k are constants.

The volume-time curves obtained in this study were found to conform fairly well to the above relationship, but it was also noted that they fitted equally well a simple exponential relationship, as would be expected for relatively small values ($\leqq 1$) of the argument of the hyperbolic tangent. This observation suggested the possibility of determining the activation energy of the process of retarded thermal expansion. Table I lists half-times of the volume-time curves for several temperatures, and Fig. 3 shows these data plotted in the usual semi-logarithmic manner (curve (a)). It is seen that a fairly straight line results, corresponding to an activation energy of 12.0 kcal. for the process. It is interesting to compare this value with the activation energy for viscous flow in polystyrene and that for high or rubber-like elasticity. It is in best agreement with an activation energy for viscous flow of polystyrene of 12 kcal., reported by Ferry[14] and obtained by studying the viscosities of solutions in xylene and extrapolating to 100 percent polystyrene. A similar study (mentioned in reference 2) of the viscosities of solutions of polystyrene in isopropyl benzene gave an activation energy of 9.9 kcal. by extrapolation to 100 percent polymer. In contrast to this, Foote[15] reports a value of 40 kcal. and the data of Wiley[16] gives an activation energy of 31.6 kcal. However, Tuckett[17] has pointed out that viscous and elastic effects have not been separated in measurements such as those of Wiley, resulting in an activation energy higher than that for pure viscous flow. He further suggests that the activation energy for viscous flow in linear polymers without special bonds should be of the order of 10–30 kcal. and that higher values, 50–100 kcal. are usually due to elastic effects.

In this connection it was thought to be of interest to determine the activation energy of rubber-like elasticity in polystyrene. A rod of polystyrene was heated, stretched to about four times its original length, and a specimen cut from its center. This specimen was placed in a quartz dilatometer of the type recommended in the ASTM test D696-42T and the initial rate of shrinkage parallel to the orientation axis determined at three temperatures. The actual shrinkage observed was so small, as compared to the total stretch, that the length-time curves were essentially linear, and no correction was made for the slightly different initial length at each temperature. Curve (b) of Fig. 3 shows a semi-logarithmic plot of rate of shrinkage against reciprocal absolute temperature, from which an activation energy of about 61 kcal. is estimated. It is quite apparent from these values that the thermal expansion process in polystyrene does not involve any very great amount of chain uncoiling, but rather viscous flow of chain segments.

Thermal expansion measurements are not usually carried out under equilibrium conditions, and it is of interest to consider the volume-temperature curves resulting from various heating conditions and initial states. Under non-equilibrium conditions, i.e., at finite rates of temperature variation, the volume changes by two mechanisms

$$d(\Delta\sigma)/dt = -B\Delta\sigma, \tag{2}$$

$$d(\Delta\sigma)/dt = -\sigma_e(273)(\Delta\beta)dT/dt, \tag{3}$$

where $\Delta\sigma$ is the difference between the actual specific volume at time t and temperature T and the equilibrium specific volume at T, B is a quantity of the form $A \exp(-E/RT)$ which may be obtained from Fig. 3, $\sigma_e(273)$ is the equilibrium specific volume at 0°C, and $\Delta\beta$ is the difference between the equilibrium and "instantaneous" cubical expansion coefficients. Combining these two equations and making temperature the independent variable, we have

$$\frac{d(\Delta\sigma)}{dt} = -\frac{B\Delta\sigma}{dT/dt} - \sigma_e(273)\Delta\beta, \tag{4}$$

where dT/dt is now to be considered as a function of T. For given initial conditions and a given temperature-time curve a graphical solution of this equation is readily obtainable by the method of isoclines.[18] This method is quite flexible, for

[14] J. D. Ferry, J. Am. Chem. Soc. **64**, 1330 (1942).
[15] N. M. Foote, Ind. Eng. Chem. **36**, 244 (1944).
[16] F. E. Wiley, Ind. Eng. Chem. **33**, 1377 (1941).
[17] R. F. Tuckett, Trans. Faraday Soc. **39**, 158 (1943).

[18] T. K. Sherwood and C. E. Reed, *Applied Mathematics in Chemical Engineering* (McGraw-Hill Book Company, Inc., New York, 1939), p.126. W. C. Johnson, *Mathematical and Physical Principles of Engineering Analysis* (McGraw-Hill Book Company, Inc. New York, 1944), p. 86.

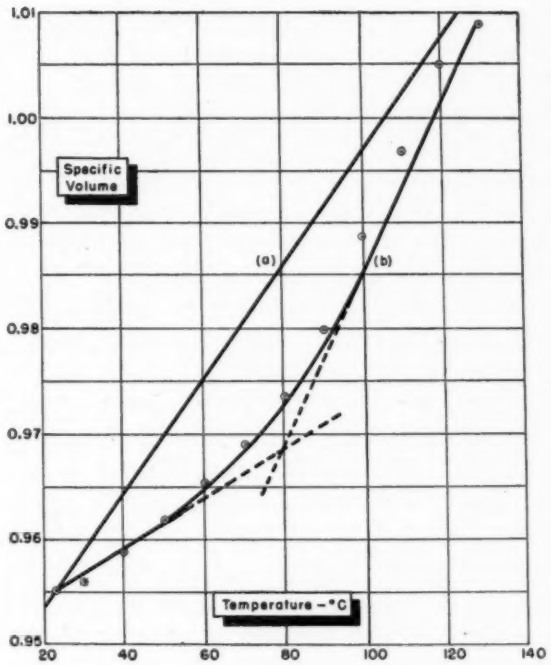

FIG. 4. Expansion of polystyrene from equilibrium at 23°C, with a heating rate of 0.82°C per minute. The circled dots are the experimental points. (a) Equilibrium curve for comparison. (b) Theoretical curve under the above conditions.

one family of curves ($\Delta\sigma$ *versus* T), corresponding to constant values of the product $B\Delta\sigma$, will suffice for any initial conditions and any temperature schedule. A comparison between theory and experiment is made in Fig. 4, where the equilibrium curve is indicated by the curve (a), the theoretical curve for constant rate of temperature rise by curve (b), and the observed curve under the same conditions by the circled points. The general features of the theoretical and experimental curves were the same, and a reasonably satisfactory fit was obtained. It is interesting to note that the system never reaches equilibrium, but rather the actual curve approaches the equilibrium curve asymptotically at the higher temperatures. Also, the non-equilibrium expansion coefficient above the apparent transition is actually greater than the equilibrium value.

Another case of interest is the thermal expansion of a quenched sample. By this we mean that a sample at equilibrium at some elevated temperature is cooled at such a rapid rate as to permit contraction corresponding to only the instantaneous expansion coefficient. The material is then immediately heated at a constant rate and the volume-temperature curve observed. The theory predicts that the volume will start out above the equilibrium curve and eventually cross it at a temperature a little below the temperature from which the sample was quenched, this temperature difference depending on the rate of heating. The volume then will dip below the equilibrium curve, to an extent depending on the heating rate, and approach the equilibrium curve asymptotically from below.

The importance of these conclusions in practical considerations such as the question of the dimensional stability of molded polystyrene objects is at once apparent. If the molded object is at equilibrium volume at some temperature and is then removed from the mold and cooled rapidly, the volume upon reaching room temperature is somewhat greater than the equilibrium volume. The object will then shrink over a period of several days, gradually approaching the equilibrium volume. The amount of shrinkage is roughly proportional to the temperature interval covered during the rapid cooling. The expansion coefficients of Fig. 2, for example, would result in a volume contraction of about 1.7 percent for a 100°C cooling interval. This shrinkage at room temperature may be reduced by an annealing process, i.e., by one or both of two procedures: first, lowering the annealing temperature, that is to say, the temperature at which the volume is allowed to come to equilibrium, and second, going to slower cooling. Graphical solution of Eq. (3) for various annealing conditions, as before indicated, permits the determination of the optimum annealing schedule for a given, allowable amount of shrinkage.

As an example of the type of chart which might prove useful in annealing problems, Fig. 5 shows the effect of temperature on the time interval necessary for the volume of a polystyrene sample to cover 50, 75, 90, 99, and 99.9 percent of its distance from the equilibrium volume, by isothermal expansion or contraction. Such a family of curves would facilitate the choice of an annealing time to correspond to any given annealing temperature. Similarly, curves might be constructed showing the deviation from equilibrium at room temperature after

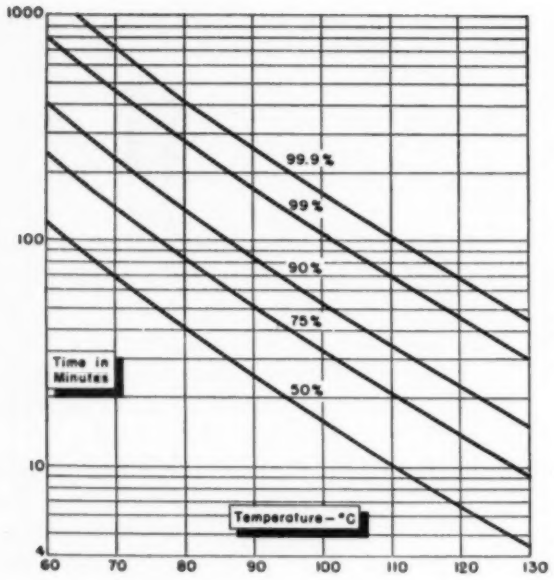

FIG. 5. Effect of temperature on the time necessary for polystyrene to travel 50, 75, 90, 99, and 99.9 percent of its initial distance from equilibrium volume by isothermal expansion or contraction.

cooling at various rates from different annealing temperatures.

It must be realized, of course, that Fig. 5 applies only to an approach to equilibrium by a viscous flow process. Certain molding techniques tend to produce objects with unrelieved stresses due to elongation of polymer chains from their equilibrium lengths, i.e., a certain amount of orientation is "frozen" into the object. This orientation is not objectionable from the standpoint of dimensional stability at room temperature due to the high activation energy for the coiling up of the chains (rubber-like elasticity). However, it does introduce optical inhomogeneities into the material and also limits its use at more elevated temperatures, thus it is frequently desirable to relieve these stresses. A more detailed study of the shrinkage of oriented specimens at various temperatures should provide data for the construction of an analogue of Fig. 5 for the annealing of slightly oriented objects.

SUMMARY

The apparent second-order transition in polystyrene has been demonstrated to be a rate effect. The equilibrium volume-temperature curve has been determined over the range of from about 20° to 140°C and no indication of a transition found within this interval. Rates of heating or cooling customarily used in thermal expansion measurements result in an apparent second-order transition in the neighborhood of 82°C. The equilibrium cubical thermal expansion coefficient was found to be 4.53×10^{-4} per °C for one sample of polystyrene, but there are indications that this value varies somewhat from one polystyrene sample to another.

At ordinary rates of heating below the apparent transition temperature, or at more rapid rates near and above the transition temperature, polystyrene exhibits a cubical thermal expansion coefficient of about 2.7×10^{-4} per °C, and this value is not dependent on the heating rate as long as it is rapid enough. This fact suggests that two mechanisms operate in the thermal expansion of polystyrene, at markedly different rates, one resulting in almost instantaneous expansion, even at room temperature, and the other being strongly temperature dependent and contributing to the expansion under normal rates of heating only at higher temperatures. The rate of expansion by the second mechanism has been determined at different temperatures, resulting in an energy of activation of 12.0 kcal. This energy of activation would seem to indicate that the second mechanism involves the viscous flow of polymer chain segments rather than the uncoiling of chains as in rubber-like elasticity, which was found to have an activation energy of about 61 kcal. for polystyrene.

Isothermal volume-time curves were found to be exponential in form and this fact, together with the instantaneous expansion coefficient, has enabled us to set up a differential equation defining the volume-temperature curve under non-equilibrium conditions, i.e., at finite heating rates. A comparison was made between an experimental volume-temperature curve and a theoretical curve under the same conditions obtained by graphical solution of the differential equation. An extension of this method of predicting volume-temperature curves to such problems as the expansion of quenched samples and annealing for dimensional stability was indicated.

Abstracts

Following are abstracts of the other papers presented on the program of the second regular meeting, Division of High Polymer Physics of The American Physical Society, Columbia University, January 24–26, 1946.

Thermal Diffusion of Polymers. PETER DEBYE, *Cornell University.*—Experiments on thermal diffusion of high molecular weight polymers in solution were performed using the Clusius-Dickel arrangement. It was found that whereas molecules of small molecular weight have a thermal diffusion coefficient of the order of 1 percent of the ordinary diffusion coefficient, both coefficients are of the same order of magnitude for polymers. It was also found in the special case of polystyrene that the thermal diffusion coefficient increases with increasing molecular weight indicating that thermal diffusion methods can be used for fractionation purposes as well as for the observation of the molecular weight distribution curve. The question whether thermal diffusion of molecules with the same molecular weight depends also on their form (for instance, branched or straight chain) has not yet been answered. The instruments which we have used are cylindrical in form, hot and cold cylinder concentric with a narrow interspace. Other experiments have shown that packing of the interspace may have practical advantages. The thermal diffusion method also seems appropriate for the purification of liquids from small amounts of impurities. The work has been done in collaboration with A. Bueche and was supported by the Rubber Reserve Company.

X-Ray Diffraction by Potassium Laurate Solutions (A Contribution to the Mechanism of Emulsion Polymerization). E. W. HUGHES, *Shell Development Company.*—This paper will describe the results of an x-ray diffraction study, mostly at small scattering angles, of aqueous potassium laurate solutions with and without other added substances. The soap concentration has been varied over the range 10 percent to 50 percent, which includes the phase change from isotropic solution to anisotropic "middle soap." The added materials include KCl up to 2.0 weight normal and more than thirty hydrocarbons and hydrocarbon derivatives. The hydrocarbons have been added in some instances up to a concentration of one mole per mole of soap. These experiments are part of a study of the role of soap in emulsion polymerization.

The Use of Color and Fluorescence Indicators for Determining the Structure of Glasses. W. A. WEYL, *Glass Science, Inc.*—The fact that light absorption and emission depend on the environment of the ions and molecules which absorb or emit light can be used to draw conclusions about the structure of liquids, glasses, and crystals. This method supplements, to a certain extent, information gained from other sources, such as x-ray diffraction data. The method is illustrated by several examples, like the influence of thermal history on the structure of glass and the constitution of the yellow fluorescing zinc orthosilicate.

The Mechanical Properties of Fibers. HENRY EYRING AND GEORGE HALSEY, *Textile Research Institute Laboratories.*—The stress-strain behavior of textiles has been interpreted quantitatively in terms of a model with a viscous element in parallel with one spring and in series with a second. Such a viscous element is of the non-Newtonian type required in plastic flow. The treatment of more complicated conditions of straining gives rise to equations best treated by the superposing of elementary processes. For any restraint, methods are given for computing the stress-strain curves from the elementary processes.

The Molecular Structure of Some Polyuronides as Revealed by X-Ray Diffraction Studies. K. J. PALMER, *Western Regional Research Laboratory,* Albany, California.*—Recent x-ray diffraction studies carried out on some naturally occurring polymers, particularly polymannuronic acid (alginic acid) and polygalacturonic acid (pectic acid), show that they are essentially long, straight chains. The symmetry of the chain in alginic acid is twofold, in sodium alginate threefold. The polygalacturonide chain remains threefold in pectin, pectinic acid, and pectic acid as well as the Na, K, and Rb pectates. The fiber axis identity period of the polygalacturonide chain is always about 13A. This identity period is compatible with the generally accepted chemical structure for this chain when the pyranose rings are assumed to have one of the two alternative transconfigurations. Moisture isotherms and x-ray data on pectinic acids show that absorbed water hydrates the polar groups and increases the interchain separation. The non-uronide material which occurs to the extent of 10–20 percent in the pectates has no detectable influence on the x-ray pattern.

* Bureau of Agricultural and Industrial Chemistry, Agricultura Research Administration, U. S. Department of Agriculture.

Statistics of Cross-Linked Polymers. WALTER H. STOCKMAYER, *Department of Chemistry, Massachusetts Institute of Technology.*—The present statistical theory of molecular distribution is highly branched and cross-linked polymer will be critically reviewed. The existing theory rests on two assumptions. The first, that all similar functional groups are equally reactive, becomes invalid for dilute solutions or for diffusion-controlled reactions. The second, that no cyclic structures can form, is more serious and must be removed before truly cross-linked polymers can be treated, but the mathematical difficulties are formidable. Experimental observations of gel points will be compared with the theory. For polycondensations, agreement is tolerably good, so that the statistical formulas may be applied with some confidence to these reactions prior to the gel point. Such an application has already been made

to a study of the viscosities of branched polyesters. The theory has now been extended to deal with a general polycondensation reaction involving any number of components. For addition polymers, the theory is generally poor, because its basic assumptions are seriously violated. Finally, the necessity of an improved theory for the gelled state will be emphasized. Flory's treatment, though qualitatively attractive, appears not to be generally applicable. It is concluded that cyclic structures must be specifically considered in the basic formulation of the theory.

Some Thermodynamic Properties of Slightly Cross-Linked Gels. R. F. BOYER AND R. S. SPENCER, *The Dow Chemical Company, Midland, Michigan.*—It has been shown recently[1] that a measurement of the deswelling of slightly cross-linked gels by high polymer solutions affords in principle a new method of determining the number-average molecular weights of polymers. In order to assess the merits of this method, it has been necessary to explore the behavior of gels in some detail. Amount of cross-linking agent, size of the sample, percentage of soluble material present in the gel, variation of swelling ratio in pure solvent for a series of supposedly identical gels, and influence of solvent type were among the factors studied. Measurements of the equilibrium swelling volumes of a series of identical gels in a wide range of solvents afford a convenient method for evaluating solvent power or solvent-polymer interaction. This is done in terms of the parameter μ_g which arises in the theory of gels. Some fifty solvents have been examined in this regard. Determination of μ_g for solvent-non-solvent mixtures leads to some interesting results. All work reported here is confined to styrene-divinyl benzene gels.

[1] R. F. Boyer, J. Chem. Phys. **13**, 363 (1945).

The Determination of Polymer-Liquid Interaction by Swelling Measurements. PAUL DOTY AND HELEN S. ZABLE, *Department of Chemistry, Polytechnic Institute of Brooklyn.*—The interaction of polymers and liquids can be fairly well characterized by the value of the quantity μ, commonly used in thermodynamics of polymer solutions and evaluated from osmotic pressure measurements. The Flory-Rehner theory of swelling relates the amount of swelling of a slightly cross-linked polymer in a liquid to μ and a parameter M_c, the average molecular weight between cross-links. M_c may be determined for a cross-linked polymer from its swelling volume in a solvent in which osmotic pressure measurements with the uncross-linked polymer have given the value of μ. The cross-linked polymer, thus calibrated, can be used to obtain the μ value for other liquids by measuring its swelling volume in them. This procedure has been carried out on polyvinyl chloride which can be cross-linked by heating. Calibration in three different liquids gave comparable values of M_c, thus checking the Flory-Rehner theory. The quantity μ was determined at two different temperatures for fifty liquids. The value of μ and the temperature dependence of μ correlate well with the observed properties of the binary systems. The variations of μ with molecular weight in an homologous series is demonstrated.

Stress-Time-Temperature Relations in Polysulfide Rubbers. M. D. STERN AND A. V. TOBOLSKY, *Princeton University.*—Polysulfide rubbers of various internal structures have been investigated by measurements of continuous and intermittent relaxation of stress and by creep under constant load at temperatures between 35°C and 120°C. Continuous stress relaxation measurements indicate that these rubbers approximately obey the simple Maxwellian law of relaxation of stress, which indicates that one definite type of bond in the network structure is responsible for stress decay. The activation energy for the relaxation process in each of the polysulfide rubbers is nearly the same, indicating that the same type of bond is responsible for the relaxation behavior of all the polysulfides investigated. In contrast to the hydrocarbon rubbers, oxygen is not the cause of high temperature relaxation in polysulfide rubbers, nor does heating in air at moderate temperatures for times comparable to the relaxation time produce permanent chemical changes or changes in modulus. Several possibilities regarding the mechanism of the relaxation process and the type of bond involved are considered in the light of the experimental results.

Viscometric Investigation of Dimethyl Siloxane Polymers. ARTHUR J. BARRY, *Dow-Corning Corporation, Midland, Michigan.*—A series of dimethyl polysiloxane fluids including pure distilled known members of linear and cyclic structures up to ten siloxane units in size as well as a series of intermediate oils of linear structure, whose number average molecular weights have been independently determined, have been studied viscometrically. The intrinsic viscosities were determined and the Staudinger constant evaluated. The molecular weights of several high viscosity polysiloxane fluids were estimated on the basis of this constant and a good fit with the Flory melt viscosity relationship found.

Some Fundamental Relationships between Intrinsic Viscosity, Diffusion and Sedimentation Constants and Thermodynamic Properties of High Polymer Solutions. ROBERT SIMHA, *National Bureau of Standards.*—Empirical relations previously proposed for the variations of the sedimentation and diffusion constants of high polymers are reviewed. If

$$s = s_0/(1+k_s c), \quad D = D_0(1+k_D c),$$

then for dilute solutions

$$k_s + k_D = 2bM/RT + v_{sp},$$

where b is the slope of the reduced osmotic pressure curve, M the molecular weight of the polymer, and v_{sp} its specific volume. Since in several instances k_D is small, while in some cases k_s is fairly well represented by the intrinsic viscosity, one may expect in general a certain parallelism between the latter quantity and the thermodynamic term. Analysis of a number of solutions of natural and synthetic polymers over a wide range of molecular weights and of varying slopes b shows the ratio between the thermodynamic factor and the intrinsic viscosity to assume values between one and two for most systems. Barring very poor

solvents, a semi-empirical equation is proposed which relates the intrinsic viscosity to equilibrium properties of the polymer-solvent system, *viz.*

$$(1-2\mu)V_2/V_1=r[\eta]V$$

is the well-known parameter in the expression for the activities, V_2/V_1 the volume ratio between the two components. $[\eta]V$ represents the intrinsic viscosity, based on volume fractions, and r is a factor which assumes values between one and two in the majority of cases considered.

Thin Section Methods for the Electron Microscopic Examination of Cured Polymers. H. C. O'BRIEN, *Research Laboratories, St. Joseph Lead Company, Josephtown, Pennsylvania.*—A method is described involving the use of the "Cyclone Knife" Ultramicrotome for the preparation of thin sections (0.1 to 1.0 micron) of cured rubber and other high polymer compounds. Such materials which do not permit the formation of film samples for the electron microscope because of their insolubility may thus be examined in thin sections for pigment dispersion and other characteristics. The Ultramicrotome, accessory apparatus, and the preparation and mounting of the specimens for the electron instrument are described. Micrographs of compounded polymers are presented to define the value of the method.

Attachment for Obtaining Angular Distribution of Scattered Light from Measurements with a Ninety-Degree Turbidimeter. J. N. WILSON, *Shell Development Company.*—A device is described which in conjunction with a ninety-degree turbidimeter permits measurement of the angular distribution of the intensity of scattered light over the range 145 to 115 degrees and 65 to 35 degrees. The apparatus consists of two mirrors by means of which the direction of the incident light beam can be varied over the required range. A discussion is given of methods of calibration and of typical results obtained.

A New Approach to the Theory of Relaxing Polymeric Media. M. S. GREEN AND A. V. TOBOLSKY, *Princeton University.*—A molecular theory of relaxing media is presented which gives an expression for the stress in terms of the strain history. At any given time the strain history produces a distribution in internal strains which for mechanical properties can be characterized by a limited number of internal strain parameters. The second law of thermodynamics is used to define dissipation of energy at constant temperature, and explicit expressions for dissipation of energy for any strain history are obtained. Inasmuch as relaxation during straining causes an essential reorganization of structure which is in fact the cause of dissipation, the kinetic theory of elasticity is extended to non-isotropic polymeric networks. A tensor expression for the stress-strain-time relations is thereby developed.

Application of Molecular Distribution Methods to the Statistical Mechanics of High Polymer Solutions. BRUNO H. ZIMM, *Polytechnic Institute of Brooklyn.*—In the expression for the osmotic pressure of a solution as a power series in the concentration, the term in the second power of the concentration determines the deviations of dilute solutions from ideality. A general expression for the coefficient, A_2, of this term has been developed for high polymer solutions using the probability distribution function of the configurations of a pair of chain molecules. In favorable cases it is found that the well-known Flory-Huggins equation arises as a first approximation, but that in general serious modifications to this equation must be made. These modifications arise from more complicated interactions of chain segments than are considered in the Flory-Huggins treatment and can be shown both theoretically and experimentally to be very considerable. It can be further shown that A_2 must depend on the molecular size, according to a relation whose first two terms are

$$A_2=A_2^0(1-kp^{\frac{1}{2}}A_2^0/R^3),$$

where A_2^0 and k are constants, p is the degree of polymerization, and R is the root-mean-square distance between chain ends.

Here and There

New Appointments

Twelve new staff members have been appointed to the University of Chicago's Institute of Nuclear Studies. They are Willard F. Libby, full professor, and the following assistant professors: Herbert L. Anderson, Nicholas C. Metropolis, Nathan Sugarman, Anthony L. Turkevich, James S. Allen, Stanley P. Frankel, Eldred C. Nelson, Harrison S. Brown, Norman S. Elliott, T. Harrison Davies, and Clyde A. Hutchison.

Robert B. Jacobs, until recently an engineer for the Kellex Corporation, has jointed the staff of Distillation Products, Inc., Rochester, New York, where he will direct the work of the physics laboratory in the study of physical phenomena at low pressures.

William A. Shurcliff, Scientific and Technical Adviser to the New York State Department, has been given temporary leave of absence by Governor Thomas E. Dewey to serve as official historian of "Operation Crossroads," to be carried out in the Marshall Islands in May and June by Joint Task Force One. Dr. Shurcliff helped edit the *Smyth Report* on the atomic bomb.

Noel C. Jamison joined Philips Laboratories, Irvington, New York, on January 2 as division chief in charge of electro-acoustics.

Charles T. Zavales recently joined the medical x-ray division of North American Philips Company as technical-commercial adviser.

Awards

Captain Ralph Decker Bennett, technical director of the Naval Ordnance Laboratory, has been awarded the Legion of Merit for his contributions in Naval ordnance research and development projects. Captain Bennett came to the Laboratory in 1940 from Massachusetts Institute of Technology, where he was professor of electrical measurements.

Enrico Fermi, Harold C. Urey, Samuel K. Allison, Cyril Smith, and Robert S. Stone, all of the University of Chicago, were presented Medal of Merit citations for their central roles in the production of the atomic bomb on March 20. Major General Leslie R. Groves, chief of the Army's Manhattan District, made the awards.

American Telephone and Telegraph Company has announced the award of five Frank B. Jewett fellowships for research in the physical sciences. Recipients are: Martin G. Ettlinger, Edward W. Fager, Bernard Goodman, Shuichi Kusaka, and Robert L. Scott.

Reinhold Rudenberg has received the Honor Award of Stevens Institute of Technology "for notable achievement in the field of electron optics as the inventor of the electron microscope."

Ohmite Laboratory

Ohmite Laboratory at Illinois Institute of Technology, established to provide service to industry in the field of electrical measurements, began in February to make its facilities available to sponsoring organizations. The result of a $32,500 contribution by David T. Siegel, president of the Ohmite Manufacturing Company, this laboratory will provide precision measurement of electrical and magnetic quantities for the Chicago area approaching in accuracy those of the Bureau of Standards in Washington. It is jointly operated by Illinois Institute's Electrical Engineering Department and the Electrical Engineering Division of the Institute's Armour Research Foundation.

Congress for Applied Mechanics

The Sixth International Congress for Applied Mechanics will be held in Paris from September 22 to 29, 1946. It will be divided into the following sections:

1. Structures. Elasticity. Plasticity.
2. Hydro- and Aerodynamics. Hydraulics.
3. Solid Dynamics. Vibration and Sound. Friction and Lubrication.
4. Thermodynamics. Heat Transfer. Combustion. Fundamentals of Nuclear Energy.

Those who desire to become members of the Congress are requested to inform the Secretary General as soon as possible of their intention to attend the Congress. They should also indicate whether they wish to present a paper, and in what section. For information address the Secretary General at Institut Henri-Poincare, 11, rue Pierre-Curie, Paris (V^e), or write to Dr. Josephine de Karman, 1501 South Marengo Avenue, Pasadena, California.

Westinghouse Forum

A science and engineering forum honoring the centennial of the birth of George Westinghouse will be held by Westinghouse Electric Corporation in Pittsburgh on May 16–18. Internationally prominent scientists will be among the speakers.

Products of Tomorrow Exposition Postponed

Because of the uncertainty of products and delivery schedules of large numbers of the nation's leading manufacturers, the Products of Tomorrow Exposition scheduled to open at the Chicago Coliseum April 27 has been indefinitely postponed. It may be held by the fall of this year or held over to early in 1947.

New Books

What Are Cosmic Rays

By Pierre Auger. Translated from the French by Maurice M. Shapiro. Pp. 128, Plates 22. University of Chicago Press, 1944.

During the last fifteen years the subject of cosmic rays has received a great deal of attention from both experimental and theoretical physicists. A great many articles have appeared in the technical literature. On the other

hand, there have been practically no books written by authoritative individuals, describing the progress made in this subject. It is therefore a particular pleasure to welcome a book by Pierre Auger. Dr. Auger is well known for his investigations and for his excellent experimental techniques, and the book therefore carries the weight of a distinguished investigator in the subject. The book was translated from the French by Dr. Shapiro who also has done experimental work in the field of cosmic rays.

The book starts with an account of the initial discovery of the residual ionization which led to the recognition that cosmic rays exist. From this beginning the development of the subject is traced through the picturesque phase of the worldwide survey expeditions which established the particle nature and energy spectrum of the radiation. The bulk of the book is devoted to the present stage of research in which most of the work is done by rather complex arrangements of Geiger counters and cloud chambers and is sometimes further implemented by high altitude balloon or airplane flights. Dr. Auger describes the experiments leading to the recognition of the positive electron and the positive and negative mesotron. The author also describes many of the more recent experiments on "cascade" shower production, knock-on electrons, mesotrons, and nuclear explosion processes. He discusses the evidence which tends to show that the primary rays are protons. This reviewer only regrets that the book was not longer.

In the preface, the translator says: "This book is written primarily for the reader who lacks a technical knowledge of physics but who wants to keep in touch with current developments in science. It is not intended for the specialist but should provide a good perspective for the physicist who wants to get a quick view of what has been done in this new field." The book is written on a semi-technical level, without recourse to mathematics, and presupposes some knowledge of the main phenomena involved. It is especially suitable for graduate students and professional physicists whose main interest is in other branches of physics, as well as for research workers in allied sciences who are familiar with physical terminology. For these persons it presents a bird's eye view of present conceptions of the subject.

The binding is of good quality, the type is easy to read, and the photographs at the end which illustrate the main cosmic-ray phenomena are both interesting and instructive.

SERGE A. KORFF
New York University

Lehrbuch der Funktionentheorie

BY L. BIEBERBACH. Two volume set. Vol. I. Elemente der Funktionentheorie. Fourth edition. Pp. 322+xiv, Figs. 77, 5½×8½ in. Vol. II. Moderne Funktionentheorie. Second edition. Pp. 370+vi, Figs. 47, 5½×8½ in. Chelsea Publishing Company, New York, 1945. Price for set $6.50.

These treatises are reprints of the latest German editions. The latest edition of Vol. I was originally published by J. Springer, Berlin, in 1934; Vol. II, in 1931.

Volume I. The first edition of this volume was published 25 years ago; yet the fourth edition still is one of the finest introductions to the theory of functions of a complex variable. The treatment, though elementary, is quite complete. Full use of the Cauchy, Weierstrass, and Riemann points of view have been made. The talent of the author in combining a clear presentation with a reasonably comprehensive treatment of the subject is almost everywhere in evidence. The reader will be quick to feel the author's deep interest in the field.

The following chapter headings give an indication of the scope of Volume I: complex numbers, series, functions of a complex variable, special functions, conformal mapping, complex integrals, Cauchy integral formula, residues, analytic continuation, algebraic functions, integrals of algebraic functions, simple periodic functions, elliptic functions, representation of analytic functions by series and products, gamma-function.

Volume II. Volume II contains a great variety of material on modern theory of functions of a complex variable. In it are reflected the many advances of the subject up to the time of its original publication.

This volume contains extensive treatments of such topics as the following: conformal mapping, elliptic modular functions, theory of analytic functions bounded in the unit circle, Professor Bieberbach's treatment of uniformization, Picard's theorem, entire functions, analytic continuation, zeta-functions.

These classical treatises will undoubtedly continue to be useful for many years to come, to those whose primary interest is in mathematics as well as to those whose concern lies mainly in the physical sciences. Serious students of physics, engineering, and related fields who make frequent use of functions of a complex variable, conformal mapping, and the like, will profit by a thorough study of these volumes.

RICHARD S. BURINGTON
Washington, D. C.

Physical Methods of Organic Chemistry, Volume I

BY ARNOLD WEISSBERGER, Editor. Interscience Publishers, Inc., New York, 1945.

In the preface to this volume, Arnold Weissberger suggests that this work has been compiled to assist the chemist in acquainting himself with physical methods and the student in understanding the principles involved in the methods described. In addition, the book should also be of value to still a third person, the engineer who desires information as to the accuracy of data and what information may be reasonably requested from the laboratory.

Beginning with the "Determination of Melting and Freezing Temperatures," the successive chapters describe the theory and apparatus necessary for measuring boiling point, density, solubility, viscosity, interfacial tension and parachor, osmotic pressure and diffusivity of pure substances and solutions. While the needs of organic chemistry are particularly stressed, the applications and principles involved need not be confined to any one field. Quite naturally, the examples used in describing operations are those of organic chemicals.

Wherever possible, the authors have included alternate methods of determination for various required degrees of accuracy or for the different types of materials to be measured. Very useful are tables, such as that on page 105 in which means of determining density are recommended in terms of the nature of the substance, the conditions required (such as speed, size of sample, etc.), and the maximum precision desired.

Particularly noticeable is the recommended use of comparative rather than absolute methods of measurement. Through this technique the sources of error inherent in many laboratory methods may be minimized. Frequently the property of a reference substance has been established as standard or can be determined very accurately by a difficult or complex method. In this case, the comparison determination may be made much more rapidly and in simpler apparatus than if an absolute determination were necessary.

Other chapters discuss the properties of monolayers and duplex films, calorimetry, microscopy, crystal form and crystallochemical analysis, diffraction (both x-ray and electronic), and refractometry.

Many references are given, including specific articles, listed by number on the same page as the corresponding item in the text, and general references, which are tabulated at the end of each chapter. Thus, a sound basis is provided for anyone who might wish to pursue any particular subject farther. However, sufficient information on formulas, constants, and standards has been included so that use of the references is not necessary and may be made at the discretion of the reader.

Volume I has been published without an index. While not absolutely necessary, as the Table of Contents and the Chapter Outlines enable any subject to be located fairly readily, an index would be a valuable addition to any book of this nature. Perhaps one is included in Volume II.

As might be expected in a work of this nature, the style of presentation varies throughout the book. This is no disadvantage as each chapter is complete in itself. Both the authors and the editor are to be commended for maintaining the uniform high quality of the work throughout the diverse subjects which are included.

THOMAS J. WALSH
The Standard Oil Company (Ohio)

New Booklets

National Research Corporation, 100 Brookline Avenue, Boston, Massachusetts, has issued a 30-page book, containing many pictures, entitled *High Vacuum for Industry*, describing the new commercial possibilities for high vacuum.

Interchemical Review for Autumn 1945, published by the Interchemical Corporation, 432 West 45 Street, New York 19, New York, has the following table of contents:

Analysis by Excited Atoms
Colors for Textiles: Ancient and Modern
Proximity Radio Fuze
Gloss Black for War Planes

Fischer and Porter Company, Hatboro, Pennsylvania, has issued an 8-page bulletin explaining Rotameter advantages and covering the most prominent styles of rotameters and their uses. Free. Request Bulletin 45-A from Fischer and Porter Company, Department 5–4, County Line Road, Hatboro, Pennsylvania.

Alemite Division of Stewart-Warner Corporation, Chicago, Illinois, has published a book entitled *Alemite Answers*, containing a discussion of man's age-long struggle with friction and a graphic presentation to demonstrate, in laymen's pictures and terms, the how, what, when, where, and why of lubrication. The book is for distribution at $3 per copy through the Alemite distributor organization, to industry and the automotive, marine, and aviation fields. In addition, copies will be made available to engineering and technical schools, designers, engineering societies, and other individuals and groups concerned with machinery.

Eitel-McCullough, Inc., San Bruno, California, has issued a 20-page brochure, fully illustrated, which presents the entire Eimac line of electronic products. Free on request.

Bakelite Corporation, 30 East 42 Street, New York 17, New York, publishes quarterly the *Bakelite Review*, the purpose of which is "to inform industry of the latest developments in plastics and synthetic resins and their applications." The January, 1946 issue contains 32 pages and many attractive illustrations.

Science and Appliance for January, 1946, a four-page folder issued monthly by The Ohio State University Research Foundation, Columbus 10, Ohio, features articles on the work of A. R. Olpin, until recently the Executive Director of the Foundation: Sonar—underwater radar; progress in aids to hearing; uses of glass fibers.

Allied Radio Corporation, 833 West Jackson Boulevard, Chicago 7, Illinois, has announced the publication of a new 1946 buying guide, *Everything in Radio and Electronics*. Free on request.

Ohmite Manufacturing Company, 4835 West Flournoy Street, Chicago 44, Illinois, has issued a four-page folder, Bulletin No. 126, on Riteohm Precision Resistors. Free on request.

Philco Corporation, Philadelphia 34, Pennsylvania, is sending to all Philco stockholders, distributors, and dealers a 32-page booklet, *Radar on Wings*. "This first complete story of airborne radar is illustrated with a large number of photographs and drawings of operational and installation views that were stamped 'Secret' until long after V-J Day and can only now be released."

Bell Telephone Laboratories, Inc., 453 West Street, New York 14, New York, has published a 28-page booklet entitled *Radar and Your Telephone*. It tells in non-technical language how the problems of radar were solved and how it accomplished so much in actual combat. Many color illustrations.